Mechanical Ventilation and Optimisation through Analytical Lung Model

Ankit Mishra

A thesis presented for the degree of

Masters of Engineering

in

Mechanical Engineering

at the

University of Canterbury,

Christchurch, New Zealand.

Acknowledgements

To my supervisor Prof. Geoff Chase. Thank you for being a great supervisor and for your valuable inputs and insight.

To Dr Geoff Shaw. Thank you for your time and assistance with clinical trials and your medical insight and inputs.

To Mike Forrester and the ICU staff. Thank you for your time and help with setting up my clinical trials. It would not have been possible without your help.

To my family and friends. Thank you for backing me up and for your love and support.

Table of Contents

List of Figures

List of Tables

Nomenclature

Intensive Care Unit (ICU)

Mechanical Ventilation (MV)

Endotracheal (ET)

Ventilator Induced Lung Injury (VILI)

Acute Respiratory Distress Syndrome (ARDS)

Acute Lung Injury (ALI)

Positive End Expiratory Pressure (PEEP)

Centimetre of Water – Pressure Measurement (cmH2O)

Tidal Volume (V_t)

Peak Inspiratory Pressure (PIP)

Functional Residual Capacity (FRC)

Dynamic Functional Residual Capacity (dFRC)

Volume Controlled Ventilation (VCV)

Pressure Controlled Ventilation (PCV)

Carbon Dioxide (CO_2)

Pressure Volume (PV)

Lower Inflection Point (LIP)

Upper Inflection Point (UIP)

Zero End Expiratory Pressure (ZEEP)

Computed Tomography (CT)

Threshold Opening Pressure (TOP)

Threshold Closing Pressure (TCP)

Standard Deviation (SD)

Transpulmonary Pressure (ΔP_L)

Specific Lung Elastance (E_{Lspec})

Plateau Airway Pressure (P_{aw})

Lung Elastance (E_L)

Chest Wall Elastance (E_{CW})

Ratio of lung elastance to total respiratory elastance (α)

Mean (μ)

Total Lung Capacity (TLC)

Inspiratory Capacity (IC)

Abstract

Mechanical Ventilation (MV) therapy is one of the most common treatments offered to patients with respiratory failure in ICU. MV assists patient recovery by completely or partially taking over the breathing process and helping with oxygen delivery and removal of carbon dioxide. However, inappropriate MV settings mismatched to a given patient's condition can cause further damage. On the other hand, suboptimal MV settings can increase the length of stay of the patient in ICU and increase the cost of treatment.

Acute Respiratory Distress Syndrome (ARDS) is a major form of Acute Lung Injury (ALI) where clinicians offer a supportive environment for patient recovery by application of MV. ARDS is characterised by inflamed and fluid filled lungs that result in alveolar collapse and thus severe hypoxemia. Application of positive end expiratory pressure (PEEP) is employed to recruit and retain lung units to maximise gas exchange. However, a delicate trade-off is required between maximising gas exchange and preventing further unintended damage to the lungs, when determining optimum PEEP level.

Currently, no specific protocols to determine optimum PEEP level exist and selection of PEEP is dependent on medical intuition and experience, primarily due to lack of easy methods to determine patient – specific condition at the patient's bedside. A mathematical recruitment model is developed in Labview to help determine patient – specific condition based on fundamental lung physiology and engineering principals in this thesis. The model utilises readily available clinical data to determine parameters that identify underlying patient – specific lung characteristics and conditions. Changes in these parameters can be monitored over time and compared between patients to determine the severity of the disease and evolution of disease with time.

A second model is developed to determine dynamic functional residual capacity (dFRC), that represents the extra volume retained in a lung through application of PEEP. The model extends previous efforts in the field that applied the stress – strain theory to lung mechanics to estimate dFRC. This model estimates the patient's dFRC using readily available clinical data (PV data) and can be monitored over time to determine changes in a

given patient's condition. The dFRC model introduces a new parameter, β_1, which is considered a population constant for the particular PEEP. The model offers an easy and reliable method to determine dFRC since other methods are normally invasive or require interruption of MV.

The models developed were validated against real – time clinical data obtained through clinical trials. The recruitment model was found to fit the clinical data well with error values within acceptable limits. It also enabled identification of parameters that reflect the underlying patient – specific lung condition. The dFRC model was able to estimate the dFRC for a patient with high level of accuracy for clinically applicable PEEP levels. The two models work well in conjunction with each other and provide a novel and easy method to clinicians to determine patient – specific lung characteristics and ultimately determine optimal MV treatment parameters, especially PEEP.

Chapter 1 - Introduction

1.1 RESPIRATORY STRUCTURE AND FUNCTION

All warm-blooded animals, including humans, require a constant supply of energy to maintain a constant body temperature and perform other necessary functions. This energy is obtained when the food consumed undergoes a chemical reaction with oxygen, oxidative cellular metabolism, as part of homeothermic (warm-blooded) physiology. The energy from food can be stored in the body in form of fat, but oxygen cannot be readily stored and a constant supply is needed.

The lungs fulfil this requirement through gas exchange. Oxygen is extracted from inspired air and is transferred to the blood through the lung alveoli. Equally, the bi-products of the metabolic chemical reaction (primarily CO_2) are removed from the blood and exhaled from the body. Thus, the lungs provide oxygen and remove waste gases from the body through gas exchange in recruited/available lung alveoli.

1.2 RESPIRATORY SYSTEM AND LUNG PHYSIOLOGY

Functionally, the respiratory system consists of two portions. First, the *Conducting section,* which includes the nose, pharynx, larynx, trachea, bronchi, bronchioles and terminal bronchioles. These structures are responsible for warming, moistening and conducting air to the lungs and second, the *Respiratory section,* which includes the respiratory bronchioles, alveolar ducts, alveolar sacs and alveoli in the lungs. These latter structures are responsible for gas exchange with alveoli being the main sites of O_2-CO_2 exchange between air and blood.

The lungs form the primary part of the respiratory structure and are located in the thoracic cavity, above the diaphragm and around both the sides of the heart. The overall shape of the lungs is maintained by the rigid rib cage. The lungs and the rib cages are separated by inner and outer plural membranes. The inner plural membrane is attached to the lungs and the outer plural membrane is attached to the inner side of the rib cage. A thin layer of fluid

fills the space between the two plural membranes. This reduces friction and allows the two membranes to slide freely relative to each other. There are no physical connections between the lungs and the rib cage or the diaphragm (Sebel et al., 1985).

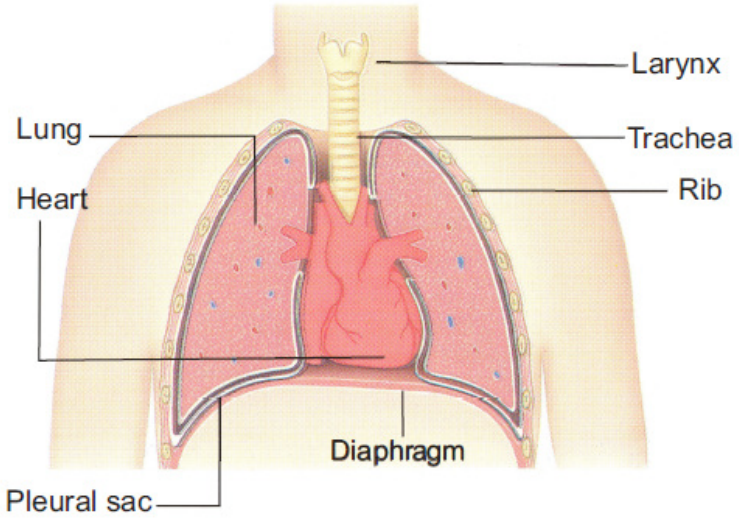

Figure 1-1: Location of lungs in thoracic cavity (Sebel et al., 1985)

The conducting section consists of the trachea, which is a c-shaped cartilage ring lined airway, with an average diameter of 2 cm. The cartilage supports and maintains the shape of the trachea and keeps this airway open. The trachea can withstand much greater pressures than the normal intrathoracic pressures observed (Sebel et al., 1985).

The trachea bifurcates into two slightly smaller lateral airways called bronchi just above the heart. Each bronchus feeds the lung on its respective side. The right bronchus is slightly larger than the left bronchus corresponding to the relative sizes of the left and right lungs. Each bronchus branches out further in its own lung, reducing in size with each bifurcation. The cartilage on these airways also becomes smaller, thinner and more irregular in shape.

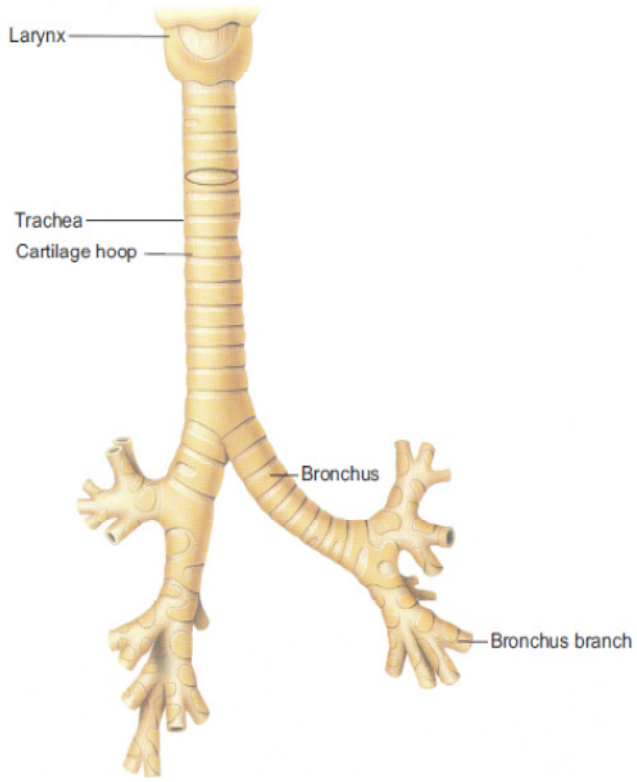

Figure 1-2: Major respiratory airways

The diameter of the bronchioles reduces to about 1 mm after about 11 generations and the cartilage lining disappears. The walls of the bronchioles now contain helical bands of muscles and the shape of the bronchioles is maintained by the lung parenchyma, which is the principal structural tissue in the bronchioles. The bronchioles branch further for about 8 generations without a rapid reduction in the diameter. Thus, the total surface area of the bronchioles increases with each bifurcation. The sole purpose of the airways until these bifurcations occur is the transport of air and maintenance of its temperature and humidity (Sebel et al., 1985, Vander et al., 2001).

The alveoli start to appear on the walls of the bronchioles after about 17 generations. The alveolus is where the gas exchange takes place. The number of alveoli gradually increases as the bronchioles branch out for further three generations. The function of the airways gradually changes from transport of air to gas exchange. The walls of the bronchioles are completely lined with alveoli after about the 20^{th} generation and the band of muscles completely disappear from the walls. These bronchioles do not reduce in diameter substantially with further bifurcation. This further bifurcation results in an increase in the

surface area of the alveoli. The bronchioles terminate into alveolar sacs after about the 23rd generation. Each alveolar sac contains approximately 20 alveoli and nearly half of all the alveoli are located in the alveolar sacs (Sebel et al., 1985, Vander et al., 2001).

An adult human lung contains approximately 600 million alveoli on an average, each of which are about 200 µm in diameter (Seeley et al., 2003). The actual number of lung units varies greatly depending on several factors including the gender and size of the lungs of the individual (Ochs et al., 2004). The alveoli are surrounded by minute capillaries that allow rapid gas exchange through the thin epithelium (2 µm) separating the gas and the blood (Vander et al., 2001). The exchange is done by transfer of gas from the region of high partial pressure to that of low partial pressure, trading oxygen and CO_2 in both directions. A typical alveolar sac is shown in Figure 1-3.

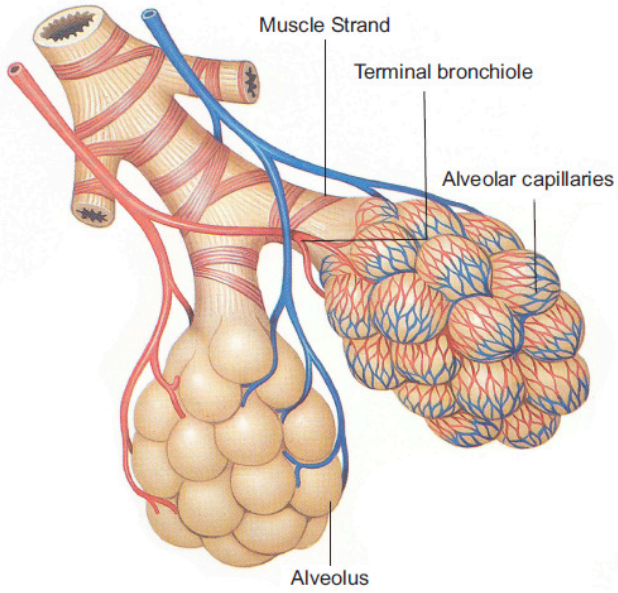

Figure 1-3: Alveolar sac and capillaries (Sebel et al., 1985)

The inner walls of the alveoli and distal bronchioles are lined with a fluid called surfactant, which maintains the spherical shape of the alveoli and prevent their collapse at smaller sizes and volumes. The surfactant is a mixture of proteins and lipids and works to control the surface tension and thus the shape of the alveoli. Specifically, surfactant acts to prevent alveolar collapse, thus maintaining the alveolar structure and function.

The concentration of the surfactant molecules on the alveoli and the bronchioles increases in the deflated state of the lung. The increase in the concentration of the surfactants decreases the surface tension and maintains the shape of the air space. The surfactant molecules become more spread out in the inflated state of the lung. This change in turn, increases the surface tension. Finally, this increase in surface tension prevents the overstretching of the alveoli and the airways by providing the restoring force.

The lung itself does not participate in the actual muscular movement required for inflation during inspiration. Instead, it is completely passive. The work is done by muscular movement of the diaphragm and the intercostal muscles of the ribs. During inspiration, the diaphragm moves downwards and the intercostal muscles move the ribs upward and outwards increasing the volume of chest cavity, as shown in Figure 1-4.

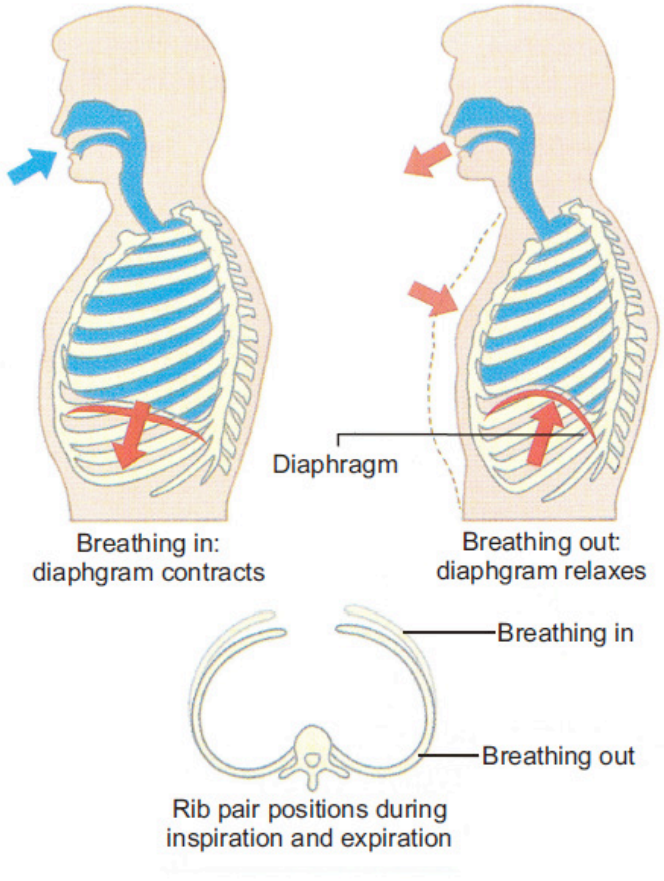

Figure 1-4: Movement of muscles and rib cage during inhale and exhale (Sebel et al., 1985)

Since there are no direct mechanical connections between the surrounding tissues and the lung, when the inspiratory muscles contract, a negative pressure gradient is created

between the thoracic cavity and the lung. This negative pressure gradient, in turn creates negative pressure gradient between the lung and the environment, which is at a higher atmospheric pressure. As a result, air is then drawn naturally into the lung , creating the inspiratory pattern of normal breathing (Sebel et al., 1985, Seeley et al., 2003).

Under normal breathing, deflation during expiration is a result of the simple elastic recoil of tissues. At the end of expiration, all the respiratory muscles are relaxed and the lung volume resumes its original equilibrium volume. The change forces the air, now exchanged with CO_2 and waste products, out of the lungs. This movement of air is caused by the elastic recoil of the surrounding tissues that were deformed during inspiration. Most of this recoil force results from deformed lung tissues and the surface tension on alveoli and distal bronchioles.

1.3 ACUTE RESPIRATORY DISTRESS SYNDROME

Acute Respiratory Distress Syndrome (ARDS), is a severe form of Acute Lung Injury (ALI), and is characterized by inflammation of the lungs and filling of the lungs with fluid. In this state, the lungs lose their ability to exchange gases effectively. The surfactant is also denatured and its production is reduced due to the inflammation. This change causes the alveoli to collapse losing its function. In particular, the collapse prevents the alveoli and the airways from filling with air during inspiration. As noted, the severely affected lung units collapse. Importantly, they cannot now be recruited without intervention and do not participate in gas exchange, resulting in a smaller and stiffer lung, also called a “baby lung” (Gattinoni et al., 2005).

The definition of ARDS was first reported in 1967 and has been evolving since then (Ashbaugh et al., 1967, Ware and Matthay, 2000). This evolution and lack of firm, clear definition occurs primarily because of lack of any specific criteria or tests that a clinician can follow to diagnose ARDS. In particular, ARDS does not have any disease specific symptoms (Artigas et al., 1998, Atabai and Matthay, 2002, Rouby et al., 2000).

The reported number of ARDS incidences varies between about 10 and 80 cases per 100,000 persons per year (Bersten et al., 2002, Luhr et al., 1999, Manzano et al., 2005, Reynolds, 1998, Rubenfeld et al., 2005, Suchyta et al., 1997, Ware and Matthay, 2000,

Zilberberg and Epstein, 1998). The mortality rate for ARDS is reported between 30% and 70% depending on severity, cause and treatment approach (Bersten et al., 2002, Esteban et al., 2002, Luhr et al., 1999, Manzano et al., 2005, Reynolds, 1998, Rubenfeld et al., 2005, Suchyta et al., 1997, Ware and Matthay, 2000, Zilberberg and Epstein, 1998). Due to the inspecific and broad definition of ARDS, different studies use different criteria to assess ARDS. There is thus significant variability in the incidence and reporting of eventual mortality. However, it is more consistently reported that the older patients have been believed to be at a significantly higher risk of ARDS and mortality rate (Manzano et al., 2005, Rubenfeld et al., 2005, Suchyta et al., 1997).

A recent cohort study suggests that, in the United States, there are 190,600 cases of ALI, including ARDS, with 74,500 associated deaths and 3.6 million hospital hours every year (Rubenfeld et al., 2005).

The damage to epithelial walls has an adverse affect on the production of surfactant which causes the alveoli to collapse. The additional pressure due to the excess fluid in the lung also facilitates the collapse of the alveoli. These factors make the gas exchange extremely difficult within the lung, resulting in a reduced concentration of oxygen and an increased concentration of CO_2. These factors have an overall effect of making the lung stiffer and require a higher pressure gradient to inflate an ARDS affected lung to the same volume as a healthy lung. This additional pressure required makes the process of breathing strenuous for the patient. This overall poor condition is further exacerbated by the non-participation of the injured and flooded lung units, further reducing the functional volume of the lung.

Inefficient gas exchange can result in severe hypoxemia which is defined as partial arterial oxygen pressure less than 50 mmHg or half the normal level. Hypoxemia can prove fatal to vital organs (especially the brain) if not treated immediately. Hence, it is pertinent to provide support for the work of breathing, and to maintain lung unit recruitment.

ARDS is caused by a range of conditions which may include direct injury to the lungs through inhalation of toxic gases or smoke, as well as diseases such as pneumonia, near drowning and direct physical injury to the lung (surgery). Indirect causes may include sepsis and severe trauma to other parts of the body, which cause an inflammatory response at the capillary level. Thus, ARDS can emerge from any condition that results in severe stress and trauma to the body.

1.4 MECHANICAL VENTILATION (MV)

No specific treatment methods for ARDS have been identified. Clinicians thus offer a supportive environment that aids patient recovery by application of mechanical ventilation (MV), which partially or completely takes over the breathing process (Ware and Matthay, 2000). This intervention is achieved through bulk movement of air in and out of the patient's lungs via the application of external pressure on the patient's airway through a high precision pump. MV may be invasive through an endotracheal tube (ETT) or, for less acute cases, non invasive, using a tightly fitted face mask. Up to 97% of the patients are treated with mechanical ventilation on admission to the ICU depending on the ICU cohort (Walsh et al., 2004), at a typical added cost of about $ 1,500 per patient a day (Dasta et al., 2005).

1.4.1 PARAMETERS OF MV

The major parameters considered in applying and setting MV are:

- **Positive End Expiratory Pressure (PEEP):** The pressure applied on the patient's airways at the end of expiration.
- **Functional Residual Capacity (FRC):** The relaxed volume of the lung at atmospheric pressure. PEEP is applied to maintain some additional volume above FRC at the end of expiration (dFRC). Application of PEEP prevents the collapse of the lung units at the end of expiration. This is particularly useful in treatment of ARDS since the lung units are vulnerable to collapse due to higher superimposed pressure and denaturing of the surfactants.
- **Tidal Volume (V_t):** The volume of air that enters the lung during each breathing cycle.
- **Peak Inspiratory Pressure (PIP):** Maximum pressure applied to the patient's proximal airway.

Together, these factors can define the entire breathing cycle for a patient. The main goal is to facilitate gas exchange and maximise recruitment, while not adding too much pressure that may cause damage to healthy lung units.

1.4.2 MODES OF MV

There are two common modes of mechanical ventilation:

- **Pressure Controlled**

  The PEEP and PIP are set by clinician in this mode of mechanical ventilation and the V_t is a result of these settings.

- **Volume Controlled**

  The PEEP and V_t are set by the clinician in this mode of mechanical ventilation and the PIP is determined as a result. The flow can be constant or can be varied over the inhale cycle and the actual flow is determined by the combination of the defined V_t and the Inspiration to Expiration (I:E) ratio.

The ventilator actively controls the inspiration cycle of the breathing cycle. The exhalation cycle is passive deflation of the lung to the applied PEEP.

1.4.3 EFFECTS OF INCORRECT MV

MV is an important form of treatment for patients with respiratory failure or lung injury and is necessary to maintain the appropriate blood oxygen level in most cases. However, incorrect ventilation mismatched to patient needs may cause further injury to the lung by the use of high air pressure (barotrauma) and high tidal volume (volutrauma).

Extended MV support to a patient may also lead to dependence which would prolong the use of mechanical ventilation and ultimately the cost of treatment (Dasta et al., 2005, McLean et al., 2006) Long term use of MV may also lead to problems such as ventilator associated pneumonia (Rello et al., 2002). Hence, there is a trade-off between quality of care and length of support as well.

In addition, the applied tidal volume is transferred to the healthy lung units from the collapsed region resulting in an increase in pressure in those areas. Application of a high pressure during MV, at any point in the cycle, may cause further unintended damage to healthy lung units. Thus tidal volume and airway pressure must also be correctly managed.

Thus, mechanical ventilation should be applied for a minimum period of time to avoid the complications arising from prolonged mechanical ventilation. Mechanical ventilator settings must also be optimized to achieve maximum lung recruitment to enable the patient to recover, while minimizing the Ventilator Induced Lung Injury (VILI).

Generally, the current methods of mechanical ventilation are based on trial and error and the application of the clinical experience and intuition of the clinicians. This results in extremely variable protocols that impact the effectiveness of the treatment. Hence, the quality and consistency of care can suffer.

1.5 EFFORTS TO STANDARDIZE MV PROTOCOLS AND PROBLEMS FACED

Current methods to determine the ventilator settings are based on trial and error and the intuition and experience of the clinicians and medical practitioners. The variability in the ventilation protocols has an adverse effect on the treatment offered to patients. Past attempts to standardize the ventilator treatment have mainly been focused on controlling the PEEP (Amato et al., 1998, Brower et al., 2004, Rouby et al., 2002, Takeuchi et al., 2002) and V_t (Brochard et al., 1998, Eichacker et al., 2002, Kallet and R.M. Jasmer., 2005).

1.5.1 STUDY OF TIDAL VOLUME TO STANDARDIZE MV PROTOCOLS

Tidal volume represents the volume of air that enters the lung during a breathing cycle and is one of the fundamental parameters of MV controlled by the clinicians and has significant impact on the MV protocol. Since an ARDS lung is characterised by heterogeneous distribution of the affected lung units (Gattinoni et al., 2001), some regions of the lung are more affected than others. The applied tidal volume may be transferred to the healthy lung units causing overstretching of these lung units, causing further damage.

Thus, the use of low tidal volumes during MV was investigated as a parameter for safe MV (Amato et al., 1998, Brochard et al., 1998, Dreyfus et al., 1985, Gajic et al., 2004, Stewart

et al., 1998). Amato et al (Amato et al., 1998), reported significantly lower mortality rates in the protective ventilation group compared to the conventional ventilation group. The ARDS network (The Acute Respiratory Distress Syndrome Network., 2000) also conducted a trial on 861 patients to study the impact of tidal volume on MV. This study showed that patients with lower tidal volumes (6.2 ± 0.8 ml/kg) had a higher number of days free of mechanical ventilation and lower mortality rates compared to those with higher tidal volumes (11.8 ± 0.8 ml/kg). However, their results and conclusions have also come under criticism for use of impractically high tidal volumes (12 ml/kg, compared to the normally used 8-10 ml/kg) during the trials for comparison (Eichacker et al., 2002) , as well as ignoring some negative effects of the use of low tidal volume (Kacmarek, 2005).

1.5.2 STUDY OF PEEP TO STANDARDIZE MV PROTOCOLS

Investigations have also been carried out to determine the optimum level of PEEP to be applied during MV. Amato et al (Amato et al., 1998) reported a decrease in the mortality rate when PEEP was set 2 cmH_2O higher than the lower inflection point of the inflation PV curve. This study theorised that the application of sufficient PEEP would prevent further collapse of the lung units and keep the lung inflated at the end of expiration, improving oxygenation, an “open lung” approach. Similar results were also presented by Villar et al (Villar et al., 2006) for the use of high PEEP.

In spite of the low mortality rates reported, the reasoning proposed to support these results have been challenged (Brower et al., 2004, Deans et al., 2005). One of the primary arguments presented suggests that the PEEP should be set according to the deflation curve instead of the inflation curve since the derecruitment of the lung units occurs during deflation (Girgis et al., 2006, Hickling, 2001, Hickling, 2002). It has also been suggested that the lower mortality rates could either be attributed to application of high PEEP or the use of low tidal volume during MV (Jonson and Uttman, 2007).

Although higher PEEP can improve oxygenation, the risk of overstretching of the lung units also increases with an increase in PEEP, particularly for healthy lung units (Ricard et al., 2003). Thus, use of the highest possible PEEP does not offer an optimal ventilator setting for MV. However, setting the PEEP too low results in continuous recruitment and derecruitment of the affected lung units (Schiller et al., 2003). Hence, an optimal PEEP

level needs to be selected to maximise recruitment while minimising any additional damage to the lung, a difficult and patient – specific trade-off.

Standardization of the MV protocols is further complicated by lack of simple and practical methods to determine and monitor the patient – specific lung condition at the patient's bedside. The most reliable method to accurately determine patient – specific lung condition is through Computer Tomography (CT) scans. However, this method has limited applications since it requires transport of the patient out of the ICU, disconnecting the patient from the ventilator and exposure to excessive radiology. Furthermore, the condition of the patient is expected to change during MV and frequent CT scans to monitor these changes offer an impractical and highly invasive solution.

The unique time – varying conditions of the patient is not accounted for in most studies. The condition of the patient varies greatly depending on several factors, such as age, gender, any pre-existing conditions etc. The condition of an individual patient also evolves with time and the use of simplified standard protocols may not be effective all the time.

1.6 SUMMARY AND PREFACE

The major problem with MV lies with the lack of standardized protocols for treating patients in the ICU. Optimal PEEP and V_t during MV would assure maximum gas exchange without causing further damage to the lungs and depend on the patient – specific conditions. The condition of the patient varies greatly depending on several factors and evolves constantly during the time MV is applied. Hence, it is extremely important to determine the patient – specific conditions during admission to the ICU and it also becomes incumbent to track the changes in these conditions during the stay of the patient in the ICU.

In particular, this outcome can be achieved through development of simple analytical models that incorporate the lung physiology and MV parameters. The specific objective of the model is to allow rapid identification of the patient – specific characteristics and thus assist in monitoring and determination of optimal MV parameters.

The primary goal of this thesis is to introduce an analytical lung model which identifies and captures the characteristics of the lung. The model uses clinically obtainable pressure

volume (PV) curves for the purpose and assists in determination of MV parameters through estimation of the recruitability of the lung. The thesis also discusses another model developed that estimates the actual volume of air contained inside the lung above the FRC due to application of PEEP by using the easily identifiable lung characteristics.

PV data is easily available from most of the modern ventilators, but often further complicated intervention is required to record and manipulate this data. This thesis thus presents a simple method for accurate measurement and recording of the PV data over a breathing cycle. This intervention allows for simple access of the data for manipulation required in fitting of the model, leading to model – based monitoring of MV therapy and guidance.

Chapter 2 - Lung Mechanics

The primary focus of the model studied is to identify the patient – specific characteristics of the lung under MV. The model developed is based on a well accepted physiology and dynamic mechanism of the lungs that contradicts traditional ideas of lung recruitment and expansion (Yuta, 2007). This new mechanism of lung recruitment and expansion is presented in this chapter. The PV curves that form the basis for identification of the patient – specific characteristics are also discussed with respect to their use in the model and their use in the clinical context of MV.

2.1 BREATHING CYCLES AND PV CURVES

Pressure volume (PV) loops are one of the fundamental pieces of data that are readily available to clinicians and illustrate lung characteristics over a breathing cycle (Hamilton Medical., 2006, Iotti and Braschi, 1999, Maquet Medical Systems., 2006). The pressure is typically measured either at the mouthpiece or directly at the ventilator. However, accurate lung pressure at the trachea can also be measured through specialized equipments and techniques (Karason et al., 1999). Clinicians often depend on the PV curves to estimate the recruitment status, lung conditions and response to therapy, and using this assessment set the ventilator accordingly. A typical PV curve is shown in Figure 2-1.

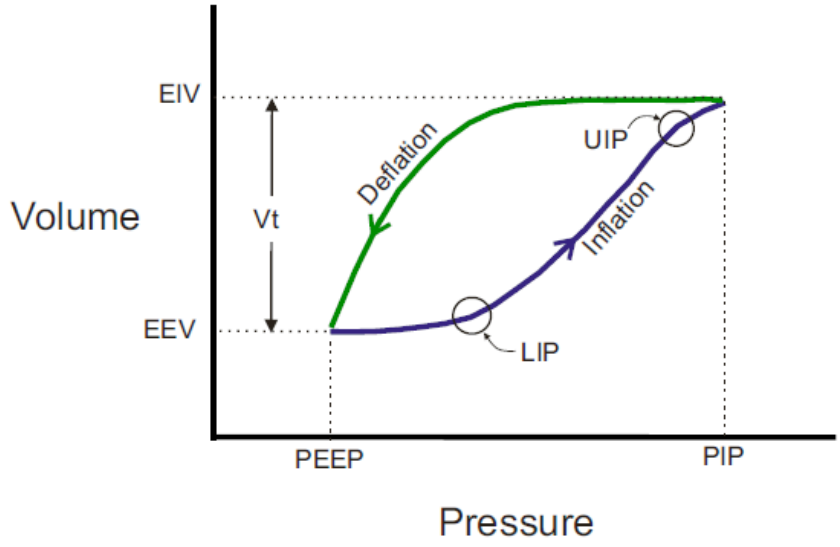

Figure 2-1: PV curve displaying inflation and deflation curves. The illustration shows a basic shape of a typical PV curve. PEEP = Positive End Expiratory Pressure, PIP = Peak Inspiratory Pressure, LIP = Lower Inflection Point, UIP = Upper Inflection Point, V_t = Tidal Volume, EIV = End Inspiratory Volume, EEV = End Expiratory Pressure

The inflation stage begins with a pressure build-up in proximal airways with no significant change in volume. This build-up is due to the presence of rigid cartilage in the airways that do not expand or stretch significantly. This portion corresponds to the low compliance area in the lower portions of the PV loop and also corresponds to the establishment of flow in MV. Once, enough pressure builds up, the air flows to the distal airways resulting in an increase in volume with increasing pressure. This increase is represented by the middle portion of the PV inspiration curve with higher compliance. The lung becomes stiff when the lung is inflated to near maximum capacity and the lung tissues are stretched at the end of inspiration. This corresponds to the low compliance area in the upper regions of the PV curve.

It can be observed that the inflation portion of the PV curve follows a sigmoid curve indicating a lower compliance at the lower and higher pressures and a higher compliance in the middle. The Lower Inflection Point (LIP) marked on the figure is the point where the slope of the curve is found to increase and the Upper Inflection Point (UIP) is the point where the slope of the curve decreases, or plateaus at higher pressures.

PV curves potentially indicate unique conditions of the patient and are readily available to the clinicians. Hence, they can be used for determining patient – specific MV treatment by

clinicians (Jonson and Svantesson, 1999, Jonson and Uttman, 2005). ARDS lungs are stiffer overall and have a lower functional volume compared to healthy lungs. A healthy lung also can be differentiated from an ARDS lung through its higher compliance and lower hysteresis. These differences can be observed through the PV loops, which indicate the aerated volume of the lung as a function of the applied pressure.

2.2 LUNG MECHANICS

In the traditional theory of lung mechanics, the expansion of the lungs was thought to be due to an isotropic balloon – like expansion of lung units (Hickling, 2002). The LIP was considered to be the point where a simultaneous massive recruitment of lung units occurs, followed by an isotropic balloon – like expansion of lung units, which corresponded to the high compliance region observed on the PV curves. The UIP was considered as the point where the overstretching of the simultaneously recruited lung units start to occur. This concept is illustrated in Figure 2-2.

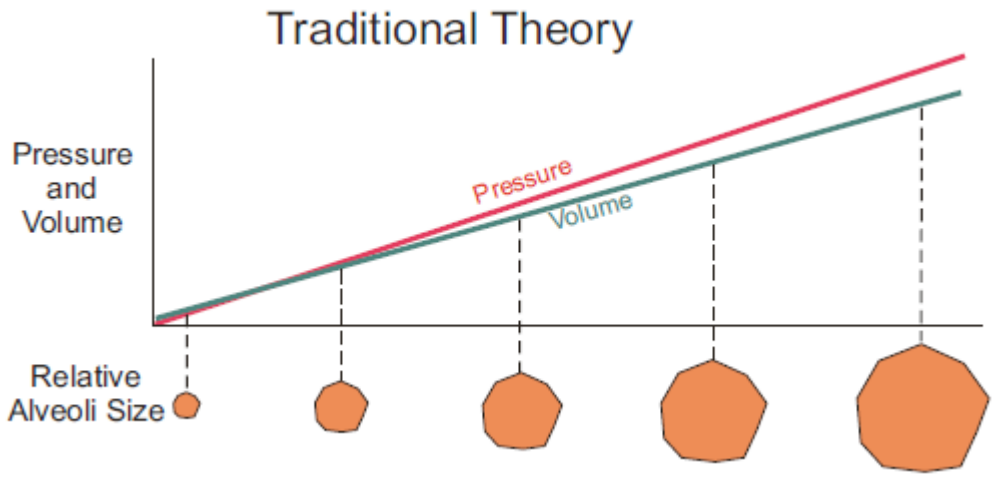

Figure 2-2: Traditional theory of lung expansion (Yuta, 2007)

However, this theory did not correspond well with observed clinical data (Hickling, 2002, Schiller et al., 2003). Recruitment and derecruitment of the lung units is thought to contribute greatly to the hysteresis observed on the PV curves (Cheng et al., 1995). It was also argued that the hysteresis observed in PV curves for different PEEP levels above LIP should be minimum and the PV curves should be superimposed on the inflation limb of the

total lung PV curve if LIP was the point of single massive recruitment of lung units. However, this behaviour is not observed clinically (Bersten, 1998).

Furthermore, it was also observed that recruitment of the lung units occurs throughout the inflation cycle, even above the LIP in several studies utilising CT scans (Albaiceta et al., 2004, Gattinoni et al., 2001, Pelosi et al., 2001). It was also observed that healthy lung units do not change in size significantly once they have been recruited (Schiller et al., 2003). Carney et al (Carney et al., 1999) used *in vivo* microscopy to study the mechanism of lung expansion in mongrel dogs. A steady increase in recruitment was observed as the lung volume was increased to 80% of the total lung capacity (TLC). Hence isotropic balloon – like expansion of the lung units was observed to contribute to only 20% of the TLC.

These studies led to development of a new theory of lung mechanics, summarised as follows:

- The air first enters the topmost region of the lungs through the upper airway where the superimposed pressure is negligible. The initial phase of the inhale cycle causes relatively small increase in volume due to the presence of stiffer airways (trachea, bronchi etc). This corresponds to the low compliance region observed in the lower portions of the PV curve.
- A derecruited lung alveoli is considered to have a volume of zero. When the applied pressure overcomes the superimposed pressure and the pressured required to recruit a lung unit, Threshold Opening Pressure (TOP), the lung unit is recruited or "pops" open. The superimposed pressure increases in the lower regions of the lung and a higher pressure is needed to be applied to recruit lung units in these regions. More lung units are recruited progressively with an increase in pressure to add a certain volume to the total until all the recruitable lung units within the applied pressure range are recruited. This is represented in Figure 2-3:

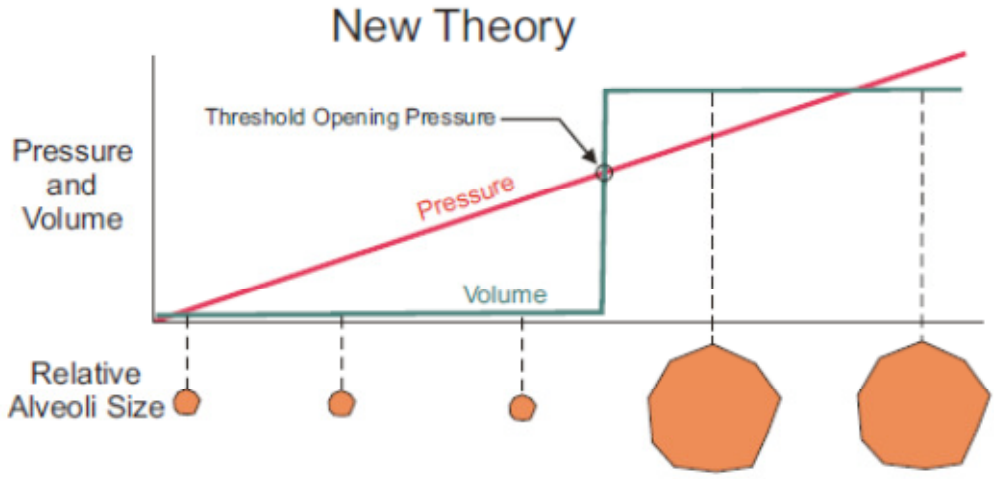

Figure 2-3: New theory of lung expansion based on recruitment and derecruitment of the lung units (Yuta, 2007)

The deflation process is the same as the inflation process. However, the pressures at which the lung units are derecruited or deflate at the Threshold Closing Pressure (TCP) are lower than the pressures at which they are recruited. The overall hysteresis observed in the PV loop is attributed to this nature of the alveoli.

2.2.1 RECRUITMENT AND DERECRUITMENT

ALI/ARDS is characterized by inflammation of the lungs and filling of the lungs with fluid. The surfactant that maintains the shape of the alveoli is also denatured and its production is reduced due to the inflammation. These changes cause the lung units to collapse and they cannot be recruited without external intervention.

As discussed in Section 2.2, recruitment of the lung units refers to the condition of the lung units when the applied pressure is higher than the TOP and the lung unit assumes a non-zero volume based on its characteristics, or the lung unit “pops open". The derecruitment of the lung unit refers to the condition of the lung unit when the applied pressure is lower than the minimum required pressure to hold the unit at a non-zero volume called the Threshold Closing Pressure (TCP). The lung unit assumes a zero volume or is “shut” close when derecruited.

The effect of PEEP on the recruitment status of the lung units can be understood by comparing the volume of the lung at a given pressure when exhaled to Zero End

Expiratory Pressure (ZEEP) and when PEEP is applied. It was found that the volume of the lung was higher under PEEP compared to ZEEP (Jonson and Svantesson, 1999). This increase in lung volume was evident even when the PEEP was set above the lower inflection point. This result further confirms that recruitment continues to occur above LIP. This conclusion was also directly confirmed through the use of Computer Tomography (CT) scans to study recruitment above LIP (Albaiceta et al., 2004, Gattinoni et al., 2001).

Cheng et al (Cheng et al., 1995) used excised rat lungs to study the energy required to rerecruit a collapsed lung unit. This was done by progressively increasing the end inspiratory pressure at the end expiratory pressures of -5 and 5 cm H_2O. It showed that additional energy was required to recruit alveoli but less energy was required to keep them inflated once they were recruited. Thus, this study emphasised the strong dependence of the recruitment and derecruitment on the End Expiratory Pressure (EEP). Overall , these studies have shown that recruitment of the lung units occurs throughout the inflation cycle, even above the LIP utilising CT scans (Albaiceta et al., 2004, Gattinoni et al., 2001, Pelosi et al., 2001) and the healthy lung units were not found to change in size significantly once they have been recruited (Carney et al., 1999, Schiller et al., 2003).

The recruitment and derecruitment of lung units as the major influence on volume change during tidal ventilation holds significance in ARDS patients since the severely affected lung units collapse and are "lost" to the disease and cannot be recruited without external intervention. This change in lung physiology affects the recruitment and derecruitment characteristics of the lung and ARDS affected lung characteristics are skewed compared to a healthy lung. The collapsed lung units do not participate in gas transfer, which leads to significant reduction in absorption of oxygen and expulsion of CO_2 from the body.

More specifically, the *in vivo* microscopic study by Schiller et al (Schiller et al., 2003) characterised the lung units in three categories based on the level of injury.

1. Type 1 alveoli do not collapse at the end of expiration and do not change in volume significantly during tidal ventilation. All the lung units in a healthy lung are Type 1 lung units.
2. Type 2 alveoli undergo a significant change in volume but do not derecruit at the end of expiration.

3. Type 3 alveoli undergo a significant change in volume during tidal ventilation and also collapse at the end of expiration cycle.

All three types of alveoli are present in a lung after denaturing of surfactant indicating that Type 2 and Type 3 alveoli are associated with ARDS affected lungs.

2.2.2 THRESHOLD PRESSURE DISTRIBUTIONS

The pressure at which a lung unit is recruited is termed as Threshold Opening Pressure (TOP) and pressure at which a lung unit is derecruited is called Threshold Closing Pressure (TCP). It is known that recruitment and derecruitment of lung units occurs throughout the breathing cycle and is not limited to LIP and UIP, as previously thought. The threshold pressures are influenced by several factors, such as the superimposed pressure and the characteristics of the lung unit (nature of the surfactant, oedema, inflammation etc).

Pelosi et al. (Pelosi et al., 2001) studied the mechanism of recruitment and derecruitment in ARDS affected lungs by inducing respiratory failure in dogs through oleic acid. Each dog was studied for a combination of V_t and PEEP levels, and the effect of pressures on recruitment was studied through CT scans at the end of inspiration and expiration cycles. They concluded that recruitment occurs continuously throughout the PV curve and that superimposed pressures play an important role in regional recruitment. They also found a strong correlation between the end inspiratory and end expiratory collapse of lung units suggesting that more lung units stay open at the end of expiration if more lung units are recruited at the end of the inspiratory cycle. Similar conclusions were drawn by the studies carried out by Crotti et al (Crotti et al., 2001) on ARDS/ALI patients.

An example of the TOP and TCP distributions obtained by Crotti et al are shown in Figure 2-4. Note that the mean of the TOP distribution is higher than the mean of the TCP distribution indicating a difference in the opening and closing pressures of a given lung unit on average. This corresponds with the hysteresis observed in PV loops.

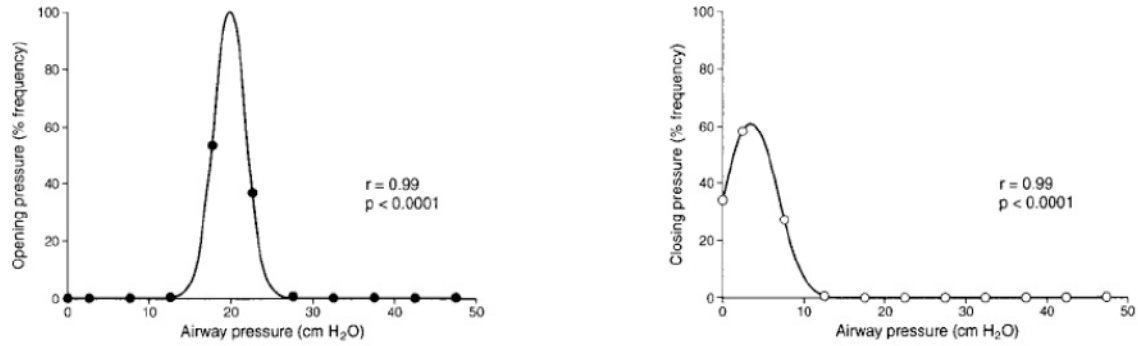

Figure 2-4: TOP (left) and TCP (right) distributions of patient 1 studied by Crotti et al.(Crotti et al., 2001)

THRESHOLD PRESSURE DISTRIBUTIONS IN NORMAL VS ARDS LUNGS

The TOP and TCP distributions are a direct result of the lung characteristics and hence can be used to assess and quantify a patient's lung condition. ARDS affected lung units tend to open or get recruited at a higher pressure compared to healthy lung units due to their physiological dysfunctions, such as oedema, inflammation and denaturing of the alveolar surfactant. This abnormality observed and the heterogeneous nature of ARDS can be represented by broader TOP distribution with the mean shifted towards higher pressure. This overall distribution captures the higher pressure required to inflate an ARDS affected lung to the same volume as a healthy lung. Similarly, the lung units tend to get derecruited at a higher pressure during exhalation cycle. This behaviour has a similar effect on the TCP distribution, as can be observed in the TOP distribution.

This is represented in Figure 2-5. These significant differences in the TOP and TCP distributions in ARDS affected lungs compared to healthy lungs can be utilized to characterize the severity of ARDS. Equally, changes in these distributions over time, based on regular assessment can enable the patient-specific monitoring of lung condition and disease state in response to therapy.

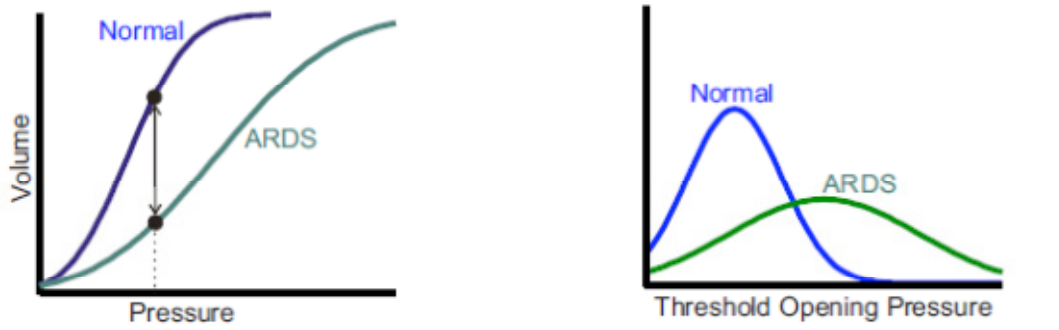

(a) An example of PV inflation curves for normal and ARDS lungs.

(b) An example of TOP distributions for normal and ARDS lungs.

Figure 2-5: ARDS affected lungs are stiffer and hence require higher pressures for inflation to similar volumes as a healthy lung. (b) A stiffer lung is represented by broader TP distribution (Yuta, 2007)

2.2.3 MODEL - BASED APPROACH TO DETERMINE OPTIMAL MV SETTINGS

The objective of MV is to assist patient breathing by partially or completely taking over the process of breathing. The primary focus is to maximise gas exchange, while minimising any further damage to the lungs. This goal is achieved in general through a bulk movement of air through the lungs by application of positive pressure to the airways and application of a suitable PEEP by the ventilator at a clinically acceptable tidal volume.

PEEP is important since ARDS affected lung units are vulnerable to collapse due to the extra pressure of the fluid and denaturing of surfactants that maintain the shape of the alveoli. PEEP prevents the collapse of lung units at the end of the exhale cycle and maintains a certain lung volume above the functional residual capacity (FRC). Application of high PEEP would maximise gas exchange, but would cause further unintended damage to healthy lung units. Thus, an optimum value of PEEP needs to be determined and constantly evaluated to provide optimal care in the face of ongoing evolution in the patient condition.

Currently, no ideal method exists to effectively determine MV parameters, and especially PEEP, based on the unique lung characteristics of the patient. Mathematical models that utilise the readily available data, such as PV data to determine the physiological

characteristics of the patient required by clinicians to determine the optimum MV settings offer a useful solution. These models add no burden to the clinical costs as they require no significant new hardware or systems, nor significantly added clinical time and effort.

RECRUITMENT MODELS

Recruitment models have been developed with the purpose of identifying the recruitment behaviour of the alveoli and to assist clinicians in setting the ventilator to enable maximum recruitment and maximise gas exchange. Hickling (Hickling, 1998, Hickling, 2001) developed a simple mathematical model to simulate and understand the shape of the PV curves in ARDS lungs based on the TOP and TCP distributions. Hickling modelled the lung as a cluster of lung units or alveoli with their compliance reducing with an increase in the applied pressure. The superimposed pressure was simulated by dividing the lung into a number of horizontal slices or compartments and each compartment associated with a certain superimposed pressure with the uppermost slice associated with a superimposed pressure of zero and the lowermost compartment associated with the maximum superimposed pressure.

The model determined the recruitment status of the alveoli based on the TOP and TCP distributions, which were uniformly distributed in the earlier model (Hickling, 1998) and normally distributed in the later model (Hickling, 2001). Unit volume was calculated using a linear PV relationship with slight adjustments at higher pressures in the original model (Hickling, 1998) and through the Salazar and Knowles (Salazar and Knowles J.H., 1964) equation in the new model (Hickling, 2001).

The model simulated the lung by estimating the volume of the lung at pressures between the applied PEEP and peak inspiratory pressure (PIP) using the entered TOP and TCP distributions, the superimposed pressure and the applied airway pressure values. The model determined whether the transalveolar pressure (applied pressure – superimposed pressure) was higher than TOP during the inflation cycle. The lung unit was considered as recruited if this condition was met and the alveolus was assigned a volume according to the unit compliance equation. During deflation, the transalveolar pressure was checked against associated TCP values. If the pressure was found to be below the TCP level, the lung unit was considered derecruited and assumed a volume of zero.

At an alveolar level, the *in vivo* microscopic study carried out by Schiller et al (Schiller et al., 2003) categorised lung units into three categories as discussed in Section 2.2.1. Yuta (Yuta, 2007) developed a mathematical model to simulate lung characteristics considering all three types of lung units. However, these models consisted of too many parameters for unique identification. Hence they were too complicated and not identifiable for clinical use. A final model was developed consisting of only one type of lung units for direct comparison to ventilator treatment and the lung characteristics directly exposed to the ventilator (Yuta, 2007).

2.3 SUMMARY

The lung mechanics modelled in this thesis are based on a newly emerging theory of lung inflation and deflation. Traditionally, isotropic balloon like expansion of the lung alveoli was thought to be the primary mechanism behind volume change. However, recent studies have questioned this traditional theory and suggest that recruitment and derecruitment of lung units are primarily responsible for the volume change observed over a breathing cycle in ARDS affected patients. It was also suggested that recruitment of lung units occurs throughout the inflation cycle in contrast to the traditional idea of LIP being a point of a single massive recruitment of lung alveoli.

This new theory was further strengthened by studies carried out using CT scans (Albaiceta et al., 2004, Gattinoni et al., 2001, Pelosi et al., 2001) and through *in vivo* microscopic studies carried out by Carney et al (Carney et al., 1999) and Schiller et al (Schiller et al., 2003). These studies showed that the recruitment and derecruitment of lung units occur throughout the breathing cycle and that once recruited, the lung units did not change in volume significantly with an increase in pressure.

More specifically lung expansion and contraction were found to be dependent on the threshold opening pressure (TOP) and threshold closing pressure (TCP) distributions of lung units. The lung units are recruited or “pop open” when the applied pressure exceeds the TOP during inflation. Similarly, the lung unit is derecruited or assumes a zero volume when the applied pressure falls below the associated TCP. The values of the threshold pressures are dependent on several factors, that represent the unique characteristics and condition of the lung unit, such as the superimposed pressure, oedema, inflammation and

condition of the surfactant. Since recruitment and derecruitment occurs throughout the breathing cycle, the TOP and TCP can take a range of values. Studies carried out by Pelosi et al (Pelosi et al., 2001) and Crotti et al (Crotti et al., 2001) proposed that the TOP and TCP values were distributed normally. More importantly, these distributions, if identified from data, capture patient-specific lung conditions.

Mechanical ventilation assists in patient breathing by completely or partially taking over the breathing process. The primary focus of MV is to improve recruitment of lung units and gas exchange while minimizing any further harm to the lungs (Ware and Matthay, 2000). However, incorrect ventilation settings can cause further unintended harm by the use of high air pressure (barotrauma) and high tidal volume (volutrauma). Hence, determination of optimum MV settings and continuous evaluation of these settings based on the changes in the patient's conditions is required.

Mathematical models created (Hickling, 1998, Hickling, 2001, Yuta, 2007) primarily are aimed at understanding ARDS. However emerging models (Sundaresan et al., 2011) are becoming more focused on providing tools to aid clinicians in determining optimum MV settings based on readily available data. These models analyse the recruitment status of the lung and can be used readily at the patient's bedside. The following chapters discuss such models developed to determine the optimum MV settings (primarily PEEP) and their clinical implications.

Chapter 3 - PV Data Measurement

3.1 PV DATA MEASUREMENT AND DISPLAY

PV curves form one of the fundamental pieces of data available to the clinicians to determine ventilator settings. The curves indicate the lung characteristics over an individual breathing cycle and are easily available from any modern ventilator (Hamilton Medical., 2006, Iotti and Braschi, 1999, Maquet Medical Systems., 2006). PV data can offer further important information on the recruitability of the lung when used in conjunction with recruitment models, such as those discussed in Chapter 2. Hence, one of the necessary goals of this project is to develop a simple and efficient method for accurate measurement and recording of PV data for analysis and model fitting, as many modern ventilators do not allow independent processing of PV data. The methods employed in this study are discussed in detail in this chapter.

3.1.1 DATA ACQUISITION (PNEUMOTACHOMETER)

The pressure (cmH_2O) and air flow rate (lpm) during a breathing cycle are measured at the mouthpiece (proximal pressure) of the patient using an instrument called a pneumotachometer (pneumotach). The pneumotach uses SensorTechnics RBI series pressure sensor to measure the pressure and SensorTechnics HCLA series miniature amplified low pressure sensors to measure flow rate. Volume is calculated by trapezoidal integration of flow over time.

More specifically, flow rate during tidal ventilation is calculated using the drop in pressure across a slit (orifice). A Hamilton single - use flow sensor, PN 279331, as shown in Figure 3-1 is used for this purpose. The pneumotach records the voltages corresponding to pressures P_1 and $(P_1\text{-}P_2)$. Pressure P_1 is the pressure applied to the airways and the differential pressure across the slit $(P_1\text{-}P_2)$ can be used to accurately determine the flow rate. The voltage values recorded for the differential pressure $(P_1\text{-}P_2)$ shall be treated as "flow" voltage and voltage values recorded for pressure P_1 shall be treated as "pressure voltage" henceforth.

The sensor is attached between the facemask/ET tube and the supply tubes with the two pressure tap-ins connected to the respective sensors in the pneumotach. The analog to digital (ADC) conversion is done using a National Instruments USB 6009 data acquisition system. National Instrument 2010 is used to acquire and store the data on personal laptop.

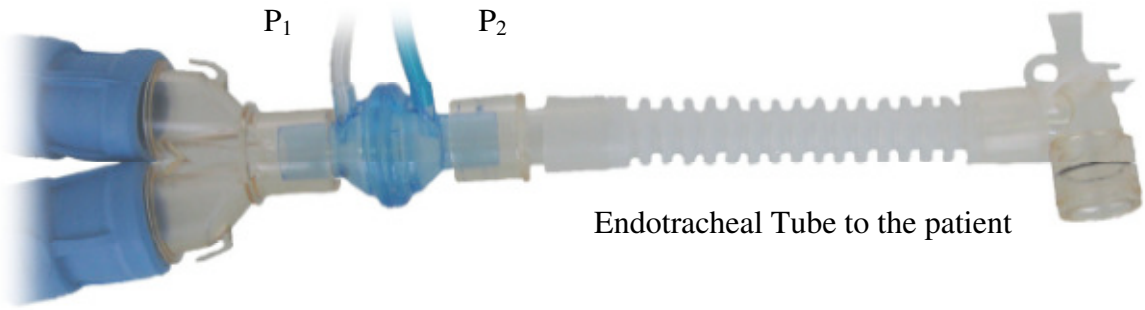

Figure 3-1: : Hamilton single use flow sensor - PN 279331 (Hamilton Medical.)

The voltage values recorded by the pneumotach are converted to their corresponding pressure and flow values using Equations 3.1 and 3.2.

$$Pressure = p_1 \times P_{voltage} + p_2 \quad (3.1)$$

$$Flow = f_1 \times F_{voltage} + f_2 \times Pressure + f_3 \quad (3.2)$$

The constants p_1, p_2, f_1, f_2 and $f_3$were determined experimentally.

EXPERIMENTAL CALIBRATION PROTOCOL TO DETERMINE FLOW AND PRESSURE COEFFICIENTS

Flow rates varying between 5 and 40 $\frac{l}{min}$ were passed through the Hamilton sensor, using a high flow device (rhotameter), at pressures varying between 5 and 40 cmH_2O. The corresponding pressure and flow voltage values were recorded by the pneumotach and substituted to Equations 3.1 and 3.2 to determine the pressure and flow coefficients.

The actual flow rate and pressure were monitored using the Performance Testing System *PTS 2000,* which allows measurement of flow rates between 0-300 lpm (under high flow conditions) and 0-150 cmH_2O pressure (under low pressure conditions). It was used in conjunction with a personal computer to display the actual flow rates and pressure in the

circuit using Puritan Bennett *Breathlab PTS*^{TM} software programme (Puritan Bennett Corporation, Pleasanton, CA, USA).

An example of the recorded voltages and corresponding flow and pressure values is shown in Figure 3-2. The pressure was maintained at 5 cmH_2O and flow was varied between 5-35 lpm with increments of 5 lpm. Figures 3-2 (a) and (b) show the flow and pressure voltages recorded respectively. Figures 3-2 (c) and (d) show the corresponding calculated flow and pressure values. A high chatter in the recorded data was observed for high flow rates but the average flow rate calculated was in compliance with the actual flow rate maintained in the system.

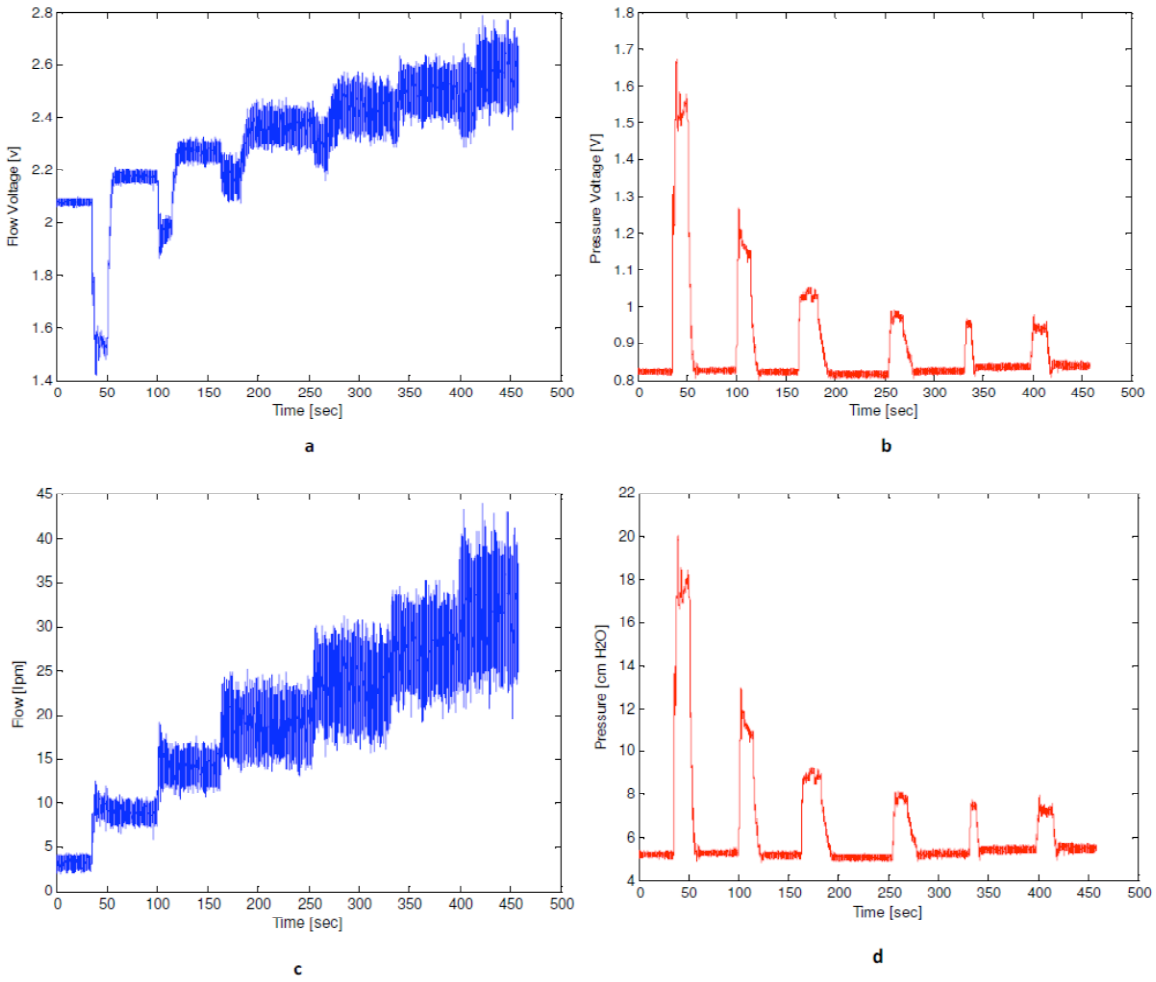

Figure 3-2: (a) flow voltage (b) pressure voltage (c) calculated flow using Equation 3.1 (d) calculated pressure using Equation 3.2

VALIDATION

Initial validation was carried out using a mechanical lung simulator (PneuView Dual Adult Training and Testing Lung), which mimicked the fundamental mechanics of a ventilated lung. Specific lung characteristics, such as the compliance and airway resistance could be varied using the variable position spring and variable parabolic resistors respectively to simulate a wide variety of lung conditions. The lung simulator is described in Figure 3-3.

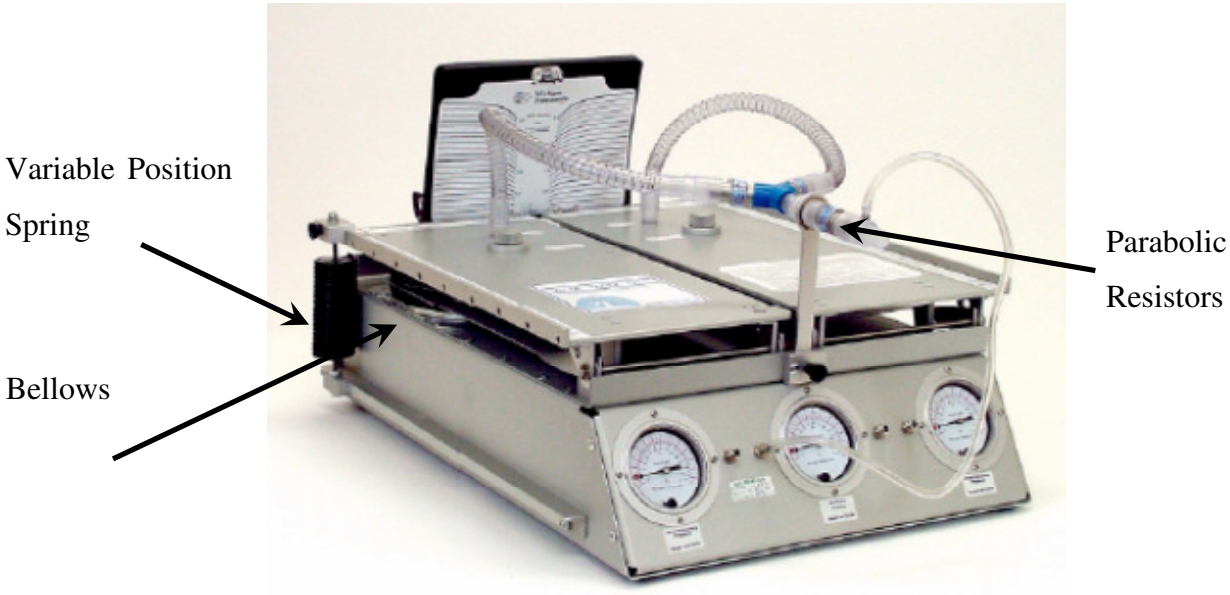

Figure 3-3: PneuView Dual Adult Training and Testing Lung. The lung compliance can be varied by changing the relative position of the springs on the sides of the lung and the different airway resistances can be simulated by changing the parabolic resistors

The mechanical lung simulator was ventilated using a Puritan Bennet PB840 ventilator (Covidien, Boulder, CO, USA). The ventilator was set to volume controlled mode with a square wave inspiratory pattern. The tidal volume was set between 350-400 ml which is a typical value. The mode of ventilation and the tidal volume were kept constant, while the PEEP and flow rate were varied. The flow and pressure voltage values were recorded by the pneumotach and were converted to their respective flow and pressure values using Equations 3.1 and 3.2, and the flow and pressure constants obtained. A standard Dell™ (Dell, Austin, TX, USA) laptop was used in conjunction with Labview 2010 (National Instruments, Austin, TX, USA) to acquire and store in a txt file.

An example of the recorded data is shown in Figures 3-4 and 3-5. Figure 3-4 shows the flow, and pressure, and Figure 3-5 shows the volume calculated over two breathing cycles. The PEEP was maintained at 10 cmH_2O and the maximum flow rate was set at 35 lpm during this particular breathing cycle in the calibration validation process.

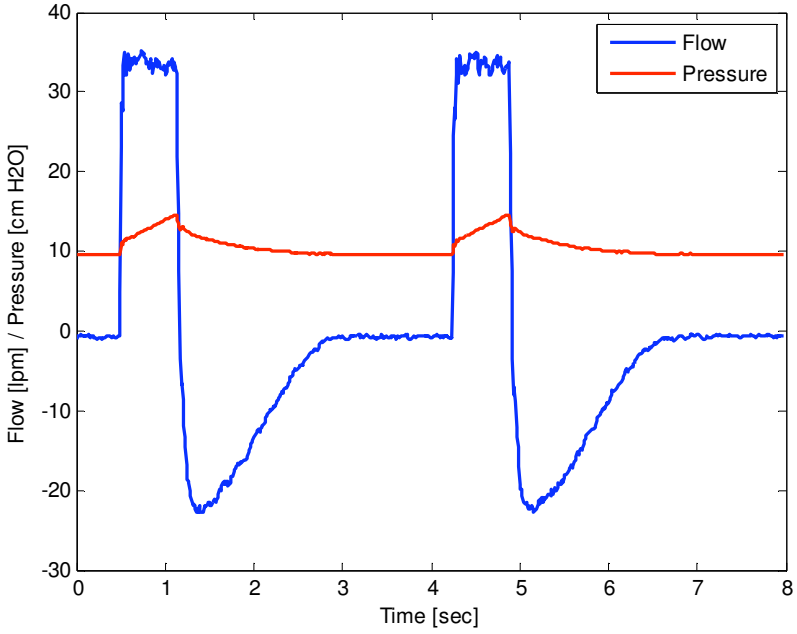

Figure 3-4: : Flow (lpm) and Pressure (cm H_2O) recorded during MV for 2 breathing cycles recorded

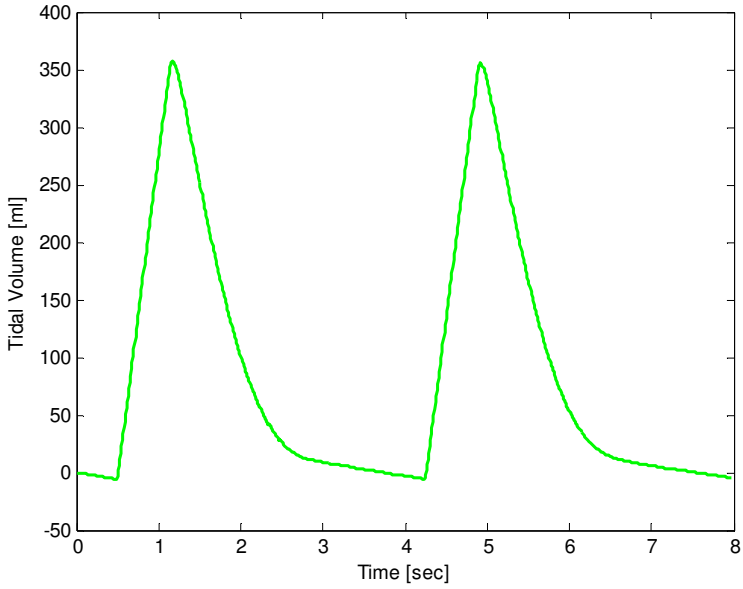

Figure 3-5: : Volume (ml) change during MV. The peak of the volume curve represents the tidal volume which is approximately 350 ml in this case

3.1.2 LIMITATIONS

PV data is measured proximally at the mouthpiece/ET tube since it is relatively non-invasive and does not require special equipment and techniques. The use of ET tubes for ventilation is common in ICU. The ET tubes are usually less than 1 cm in diameter and thus offer significant resistance to air flow in certain flow patterns (Karason et al., 2000, Karason et al., 2001). Thus the PV data recorded before the ET tube does not exactly reflect the true overall lung characteristics. This is illustrated in Figure 3-6 where the data measured before (at the mouthpiece) and after the ET tube (at the trachea) are compared. This effect is more prominent when the pressure is measured at the ventilator due to the extra resistance offered by the tubes from the ventilator to the mouthpiece.

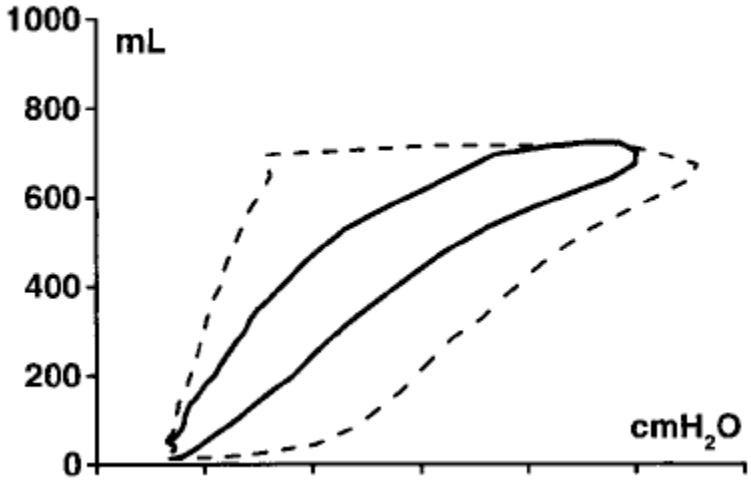

Figure 3-6: : Effect of ET tube on the PV loop. The outer loop (dotted line) shows the PV data recorded before the ET tube, and the inner loop shows the PV data measured after the ET tube (Karason et al., 2000)

The inspiratory cycle during tidal ventilation is controlled by applying positive pressure to the airways till either the pressure increases to a predefined maximum allowed PIP or a desired tidal volume is achieved depending on the mode of ventilation chosen. The exhalation cycle is essentially passive and lung is simply allowed to deflate to a predefined PEEP by removing the added pressure and flow. Thus the transition between inflation and deflation is highly dynamic as indicated by the sparsely distributed points in the transition region in Figure 3-7. This transition phase is prone to error due to the lack of sampled points and lack of sensor sensitivity at lower flows. Hence, this phase does not reflect the

true lung mechanics and the data acquired is noisy. This problem is overcome by fitting the model to about last 80-90% of the data during inflation and 80-90% during the deflation curve.

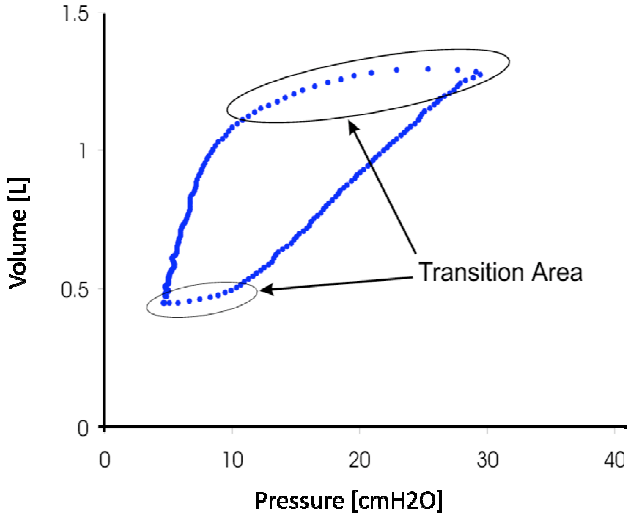

Figure 3-7: : Transition between inflation and deflation curves (Sunderesan, 2010, Yuta, 2007).

3.2 SUMMARY

PV data forms one of the fundamental pieces of data available to the clinicians to base their decisions on regarding MV. An effective and easy method of measuring the PV data and recording it in easily usable form (txt files) is developed as a necessary and fundamental part of this project. An instrument called Pneumotachometer (pneumotach) is used to measure the flow and pressure data at the patients mouthpiece (proximal data), which is safely and easily accessed, as well as typically used within the research field.

The pressure drop observed across a slit in a Hamilton single - use flow sensor is utilised to estimate the flow during MV. The pressure is measured right before the slit in the Hamilton sensor, which represents the true pressure applied to the airway. It should be noted that the pressure measured at the patient's mouthpiece would differ from the pressure measured at the ventilator. The pressure measured by the pneumotach would particularly be slightly lower than the pressure measured at the ventilator due to the resistance offered by the ventilator tubes to the airflow. Hence, it is a more relevant

representative value to use to assess patient-specific response. The method employed for measurement of flow and pressure, and the validation of this process is discussed in detail in the chapter.

However, the procedure detailed in this chapter has certain limitations. The effect of resistance to flow rate due to the ET tube is neglected in the PV data measured here. The ET tubes are usually less than 1 cm in diameter and thus offer significant resistance to air flow in certain flow patterns (Karason et al., 2000, Karason et al., 2001). Another drawback observed is the presence of a highly dynamic transitional area between inspiration and expiration cycles. This problem is overcome by fitting the recruitment model to approximately last 80-90% of the inflation and deflation data which represent the more densely populated data points.

.

Chapter 4 - Model-Based dFRC

The data obtained by Bersten et al (Bersten, 1998) required deflation of the lung to FRC to capture the pulmonary lung volume above FRC due to PEEP (dFRC). This method is invasive and sudden deflation of the lungs to atmospheric pressure can prove harmful to ARDS patients. Thus, dFRC offers useful clinical information regarding the recruitability of the lung, but is not normally measured at the patient's bedside. A model - based approach to determine the dFRC is presented in this chapter.

4.1 MODEL BASED DFRC

Functional Residual Capacity (FRC) represents the pulmonary lung volume when exhaled to atmospheric pressure or Zero End Expiratory Pressure (ZEEP). Application of PEEP prevents the lung from deflating to the FRC and maintains a certain volume of air above the FRC inside the lung at the end of the exhale cycle. This additional volume of air above the FRC is the dynamic functional residual capacity (dFRC), and includes FRC as shown in Figure 4-1.

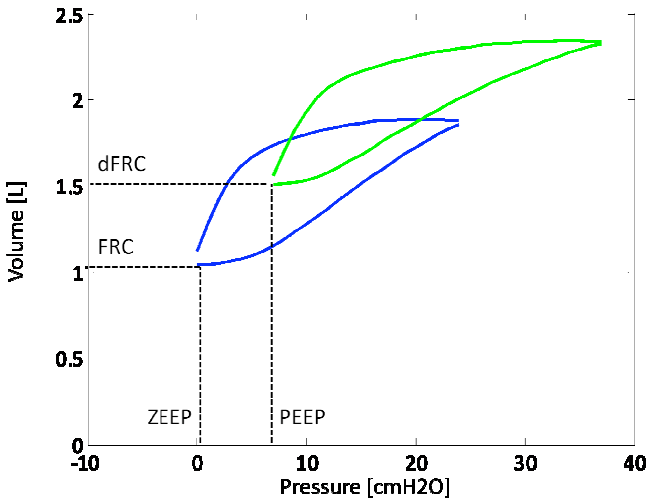

Figure 4-1: PV loops showing FRC and dFRC

Currently, there are few techniques that can be used to measure dFRC. Computer Tomography (CT) scans timed at the end of expiration allows accurate assessment of alveolar recruitment and FRC/dFRC (Gattinoni et al., 2001, Malbouisson et al., 2001). This method has limited or no clinical application since it requires transport of the patient out of the ICU, disconnecting the patient from the ventilator and exposure to radiology. Other methods used include, washin/washout of tracer gases (Heinze et al., 2007, Olegard et al., 2005) which is not readily available in most ventilators. Specialised ventilators [GE Ventilators (GE Healthcare., 2006)] allow FRC measurement and can re – estimate FRC with PEEP changes, but most standard ventilators do not have this facility. Thus, in these situations, there is no practical method that can be used to estimate dFRC at the patient's bedside. In addition, existing methods require intervention of the clinicians and do not allow for continuous tracking of dFRC, which could change with evolution of the patient's condition and thus provide added useful data to guide decision making and treatment if automatically measured at regular intervals. Hence, dFRC value offers clinicians useful information regarding lung recruitability. The model proposed here does not calculate the absolute value of dFRC but captures it effectively by estimating the extra volume in the lung above FRC due to PEEP.

4.1.1 MODEL SUMMARY

Sundaresan et al (Sundaresan et al., 2011) developed a model to estimate dFRC based on the stress – strain approach proposed by Chiumello et al (Chiumello et al., 2008), which studied the relationship between the global stress and strain within the lung during MV. The proposed model required PV data at a minimum of two different PEEP levels to determine the necessary lung characteristics. This requirement limited its application in continuous monitoring of dFRC. A new model and method are proposed in an attempt to overcome this limitation. The new model is based on a similar approach followed by Sundaresan et al (Sundaresan et al., 2011) and is discussed in detail in this chapter.

Chiumello et al (Chiumello et al., 2008) studied the relationship between global stress and strain within a lung during MV. Their study considered patients in four subgroups: Control Subjects (patients after elective surgery excluding thoracic and abdominal surgery), intensive care patients with medical diseases, patients with ALI (Acute Lung Injury), and patients with ARDS. The stress-strain relationship is defined by Equation 4.1:

$$stress = k \times strain \qquad (4.1)$$

Where k is the constant of proportionality (Modulus of Elasticity in the traditional stress-strain approach).

Chiumello et al (Chiumello et al., 2008) proposed the Transpulmonary Pressure (ΔP_L), defined as the airway pressure minus the pleural pressure, as the clinical equivalent of stress, and the ratio of the change in volume (ΔV) to FRC as the clinical equivalent of strain. FRC represents the volume during which the fibres of the lung skeleton are in their natural "resting" position and the respiratory muscles are relaxed. Hence FRC was considered as the reference volume to calculate the applied strain to the lung. The linear relationship between the lung stress and strain was thus defined:

$$\Delta P_L(Stress) = E_{LSpec}(Specific\ Lung\ Elastance) \times \frac{\Delta V}{FRC}(Strain) \qquad (4.2)$$

The proportionality constant ,E_{LSpec} (Specific Lung Elastance), can be defined as the Transpulmonary Pressure at which the change in volume (ΔV) is equal to the FRC. The specific lung elastance was found to be similar in the four groups studied by Chiumello et al (Chiumello et al., 2008) and were reported as 13.4 ± 3.4 cmH_2O in control subjects (group 1), 12.6 ± 3.0 cmH_2O for intensive care patients with medical diseases (group 2), 14.4 ± 3.6 cmH_2O for patients with ALI (group 3) and 13.6 ± 4.1 cmH_2O for patients with ARDS (group 4). Hence, the study indicated that the specific lung elastance does not vary significantly within subgroups.

The relationship between the transpulmonary pressure (stress) and the plateau airway pressure ΔP_{aw} is further defined:

$$\Delta P_L(Stress) = \Delta P_{aw}\ (Plateau\ Airway\ Pressure) \times \propto \qquad (4.3)$$

$$\propto = \frac{E_L}{E_L + E_{cw}} \qquad (4.4)$$

Where α represents the static lung elastance, defined by the Lung Elastance (E_L) and the Chest Wall Elastance (E_{CW}). It was observed in Chiumello's study that patients in the ALI/ARDS subgroups reached higher values of $\propto$ compared to the other two groups. However, the $\propto$ values for individual regressions were not found to differ significantly in the four groups and were reported as 0.69 $\pm$ 0.15 in the surgical control subjects (group 1),

0.74 ± 0.16 for intensive care patients with medical diseases (group 2), 0.64 ± 0.15 in the subgroup of patients with ALI and 0.71 ± 0.16 in the ARDS subgroup.

Chest wall elastance plays an important role in MV as part of the airway pressure applied is used to inflate the lungs and the rest is utilized to overcome chest wall pressure. This relation is schematically shown in Figure 4-2. It can be observed that the total elastance is the same in both the cases shown in Figure 4-2. Case (a) is typical of ARDS patients where a stiffer lung is represented by the higher lung elastance compared to case (b), which shows a healthy lung. Hence, the value of α indicates the severity of ALI or ARDS, where a higher value of α indicates a higher severity of ARDS.

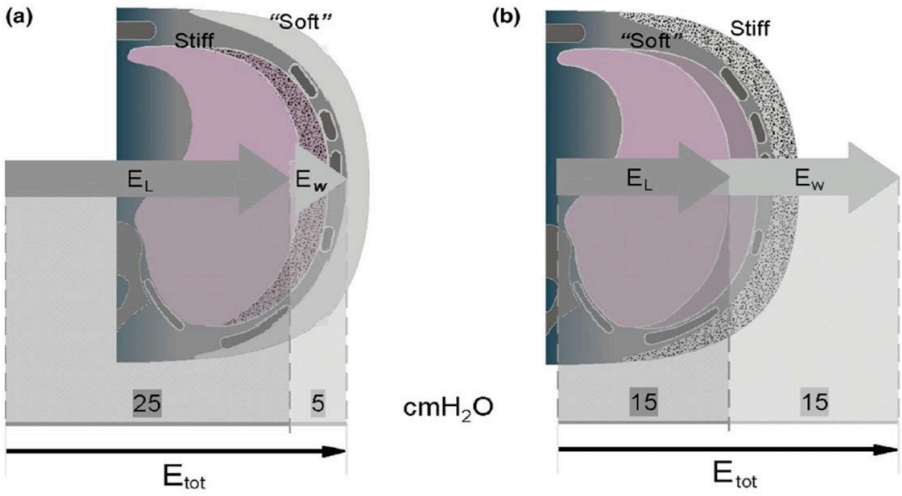

Figure 4-2: Effects of different lung and chest wall elastance (Gattinoni et al., 2004)

Combining Equations 4.2 and 4.3 yields:

$$FRC = \frac{\Delta V}{\Delta P_{aw}} \times \frac{E_{Lspec}}{\propto} \qquad (4.5)$$

Equation 4.5 defines FRC as a function of the compliance ($\frac{\Delta V}{\Delta P_{aw}}$) of the lung, E_{Lspec} and α of the patient.

The dFRC is the volume contained within a lung comprising of the Function Residual Capacity (FRC) and the additional volume at the end of expiration due to the application of PEEP. The dFRC increases with an increase in the PEEP applied. This concept is used in

recruitment manoeuvre where additional PEEP is applied to recruit extra lung units. Some of the re-inflated lung units remain open when the additional PEEP is removed. This change helps increase the FRC of the patient. Thus, the dFRC at this stage includes the FRC, the additional volume due to the applied PEEP and the extra volume at that PEEP resulting from the recruitment manoeuvre.

Importantly, the FRC component is not estimated in the model proposed here and was also not included in the clinical data obtained. The change in the FRC due to the recruitment manoeuvre is also not considered as it is very difficult to measure independently in typical clinical situations. The model solely aims at estimating the increase in dFRC value due to PEEP. Since FRC is considered as the reference volume in this study but is not estimated or measured, it can be considered zero for each patient without compromising the clinical significance of the model. Hence, the additional volume in the lung calculated by the model is expressed as dFRC for simplicity here on. However, it should not be confused with absolute dFRC discussed earlier.

It was hypothesised that dFRC follows a similar mathematical form as Equation 4.5. Hence, the total lung volume under PEEP at the end of expiration, End Expiratory Volume (EEV), can be defined as:

$$FRC + dFRC = \frac{\Delta V}{\Delta P_{aw}} \times \frac{E_{Lspec}}{\propto}(1 + x) \qquad (4.6)$$

dFRC in Equation 4.6 represents the additional volume in the lung due to PEEP.

Equation 4.6 defines dFRC as:

$$dFRC = \frac{\Delta V}{\Delta P_{aw}} \times \frac{E_{Lspec}}{\propto} x \qquad (4.7)$$

Where x is a function of the PEEP level at which dFRC is estimated. As presented earlier, $\propto$ and E_{LSpec} values were relatively constant throughout the groups studied by Chiumello et al (Chiumello et al., 2008) and can be combined into one parameter, β, yielding:

$$dFRC = \frac{V_t}{\Delta P_{aw}} \times \beta \qquad (4.8)$$

Where ΔV is replaced by tidal volume, V_t and β is a function of the PEEP, E_{Lspec} and $\propto$. The assumption that α is constant is true only for the linear portion of the PV loop (Sundaresan et al., 2011).

Sundaresan et al (Sundaresan et al., 2011) proposed a model to estimate dFRC defined as:

$$dFRC = \frac{\Delta dFRC}{\Delta PEEP} \times \beta \qquad (4.9)$$

It should be noted that the β values defined in Equations 4.8 and 4.9 are different and represent different values due to the different approach in calculation of the compliance in the two models. Sundaresan et al (Sundaresan et al., 2011) hypothesised that the value of β for a particular level of PEEP stays constant throughout the entire population for the corresponding level of PEEP. This hypothesis is maintained in this model as well.

METHODS

Retrospective data recorded by Sundaresan (Sunderesan, 2010) was obtained for a total of 9 patients. The demographics of the 9 patients are shown in Table 4-1.

Table 4-1: Characteristics of patients studied

	Sex	**Age [years]**	**Cause of lung injury**
Patient 1	Female	61	Peritonitis
Patient 2	Male	22	Trauma
Patient 3	Male	55	Aspiration
Patient 4	Male	88	Pneumonia
Patient 5	Male	59	Pneumonia
Patient 6	Male	69	Trauma
Patient 7	Male	56	Legionnaires
Patient 8	Female	45	Aspiration
Patient 9	Male		H1N1

The patients were characterised by different levels of lung injury and included PV data for each patient for at least 3 PEEP levels. The PV data for each patient analysed in this research corresponds to an average breath observed for each PEEP level. The data did not contain information on the FRC of the lung but contained information on additional volume due to PEEP for each patient at each PEEP level.

Since the FRC values were not known, $\frac{E_{Lspec}}{\propto}$ could not be estimated. Instead, the values of β were analytically calculated using Equation 4.8 for each PEEP level and for each patient. Calculated β values were normalized by the respective tidal volumes (V_t) as dFRC can vary with the V_t applied, yielding:

$$\beta_1 = \frac{\beta}{V_t} \qquad (4.10)$$

A median β_1 value was then calculated for each PEEP level over all patients, and used as a population constant for the particular PEEP level. This approach mirrors that followed by Sundaresan et al (Sundaresan et al., 2011).

The individual β_1 values along with the median β_1 values for each PEEP and the interquartile range (IQR) are shown in Table 4-2. The dFRC value for each PEEP level for each patient was then re-calculated by substituting the corresponding median β_1 value in Equation 4.8 and multiplying the resulting value with the applied V_t. Percentage errors between the estimated and measured dFRC values were calculated and presented as median and IQR, as shown in Table 4-3. The estimated vs. the measured dFRC values is presented in Figure 4-5.

It can be observed from Equation 4.8 that the value of β is dependent on the lung compliance ($\frac{V_t}{\Delta P_{aw}}$). The lung compliance was observed to change with a change in PEEP in many patients. This can be clearly observed in Figure 4-3 that shows the PV data for Patient 1 at different PEEP levels. The lung compliance is observed to decrease at higher PEEP levels indicating overstretching of lung units at these PEEP levels. In particular the compliance observed for the middle PEEP levels which are most likely to be used clinically are relatively constant.

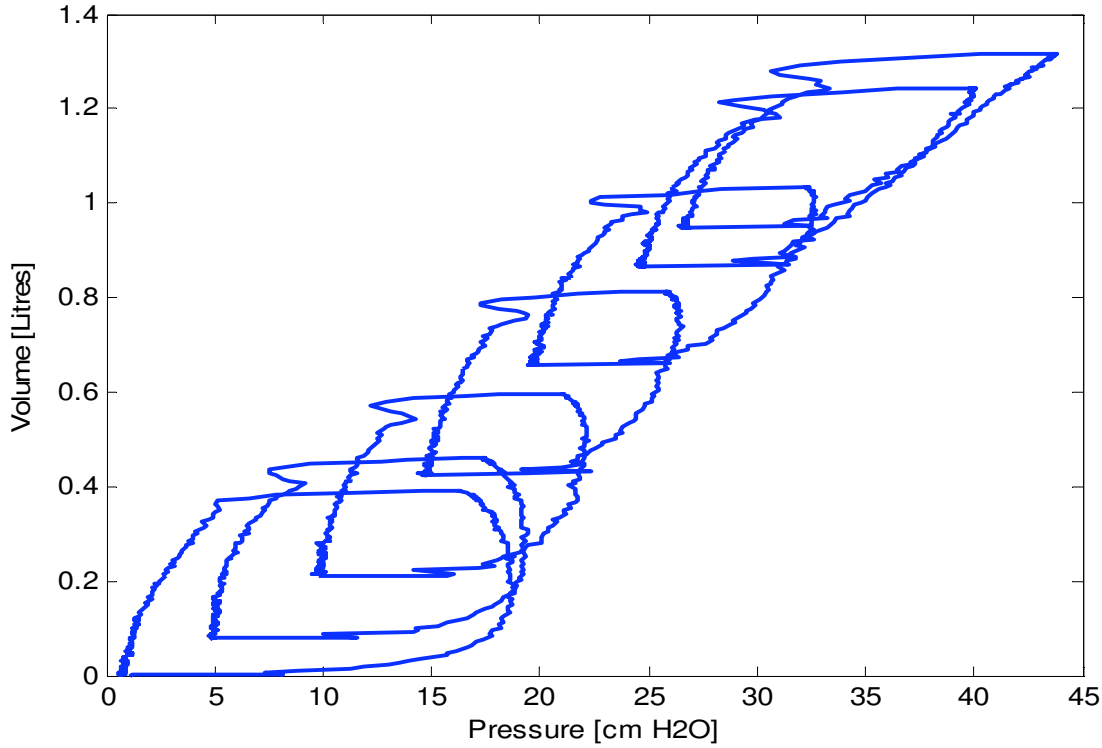

Figure 4-3: P-V loops indicating change in lung compliance with PEEP for the same patient. The compliance is observed to decrease with increase in PEEP

Hence, a representative breath, with plateau airway pressures normally observed in clinical settings was selected to calculate the lung compliance for each patient. The representative breath offered an accurate assessment of the lung compliance compared to the compliance observed in individual breaths, especially at lower and higher PEEP levels. The β values were recalculated for each PEEP level by substituting the lung compliance observed in the representative breath. Equation 4.8 was thus modified to Equation 4.11.

$$dFRC = \left(\frac{V_t}{\Delta P_{aw}}\right)_{rep} \times \beta_{rep} \qquad (4.11)$$

Where $\left(\frac{V_t}{\Delta P_{aw}}\right)_{rep}$ is the lung compliance observed in the representative breath chosen and β_{rep} is the corresponding β value calculated for each PEEP for each patient.

The β_{rep} values were analytically calculated using Equation 4.11 and V_t normalised to yield a new set of β_1 (β_{1rep}) values yielding :

$$\beta_{1rep} = \frac{\beta_{rep}}{V_t} \qquad (4.12)$$

Median β_{1rep} values were calculated and were used to estimate the dFRC values by substituting the median β_{1rep}values in Equation 4.11 and multiplying the resulting value with the corresponding V_t applied. The β_{1rep} values along with their median and IQR are detailed in Table 4-4. The percentage errors observed between the estimated and measured dFRC values are presented in Table 4-5. The estimated vs. the measured dFRC is shown in Figure 4-7.

Hence, two sets of β_1 values were calculated, 1) using the lung compliance observed in individual breaths for a patient (β_1) and 2) using the lung compliance observed in the representative breath chosen for each patient (β_{1rep}). The dFRC values for each PEEP level for each patient were calculated using the corresponding median β_1 values for both sets separately.

4.1.2 RESULTS

Table 4-2 shows the analytical solution for β_1 calculated for the lung compliance observed in individual breaths during MV. The median β_1 values for each PEEP level and the interquartile range are also shown. Figure 4-4 shows the variation of median β_1 with respect to PEEP:

Table 4-2: β_1 values calculated for each patient based on the compliance observed in individual breaths during MV, where 4_2 and 6_2 are second trial on the same patient 3 and 8 days later respectively

PEEP [cm H_20]	5	10	15	20	25	30
Patient						
1	0.0067	0.0153	0.0317	0.0611	0.0963	
2	0.0085	0.0208	0.0374	0.0607		
3	0.0078	0.0188	0.0386	0.0686	0.1045	
4	0.0020	0.0072	0.0214	0.0358	0.0547	0.0805
5	0.0040	0.0061	0.0132	0.0310	0.0544	
5_2		0.0070	0.0194	0.0494	0.0711	
6	0.0112	0.0243	0.0438	0.0758	0.1107	
6_2	0.0132	0.0348	0.0689	0.1127		
7	0.0209	0.0493	0.0880			
8	0.0108	0.0234	0.0387	0.0573	0.0825	0.1108
9	0.0074	0.0083	0.0195	0.0270	0.0544	0.0819
Median	0.0082	0.0188	0.0374	0.0590	0.0768	0.0819
IQR	0.0067, 0.0112	0.0075, 0.0241	0.0200, 0.0425	0.0358, 0.0686	0.0546, 0.1004	0.0809, 0.1036

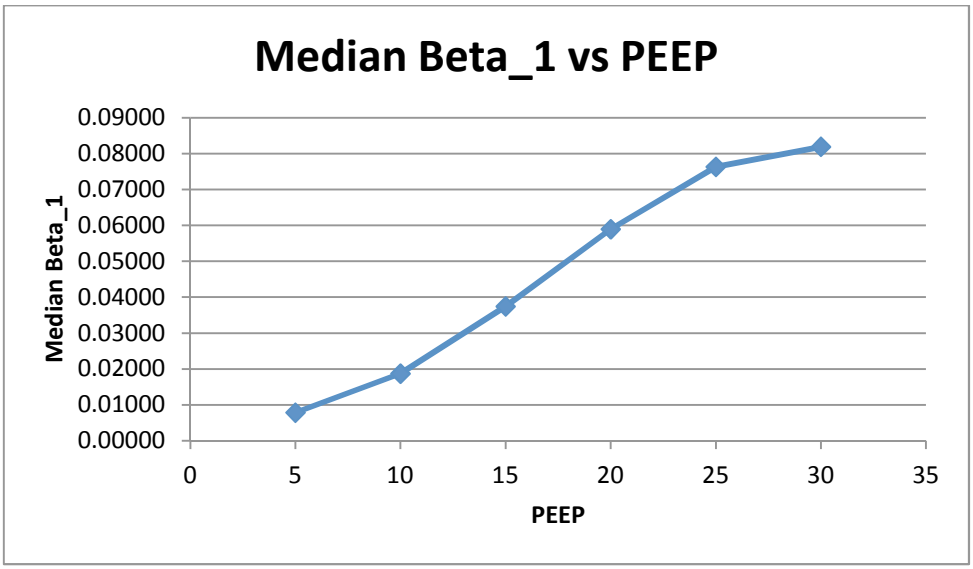

Figure 4-4: Median β_1 with respect to PEEP applied

Figure 4-5 shows the general trend observed between the estimated and measured dFRC values with R^2 value of 0.730. It should be noted that the dFRC estimated is based on the lung compliance observed in individual breaths during MV, which may vary with PEEP as discussed earlier. Percentage errors between the estimated and measured dFRC values were calculated and are presented in Table 4-3. The median and IQR of the percentage errors are also presented.

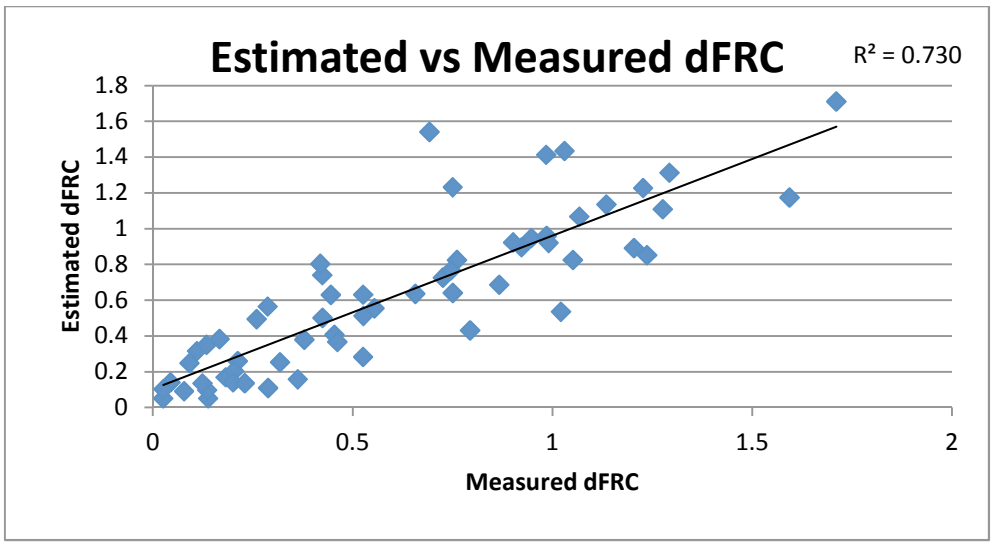

Figure 4-5: Estimated vs. Measured dFRC. The dFRC estimated is based on lung compliance observed in individual breaths during MV

Table 4-3: Percentage error between the estimated and measured dFRC values. The dFRC estimated is based on lung compliance observed in individual breaths during MV

PEEP [cm H_20]	5	10	15	20	25	30
Patient						
1	16.45	22.91	17.10	3.34	20.20	
2	7.86	9.79	0	2.80		
3	0	0	2.92	14.01	26.47	
4	292.97	162.18	74.78	64.67	40.33	1.82
5	96.17	209.62	183.46	90.62	41.21	
5_2		169.85	92.61	19.43	7.98	
6	30.30	22.57	14.59	22.18	30.59	
6_2	40.43	45.89	45.69	47.62		
7	62.54	61.83	57.46			
8	27.39	19.53	3.39	2.96	6.88	26.05
9	6.36	126.85	91.56	118.52	41.27	0
Median	28.84	45.90	45.69	20.80	28.53	1.82
IQR	7.86, 62.54	20.29, 153.31	6.19, 87.37	3.34, 64.67	14.09, 40.77	0.45, 19.10

Table 4-4 shows the analytical solution for β_{1rep} calculated for the lung compliance observed in the representative breath chosen. The median β_{1rep} values for each PEEP level and the interquartile range are also shown. The variation in β_{1rep} with respect to PEEP is

shown in Figure 4-6 which shows a more linear relationship compared to that observed in Figure 4-4.

Table 4-4: β_{1rep} values calculated for each patient based on the compliance observed in the representative breath chosen for each patient, where 4_2 and 6_2 are second trial on the same patient 3 and 8 days later respectively

PEEP [cm H_20]	**5**	**10**	**15**	**20**	**25**	**30**
Patient						
1	0.0058	0.0160	0.0317	0.0513	0.0679	
2	0.0083	0.0209	0.0338	0.0480		
3	0.0085	0.0231	0.0385	0.0546	0.0678	
4	0.0013	0.0070	0.0214	0.0352	0.0442	0.0542
5	0.0029	0.0051	0.0130	0.0307	0.0545	
5_2		0.0059	0.0190	0.0355	0.0512	
6	0.0105	0.0235	0.0399	0.0548	0.0657	
6_2	0.0132	0.0303	0.0456	0.0589		
7	0.0189	0.0387	0.0484			
8	0.0098	0.0233	0.0385	0.0545	0.0733	0.0892
9	0.0057	0.0076	0.0195	0.0322	0.0454	0.0606
Median	0.0084	0.0209	0.0328	0.0480	0.0545	0.0606
IQR	0.0057, 0.0105	0.0072, 0.0235	0.0200, 0.0396	0.0352, 0.0546	0.0483, 0.0678	0.0558, 0.0821

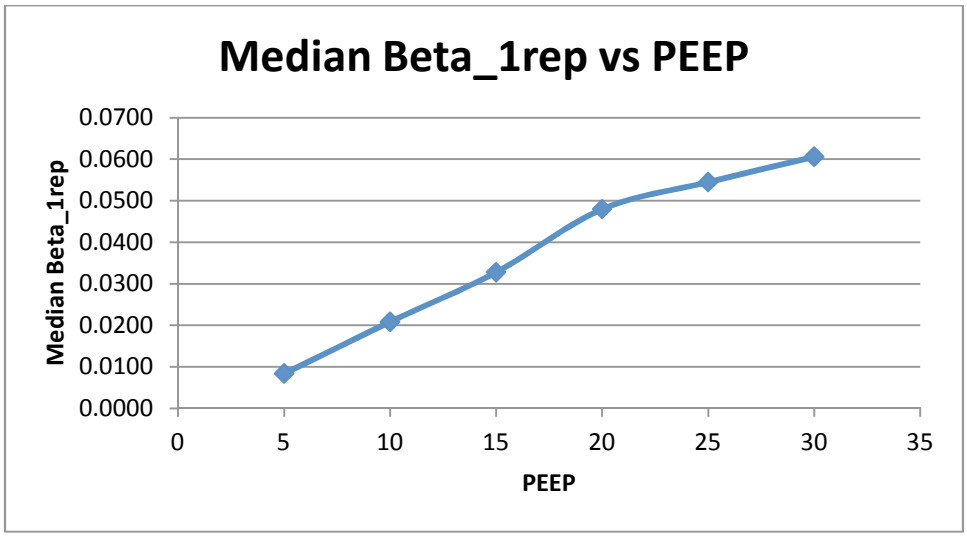

Figure 4-6: Median β_{1rep} with respect to PEEP applied

Figure 4-7 shows the general trend observed between the estimated and measured dFRC value with R^2 value of 0.862. It should be noted that the dFRC estimated is based on the lung compliance observed in representative breath chosen for each patient and median β_{1rep} values. Percentage errors between the estimated and measured dFRC values were calculated and are presented in Table 4-5. The median and IQR of the percentage errors are also presented.

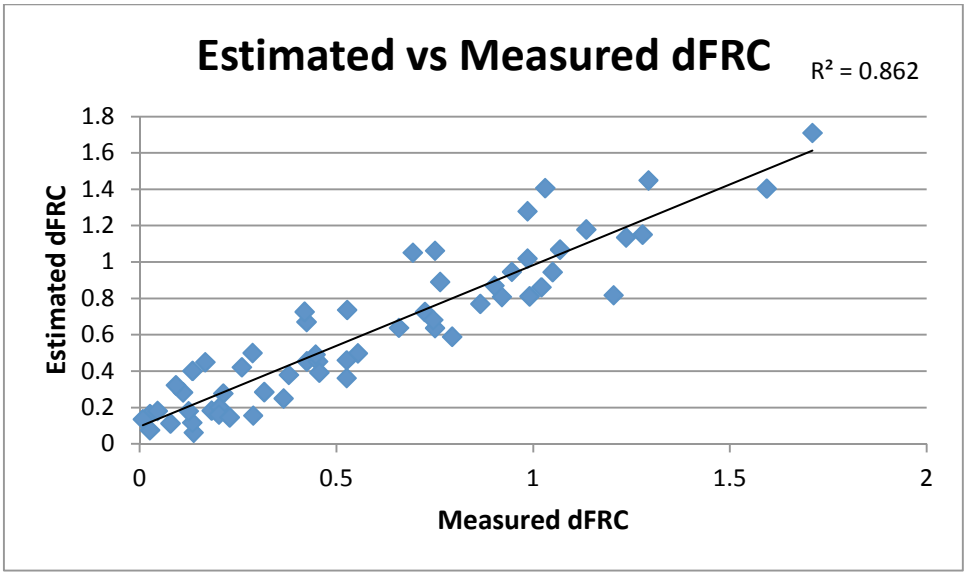

Figure 4-7: Estimated vs. Measured dFRC. The dFRC estimated is based on lung compliance observed in the representative breath chosen for each patient.

Table 4-5: Percentage error between the estimated and measured dFRC values. The dFRC estimated is based on lung compliance observed in the representative breath chosen for each patient.

PEEP [cm H_20]	5	10	15	20	25	30
Patient						
1	44.18	30.65	14.00	6.42	19.75	
2	0.94	0.00	6.87	1.12	0.00	
3	0.93	9.50	6.17	12.15	19.7	
4	527.41	198.63	68.62	36.18	23.22	11.78
5	192.84	311.93	177.03	56.35	0.00	
5_2		253.81	89.93	35.28	6.38	
6	19.93	11.16	9.42	12.40	17.05	
6_2	36.40	31.12	20.80	18.48		
7	55.39	46.06	25.27			
8	14.20	10.32	6.04	11.92	25.68	32.74
9	47.96	174.96	85.20	48.96	19.96	0.06
Median	40.29	31.12	20.8	15.44	19.7	11.78
IQR	14.20, 55.39	10.53, 192.71	7.51, 81.06	11.92, 36.18	4.79, 20.76	2.99, 27.5

4.1.3 DISCUSSION

The model presented was developed to estimate the dFRC as a function of PEEP using only readily available PV data without interrupting MV treatment. It estimates dFRC using the compliance observed. Overall, dFRC offers important information on the status of the lung and recruitability, and can be tracked continuously as it changes with the evolution of the disease using a model based approach.

The model uses the overall stress-strain approach proposed by Chiumello et al (Chiumello et al., 2008). It also extends a model previously proposed by Sundaresan et al (Sundaresan et al., 2011) using a similar overall approach. This model is an extension to these previous efforts as it utilizes lung compliance instead of a more difficult to measure volume responsiveness of the lung to a change in PEEP. Hence, it can be employed using bedside PV loop measurements with no added intervention or interruption. In particular, only a single PEEP value is required rather than two or more, which requires interrupting MV therapy.

The patients considered in this study were ventilated at a wide range of PEEP levels, which were often outside the pressure levels normally observed in a clinical setting. This aspect resulted in variable lung compliance values observed for the same patient for different PEEP levels, particularly at high and low PEEP extremes. Hence, a representative breath was chosen for each patient to estimate the lung compliance expected to be observed in normal clinical settings to take the variability in lung compliance values into consideration. This approach provides a closer estimate of the dFRC values compared to individual breaths as can be clearly observed in Figures 4-5 and 4-7, and is clinically acceptable as several breaths can be averaged.

The dFRC values observed were also dependent on the tidal volume applied during MV. dFRC was generally found to be higher for patients where a higher tidal volume was used for similar PEEP and lung compliance values. One of the shortcomings of the model proposed by Sundaresan et al (Sundaresan et al., 2011) was that the effect of tidal volume on dFRC was not considered. This enhanced model takes the effect of tidal volume on dFRC into consideration using Equations 4.10 and 4.12.

It can also be observed that median β_{1rep} shows a linear trend with respect to PEEP as observed in Figure 4-6. This linear trend can be used to estimate the median β_{1rep} values at different PEEP levels, which, in turn, can be used to estimate the dFRC values at those PEEP levels. Figure 4-8 shows the trend observed between the estimated and measured dFRC values calculated using the estimated β_{1rep} obtained from the linear relationship observed in Figure 4-8 with R^2 value of 0.85. Importantly, while errors exist, it is not necessarily clinically significant. Thus, this approach could show very good resolution, based on these results, in tracking dFRC and thus guiding clinical decision making.

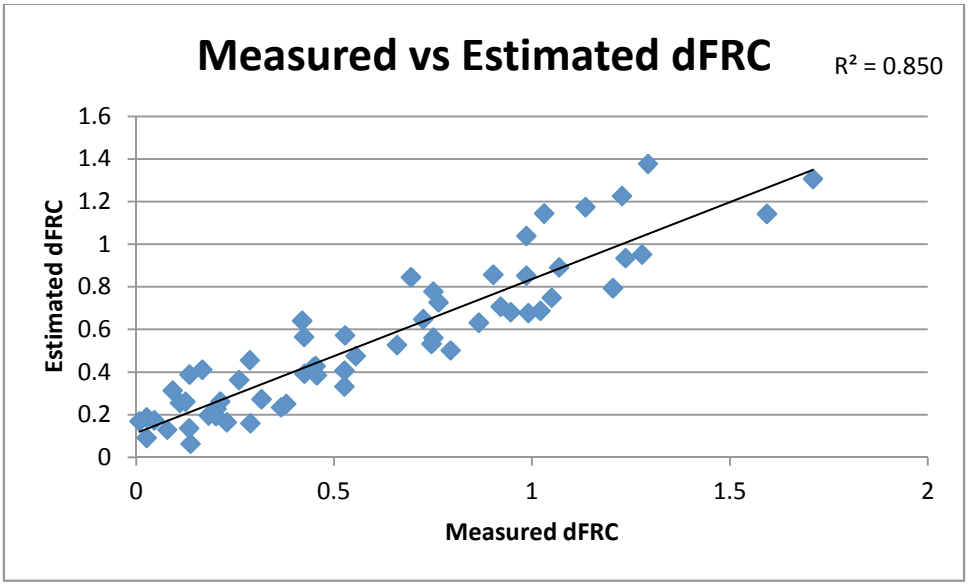

Figure 4-8: Estimated vs. Measured dFRC values using estimated median β_{1rep} values against observed median β_{1rep} values used previously

LIMITATIONS

The model has some limitations in its predictive capabilities. In some cases, the percentage error observed between the estimated and observed dFRC values was extremely high. Larger errors were primarily found at very low PEEP levels of 5 cmH_2O, which is less common in MV therapy in critical care. Large estimation errors can limit the use of this model for estimating the recruitment potential of the lung. However, median percentage errors were found to be between 20-45% in individual breaths and 10-30% in

representative breaths studied. Importantly, these errors were generally lower as PEEP rose into ranges where dFRC would be clinically more useful.

Equally, it was observed that the estimated dFRC follows a similar trend with respect to PEEP as the measured dFRC. Hence, in spite of high error values, the model is still capable of predicting the general trend in dFRC with respect to PEEP. This aspect is exampled in Figure 4-9, which shows the measured and estimated dFRC values for Patient 4 (representative breath) where the percentage errors observed were high.

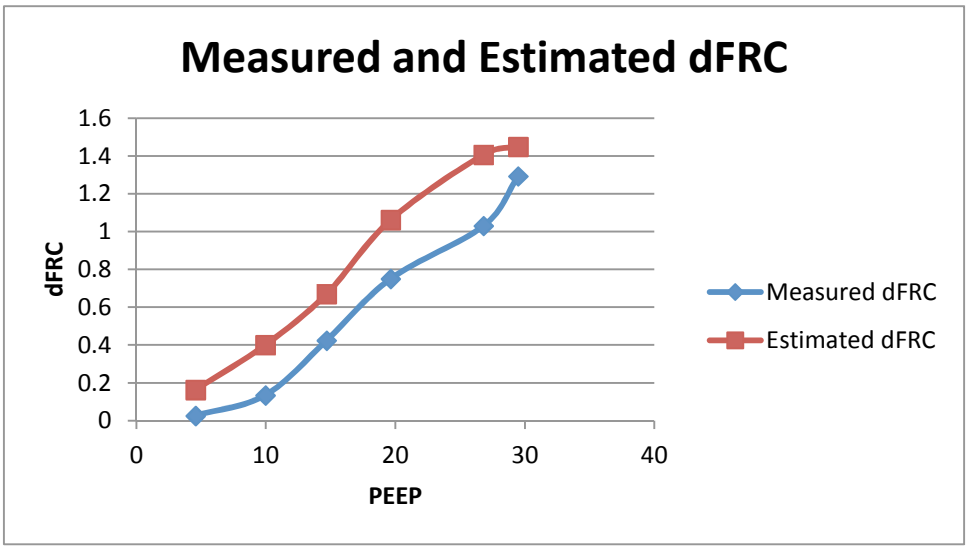

Figure 4-9: Measured and Estimated dFRC values for Patient 4 (Representative breath only)

Another limitation of this model is the assumption that the specific lung elastance E_{Lspec} and α remain constant. It should be noted that these values remain constant over the linear portion of the PV curve. The compliance calculated is expected to follow the linear portion of the PV curve, but this assumption may not always be true. It is possible that changes in compliance observed in measured PV loops could be used to scale these errors and further improve accuracy of the model.

4.2 SUMMARY

The model uses the lung stress strain theory proposed by Chiumello et al (Chiumello et al., 2008) to estimate the dFRC at any given PEEP level which considered transpulmonary pressure (ΔP_L) as the clinical equivalent of stress and the ratio of volume change to FRC ($\frac{\Delta V}{FRC}$) as clinical equivalent of strain. The model utilises a parameter, β_1/β_{1rep}, along with observed lung characteristics, such as the lung compliance to evaluate the dFRC. Validation of the model carried out on clinical data showed that the model offers an easy and reliable method to estimate dFRC values over a range of PEEP levels and the assumption that β_1/β_{1rep} values stay constant throughout the population for a particular PEEP level holds true in general. The limited number of datasets used in this validation implies further validation is required to justify the use of β_1/β_{1rep} as population constants.

The lung compliance was observed to change with PEEP as expected at very high or low PEEP levels for a given patient. Specifically, it was found to be lower at higher PEEP levels as observed in Figure 4-3. This could be attributed to reduction in recruitment at high pressures and overstretching of already recruited lung units when the lung is ventilated near its inspiratory capacity. Hence, two sets of β_1 values were evaluated for the patients studied. One set represented the lung characteristics observed in the PV data recorded for each breath irrespective of the PEEP level it was recorded at (β_1) and the other set represented the lung characteristics observed in a representative breath chosen (β_{1rep}) specifically to identify overall lung characteristics and eliminate variability in the lung characteristics observed. It was observed that the model was more effective when used with the lung characteristics observed in the representative breath compared to individual breaths recorded.

The predictive capability of the model was found to be limited at very low PEEP levels. However, such low PEEP levels are usually not observed in normal clinical settings. The error between the estimated and measured dFRC values was generally found to reduce with an increase in PEEP. Thus, the model was successful in capturing the trend of change in dFRC with PEEP in most cases and provided a useful real – time metric.

Chapter 5 - Recruitment Model

The recruitment model developed by Yuta (Yuta, 2007) used in this study is introduced in this chapter. A preliminary validation of the model was carried out by Sundaresan (Sunderesan, 2010) using the clinical data recorded by Andrew Bersten (Bersten, 1998).

5.1 MODEL SUMMARY

The recruitment model proposed by Yuta (Yuta, 2007) is based on previous models proposed by Hickling (Hickling, 1998, Hickling, 2001). It models the lung as a collection of lung units, comprising of a cluster of alveoli and/or distal airways. The number of units can be varied depending on the desired resolution. The superimposed pressure, which is the pressure resulting from the weight of the lung at different depths is captured in the model by dividing the lung into several horizontal layers. Each layer of the lung corresponds to a certain value of the superimposed pressure, depending on its relative position. The compartment at the bottom experiences the maximum superimposed pressure and the top layer experiences minimum superimposed pressure. Figure 5-1 shows the model schematically.

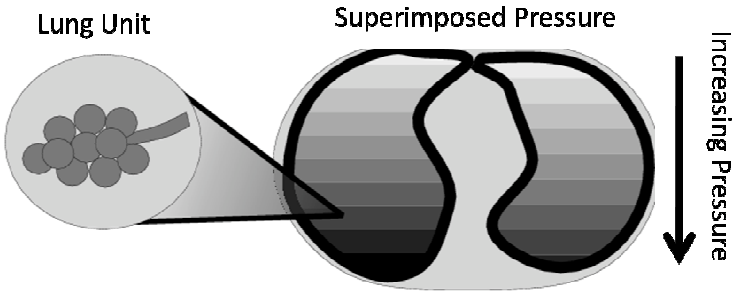

Figure 5-1: The lung modelled as a cluster of units. The units are distributed into the horizontal layers/compartments which allow modelling of the superimposed pressure (Yuta, 2007)

The model considers recruitment and derecruitment as the major cause of volume change during tidal ventilation. When the pressure in any lung unit exceeds the corresponding

threshold opening pressure (TOP), the lung unit "pops" open or is recruited. Similarly, when the pressure in any lung unit falls below the threshold closing pressure (TCP) the lung unit closes or is derecruited. This dynamic is illustrated in Figure 5-2. The TOP and TCP can be different for each lung unit due to the heterogeneous nature of ARDS. The lung units are thus recruited and derecruited at different pressures. The threshold pressures can be widely distributed over a range as a result.

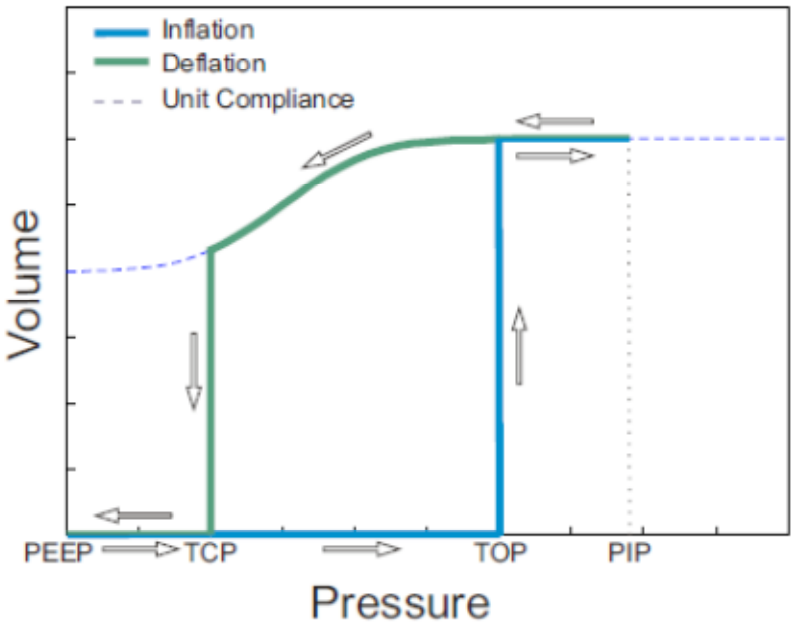

Figure 5-2: PV mechanics of a single lung unit (Yuta, 2007)

5.1.1 MODEL PARAMETERS

The two major parameters considered in the model are 1) Unit Compliance and 2) Threshold Pressure Distribution.

UNIT COMPLIANCE

The Unit Compliance describes the volume of the lung unit once it is recruited at any given pressure above the TOP. The volume of a derecruited lung unit is zero based on the new theory of lung mechanics discussed in Chapter 2. The unit compliance curve is described as a sigmoid curve (Venegas et al., 1998):

$$V(P) = a + \frac{b}{1 + e^{(-P+c)/d}} \tag{5.1}$$

Where V is the unit volume, P is the pressure, a is the minimum volume of a recruited lung unit, b represents the maximum volume, c represents the midpoint and d represents the curvature. The minimum possible volume of a recruited lung unit physiologically represents the Functional Residual Capacity (FRC) of that unit. The maximum volume is the largest physiologically possible volume of a lung unit above the TOP and thus, in summation over the model, also controls the maximum possible total lung volume. A unit compliance curve based on the Venegas equation (Venegas et al., 1998) is represented in Figure 5-3.

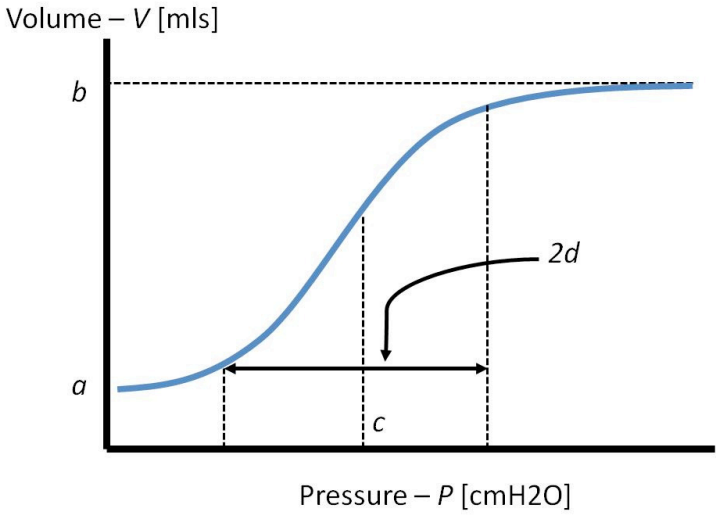

Figure 5-3: Unit Compliance curve using Venegas equation (Sunderesan, 2010)

It can be observed that the lung unit shows low compliance at low and high pressures and has a high compliance region in the middle. The inflation of a lung unit is analogous to inflation of a balloon, where initially the pressure increases without much increase in volume which is followed by a sudden increase in volume with relatively small pressure increase when a certain pressure is reached and stretching of the lung unit at high pressure corresponding to the low compliance.

The model considers recruitment and derecruitment of the lung units as the predominant cause of volume change and hence unit compliance is not expected to play a significant role in model fitting and lung characteristics.

5.2 THRESHOLD PRESSURES (TOP/TCP)

Any given lung unit has only two possible states at any given pressure: 1) recruited or 2) derecruited. The recruitment and derecruitment of the lung units in the model are governed by the TOP and TCP distributions respectively.

Studies carried out by Pelosi et al (Pelosi et al., 2001) and Crotti et al (Crotti et al., 2001) showed that recruitment and derecruitment occur throughout the PV curve and that the TOP and TCP were normally distributed. Hence, the threshold pressure distributions are modelled as a Gaussian function that can be described by two parameters: 1) mean (μ) and 2) standard deviation (SD). The TOP and TCP distributions are influenced by several factors including superimposed pressure and the characteristics of the lung units. Hence, the mean and SD values describing threshold pressure distributions can be used to uniquely identify a patient's condition.

This distribution is well known and the equation is simple to use. The equation for Gaussian distribution is defined:

$$N(P) = \frac{1}{SD\sqrt{2\pi}} e^{\frac{(P-\mu)^2}{2SD^2}} \tag{5.2}$$

Where $N(P)$ is the number of units, P is the pressure (normal physiological pressure range of 0-60 cm H_2O is used), μ is the mean, SD is the standard deviation of the distribution. These parameters are shown in Figure 5-4.

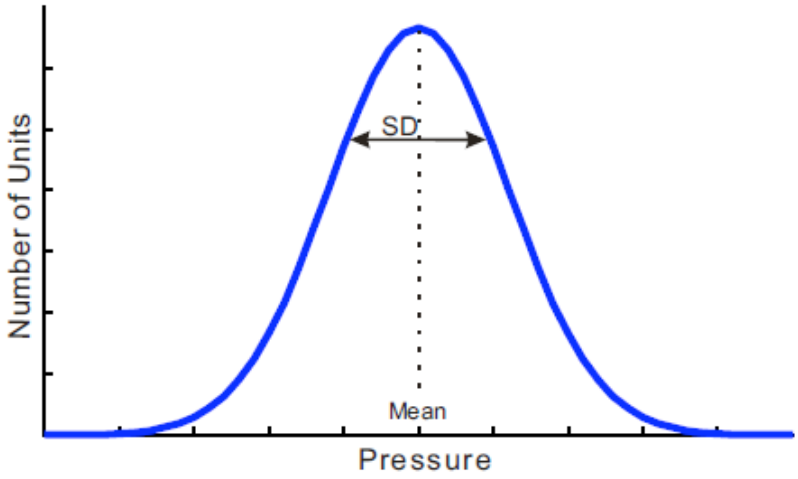

Figure 5-4: E.g. of normal (Gaussian) distribution of threshold pressure. (Yuta, 2007)

5.2.1 THRESHOLD PRESSURE DISTRIBUTION PARAMETERS AND THEIR PHYSIOLOGICAL INTERPRETATION

The normal distribution function described by Equation 5.2 can be defined by two parameters, mean and SD. These parameters and their physiological relevance are discussed in this section.

MEAN

The mean in a Gaussian distribution represents the point where the maximum value occurs. The mean values of the TOP and TCP distributions represent the pressures at which the rate of recruitment and the rate of derecruitment are maximum respectively (Yuta, 2007).

ARDS affected lungs are stiffer compared to healthy lungs and thus require a higher pressure to inflate to a similar volume. This characteristic of ARDS affected lungs can be represented by shifting the mean of the TOP distribution towards higher pressure. Similarly, lung units tend to get derecruited at a higher pressure during the exhale cycle. This behaviour can again be represented by shifting the mean of the TCP distribution towards a higher pressure. This effect is shown in Figure 5-5.

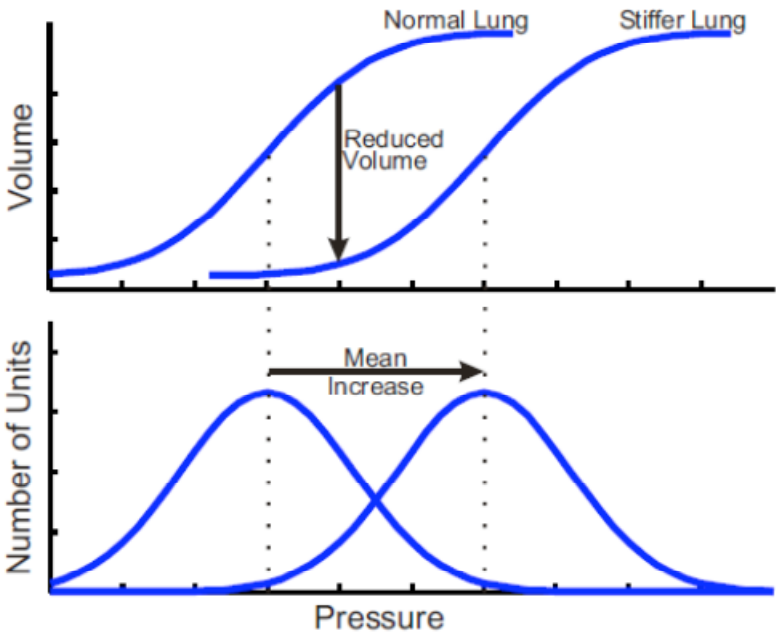

Figure 5-5: ARDS affected lung represented by an increase in mean. The increase in mean of the TP distributions results in shifting of the PV loop towards higher pressure (Yuta, 2007)

STANDARD DEVIATION (SD)

The standard deviation describes the shape of the distribution with higher SD values representing a broader distribution. About 68% of the population is within one standard deviation of the mean and 99.7% within three standard deviations. A low SD in the TOP distribution indicates rapid recruitment with increase in pressure and thus a higher lung compliance. Equally, a high SD indicates lower compliance and a stiffer lung.

An ARDS affected lung unit is recruited at a higher pressure compared to a normal lung unit. This results in a stiffer lung and thus a lower compliance compared to a healthy lung. The result is a broader set of threshold pressure distributions compared to a healthy lung. This behaviour is illustrated in Figure 5-6.

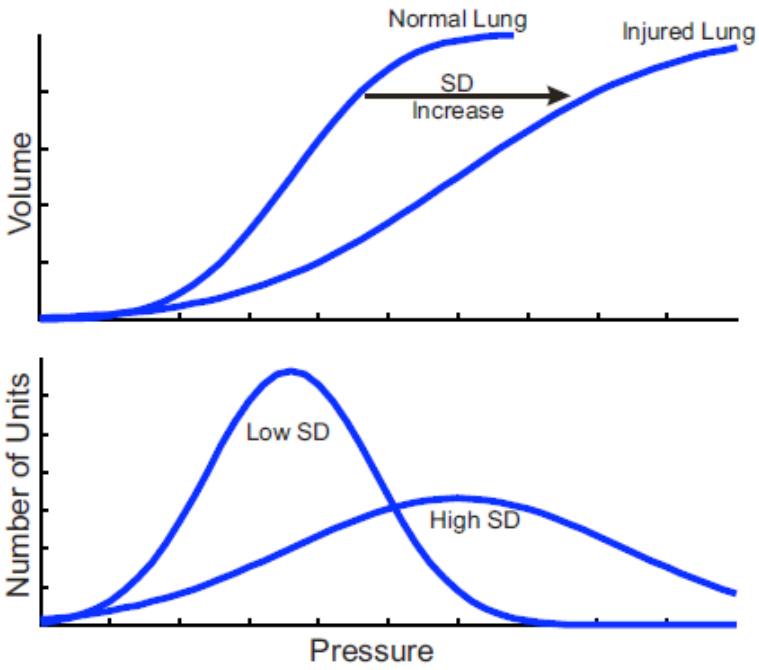

Figure 5-6: ARDS affected lung represented by an increase in SD. The increase in SD indicates a reduction in compliance and hence a stiffer lung (Yuta, 2007)

5.2.2 PHYSIOLOGICAL MODELS

Three physiological models were developed by Yuta (Yuta, 2007) based on the parameters described in prior sections. The first model developed was the most detailed model which included three different types of lung units as described by Schiller et al (Schiller et al., 2003, Yuta, 2007). Distal airways were also considered as separate lung units in this model making a total of 4 types of lung units considered. Each unit type was associated with its own unit compliance and threshold pressure distribution (Yuta, 2007).

This full physiological model was described by 12 parameters per unit type per respiration limb. Hence a total of 48 parameters were required to describe this model. Identification of most of these parameters was found to be impractical under normal clinical settings making the use of the model unfeasible (Yuta, 2007).

The second model developed by Yuta considered only two types of lung units, healthy and ARDS effected. This simplification reduced the physiological accuracy compared to the first full physiological model. However, this change also reduced the number of parameters

to be uniquely identified to a total of 20. This model was also found to be impractical to use due to the large number of parameters to be identified (Yuta, 2007).

The third and final model developed consisted of a single lung unit type and could potentially be described by two parameters per respiration limb, mean and SD for the TOP and TCP distributions. This model further simplified the parameter identification by allowing calculation of some of the parameters directly from the PV data (Yuta, 2007). The unit compliance curve defined in this model does not exhibit hysteresis in individual lung units and the influence of the unit compliance on lung mechanics is considered small compared to recruitment and derecruitment. Thus the hysteresis observed in PV curve is caused in this model by the difference in the TOP and TCP distributions. The final model is considered in this thesis and fitting of the patient data shall be done using this model.

5.2.3 MODEL FITTING AND PARAMETER IDENTIFICATION

The unit compliance and threshold pressure distributions are described by a set of governing equations and parameters. These parameters are determined by fitting the model to the clinical data available. The parameters that produce the best fit represent lung conditions unique to the patient and state of the disease. The method of fitting the model to the clinical data is based on simulating the entire inspiratory capacity of the lung and thus also shows the ventilated volume relative to the potential inspiratory capacity of the lung. This approach also minimises the exposure to the transitional and dynamic region of the PV curves since the model is fit to approximately last 80 - 90% of the data in the inspiration cycle and 80 - 90% of the data in exhale cycle. An example of the fitting approach is shown in Figure 5-7.

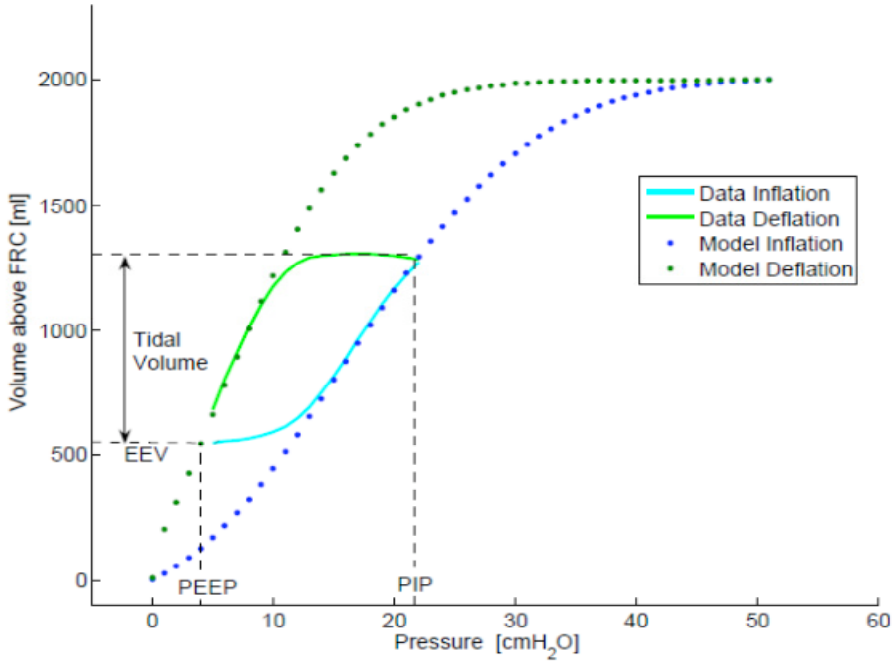

Figure 5-7: E.g. of the model fit. The plot shows the modelled inflation and deflation and the data for inflation and deflation. The model fits the entire lung capacity (Yuta, 2007)

The minimum and maximum threshold pressures are set at 0 and 60 cm H_2O, respectively. The volume ranges from FRC to the total inspiratory capacity. The inflation and deflation limbs are generated by different independent parameters and hence can be fitted separately.

The model is based on the new theory of lung recruitment that hypothesises that recruitment and derecruitment of lung units primarily contribute to volume change (Carney et al., 1999, Hickling, 2002) and that the contribution of the unit compliance is less significant in the overall PV curve. Hence the parameters defining the unit compliance curve can be fixed at generic population values. However, these parameters were fit iteratively through grid-search in the model presented in this thesis for greater physiological accuracy.

The other parameters that define the model are:

- TOP distribution Mean
- TOP distribution SD
- TCP distribution Mean
- TCP distribution SD

The standard deviation of the threshold pressure distributions describes the shape of the distribution and primarily controls the slope of the fitting curve. The mean value represents the point/pressure of maximum recruitment rate and derecruitment rate in TOP and TCP distributions, respectively. The TOP and TCP distribution parameters (mean and SD) effectively capture the severity of ARDS and its evolution with time.

As discussed earlier, an ARDS lung is stiffer and less compliant compared to a healthy lung and thus requires a higher pressure for inflation to similar volumes as a healthy lung. This behaviour is represented by a higher mean of the TOP distribution. Similarly, an ARDS unit tends to collapse at a higher pressure compared to a healthy lung unit and is represented by a higher mean of the TCP distribution. Hence, tracking of the TOP and TCP distribution mean values for similar PEEP level over a period of time for a patient could offer useful information on the evolution of the disease and thus guide clinical decisions.

Similarly, the SD represents the compliance of the lung. A lower SD in the TOP distribution represents a higher rate of recruitment and thus a higher lung compliance. A higher SD indicates a greater severity of the disease and a lower compliance. Hence, the threshold pressures distribution parameters can be tracked to evaluate the condition of the lung and state of the disease over time.

Parameter identification is carried out by iteratively changing the unit compliance and threshold pressure distribution parameters to minimise the least sum squared error between the model and the clinical data for each limb of the breathing cycle. The model is fitted to each breath independently and attempts to model the lung based on lung mechanics observed in each breath during tidal ventilation. This approach differs from the fitting procedure followed by Yuta et al (Yuta, 2007) where the lung mechanics are estimated based on PV data recorded at different PEEP levels which required a minimum of two PV loops recorded at different PEEP levels and limited the application of the model.

Moreover, certain parameters such as the SD of the TOP and TCP distributions are held constant for all PEEP levels for a patient during a trial in the method proposed by Yuta (Yuta, 2007). As discussed in Chapter 4, the lung compliance and thus lung characteristics tend to change with a change in PEEP and the lung compliance is observed to decrease at higher PEEP levels. This phenomenon is captured in this model by fitting the model parameters iteratively to each breath. Hence, they are allowed to change according to the

lung characteristics in the particular breath analysed. However, the overall basic computational fitting process is similar to that proposed by Yuta.

5.2.4 SUMMARY

The recruitment model presented here considers a lung as a group of lung units, which may include alveoli and/or distal airways. Recruitment and derecruitment of lung units is considered as the primary mechanism of volume change which was in confirmation with the clinical observations (Albaiceta et al., 2004, Gattinoni et al., 2001). Two primary parameters: 1) unit compliance, and 2) threshold pressure distributions are considered in this model.

The unit compliance describes the volume of a recruited lung unit at a particular pressure. It is applicable only to recruited lung units since the volume of a derecruited lung unit is considered zero here. Threshold pressures define the recruitment status of the lung units with threshold opening pressure (TOP) defining the pressure at which the unit "pops" open or is recruited and threshold closing pressure (TCP) is the pressure when the unit gets derecruited and assumes a zero volume. Due to the heterogeneous nature of an ARDS lung, the TOP and TCP values can be distributed over a wide range of pressures and can be described as normal distribution over a pressure range (Crotti et al., 2001, Pelosi et al., 2001).

Each of these parameters is defined by a set of governing equations. The unit compliance can be defined using the Venegas equation (Venegas et al., 1998) and the TOP and TCP distributions are defined by the mean and SD, respectively. Simulation is carried out by fitting the model to the clinical data available and determining the parameter variables that produce the best fit to the clinical data. These parameters can be used to describe the unique condition of the patient and status of the disease. The fitting method utilised here simulates the entire inspiratory capacity of the lung.

Earlier models developed by Yuta (Yuta, 2007) were fitted to PV loops obtained at different PEEP levels and had an inherent requirement of a minimum of two PV loops at different PEEP levels to determine the unique characteristics of the lung. The model approach presented here is fitted to individual PV loops obtained and attempts to identify overall lung characteristics based on the behaviour of the lung at different PEEP levels, as

discussed in subsequent chapters which will make it less invasive and more useful clinically.

Chapter 6 - Model Fitting to Clinical Data

The model developed by Yuta (Yuta, 2007) was fitted to the clinical data obtained by Sundaresan (Sunderesan, 2010) for validation. The recruitment model was implemented in Labview for the purpose.

The clinical data fitted in this study was taken at different PEEP levels for each patient and included information on dFRC. The model is fitted to the PV data of 9 patients collected by Sundaresan (Sunderesan, 2010). Consented patients were sedated, or sedated and paralysed using muscle relaxants, to prevent spontaneous respiratory efforts. The patient's initial ventilator settings, plateau pressure, tidal volume, and initial PEEP setting were recorded. All patients were ventilated using the volume controlled mode, synchronised intermittent mandatory ventilation (SIMV) during the study. The tidal volume was selected by the clinician accordingly and was kept constant while the data was recorded (Sunderesan, 2010).

The model is fitted to each breath independently and attempts to model the lung based on lung mechanics observed in each breath during tidal ventilation. This differs from the model fitting approach used by Yuta (Yuta, 2007) where the lung mechanics were estimated based on the collective PV data recorded at different PEEP levels for each patient during one trial. This outcome was achieved by keeping all the parameters except threshold pressure distribution mean values constant for all PEEP levels for a patient, enforcing consistency that may not be known or possible in regular clinical use.

The parameters uniquely representing the unit compliance curve and threshold pressure distributions (SD and mean) were identified through model fitting in the study presented here.

6.1 PARAMETER IDENTIFICATION

The model was fitted to the clinical data using the fitting method discussed in Chapter 5. The model was fitted only to the non-dynamic section of the PV data as discussed in

Chapter 3. Subsequently, the fitting error between the clinical data and model fit was calculated for only this section of the data and presented as percentage error.

The unit compliance curve in this model is described using a cumulative distribution function. The function produces a similar curve as described by the Venegas equation (Venegas et al., 1998), but is now described by mean and SD. For this study, the parameters defining the unit compliance curve were iteratively changed to determine the parameters that result in the best fit to the clinical data. The mean of the curve was varied between -2 to 20 cmH_2O in increments of 11 and the SD was varied between 1 to 11 cmH_2O in increments of 5 and the values that produced the best fit were identified. It should be noted that recruitment and derecruitment form the primary mechanisms of volume change during MV. Hence unit compliance is not expected to have a significant influence. Similar conclusions were reached by Yuta (Yuta, 2007).

The maximum volume of a lung unit was fixed at 0.01 ml in the model. This provided sufficient resolution and also simplified calculations and fitting. The size of the alveoli does not differ significantly between lungs of different sizes. Instead, the lung volume is defined by the total number of lung units present (Ochs et al., 2004). The inspiratory capacity is also not the same for all lungs and differs between subjects. This variation in the inspiratory capacity is taken into consideration by varying the total number of lung units as one of the parameters in this model.

As discussed in Chapter 2, the TOP and TCP values are distributed over a wide range of pressure values due to the heterogeneous nature of lung units and can be described as normal distribution function (Crotti et al., 2001, Pelosi et al., 2001). The threshold pressure distributions are thus defined by the SD and mean values in this model.

The SD values were iteratively changed for the threshold pressure distributions and the mean values that produce the best fit for each of the inflation and deflation cycles are calculated using a curve fitting algorithm in Labview. The parameters that produced the best fit were identified and recorded as the parameters describing the lung characteristics observed over the breathing cycle.

6.2 RESULTS

The data acquired by Sundaresan (Sunderesan, 2010) included PV curves from ZEEP to the maximum PEEP applied. A sudden increase in lung compliance was observed in the PV loops at low PEEP levels in some patients. This behaviour is shown in Figure 6-1, which shows the PV loops for Patient 1 at PEEP levels of 0 and 5 cmH_2O. This phenomenon is attributed to auto-PEEP which represents the pressure that is already in the lungs even in the absence of any external ventilation. Auto-PEEP was measured by Sundaresan for each patient by performing an end expiratory hold (Sunderesan, 2010).

A collapsed airway or an obstruction causes gas to be trapped in an alveolus due to the presence of auto-PEEP (Fernández et al., 1990, Mughal et al., 2005) as shown in Figure 6-2. When this obstruction is opened by application of higher pressures, the compliance suddenly increases due to the sudden addition of the volume of the lung units prerecruited due to auto-PEEP. Since the presence of auto-PEEP does not accurately reflect the state of the disease, the model was fitted only to the PV loops obtained at PEEP levels higher than the auto-PEEP recorded. In some cases, this trend was observed in some PV loops recorded at PEEP levels above the auto-PEEP as well. Those PV loops were also not considered in this study. Note that since auto-PEEP can be identified from the data as recorded, this choice implies no loss of clinical relevance.

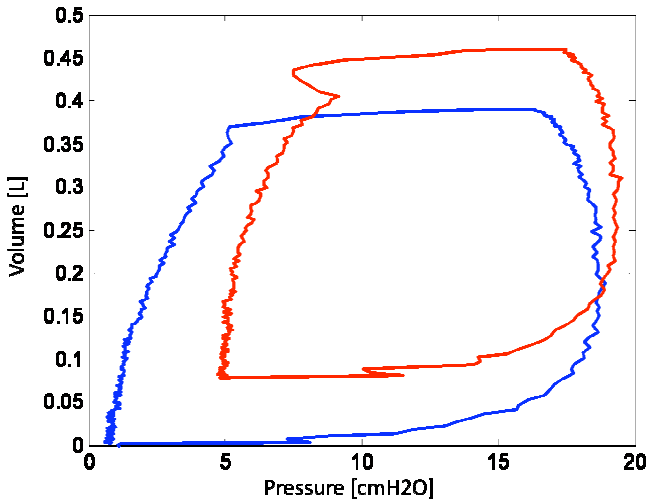

Figure 6-1: Patient 1 PV loops for PEEP 0 and PEEP 5 cmH_2O. The auto-PEEP for Patient 1 was 10 cmH_2O. A sudden increase in lung compliance can be observed in both PV loops.

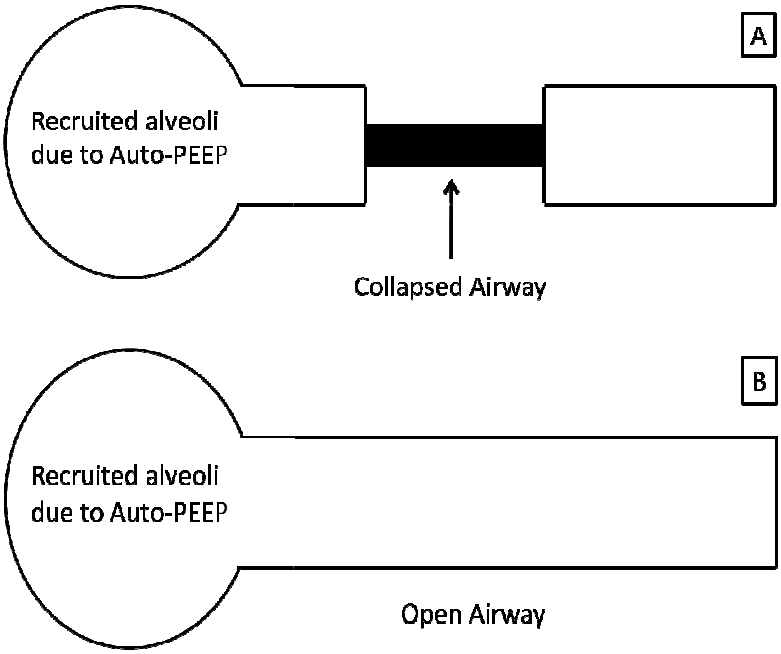

Figure 6-2: Schematic highlighting concept of Auto-PEEP. Figure (A) shows the presence of a collapsed airway, with recruited alveoli causing a level of auto-PEEP. Figure (B) shows the collapsed airway opening up when additional PEEP is applied (Sunderesan, 2010)

6.2.1 MODEL FITTING

Tables 6-1 – 6-12 show the results for each patient. The model was able to fit the data well. The average percentage error found between the fitted data and the model was 1.45% for inflation and 3.85% for deflation cycles. The model estimated the total inspiratory capacity of the lung based on the lung characteristics observed in each PV loop recorded. However, the estimated inspiratory capacity varied with PEEP in most cases for a given patient and this observed variation is also presented. However, this variation in inspiratory capacity was lower for patients ventilated at PEEP levels normally seen in clinical settings and was generally higher at lower PEEP levels.

The average mean value for TOP distribution was found to be higher at 27.68 cmH_2O compared to 19.66 cmH_2O for TCP distribution. This result is as expected since a lung unit generally gets recruited at a higher pressure compared to the pressure at which it gets derecruited and assumes a zero volume. This difference in pressure causes the hysteresis

observed in the PV loops. The average SD for TOP distribution was also found to be higher (16.73 cm H_2O) compared to the average SD for TCP distribution (11.36 cm H_2O).

Table 6-1: Patient 1 model fitting parameters

Patient 1 Fitting Results

AutoPEEP [cm H_2O] 10

IC 1.4 – 2.04 L

	Inflation			Deflation			
PEEP [cm H_2O]	Mean	SD	Error perc	Mean	SD	Error perc	Number of Units Estimated
15	27.83	15	0.07	17.58	8	0.43	140,000
20	36.46	25	0.06	24.33	15	2.49	204,000
25	25.7	15	0.01	21.44	8	0.07	140,000
27	25.002	15	2.635	20.56	8	9.12	144,000

Table 6-2: Patient 2 model fitting parameters

Patient 2 Fitting Results

AutoPEEP [cm H_2O] 2

IC 1.6 – 5.4 L

	Inflation			Deflation			
PEEP [cm H_2O]	Mean	SD	Error perc	Mean	SD	Error perc	Number of Units Estimated
5	35.04	15	20.91	17.19	8	44.51	540,000
10	24.17	15	0.741	14.56	8	0.86	180,000
15	20.47	15	1.269	14.65	8	5.19	160,000
20	27.07	15	0.0315	19.75	15	2.47	216,000
22	18.44	15	2.313	13.75	8	13.57	160,000

Table 6-3: Patient 3 model fitting parameters

Patient 3 Fitting Results

AutoPEEP [cm H_2O] 0

IC 2.0 – 6.0 L

	Inflation			Deflation			
PEEP [cm H_2O]	Mean	SD	Error perc	Mean	SD	Error perc	Number of Units Estimated
5	35.12	15	4.135	18.35	8	5.95	600,000
10	31.91	15	0.045	26.58	15	2.50	500,000
15	21.11	15	0.276	16.30	8	0.025	220,000
20	15.02	15	6.65	10.68	8	23.34	200,000
25	19.14	15	0.64	10.62	15	6.15	220,000
28	21.33	25	0.002	21.672	15	0.013	260,000

Table 6-4: Patient 4 model fitting parameters

Patient 4 Fitting Results

AutoPEEP [cm H_2O] 9

IC

	Inflation			Deflation			
PEEP [cm H_2O]	Mean	SD	Error perc	Mean	SD	Error perc	Number of Units Estimated
25	35.483	25	0.112	23.81	15	0.030	220,000
30	30.885	25	0.010	21.61	15	0.010	220,000

Table 6-5: Patient 5 model fitting parameters

Patient 5 Fitting Results

AutoPEEP [cm H_2O] 13

IC 1.6 – 5.6 L

	Inflation			Deflation			
PEEP [cm H_2O]	Mean	SD	Error perc	Mean	SD	Error perc	Number of Units Estimated
15	52.26	15	0.092	41.60	15	1.52	560,000
20	41.95	15	0.27	33.34	15	0.67	160,000
25	48.26	25	0.421	34.65	15	4.64	200,000

Table 6-6: Patient 5 (second trial) model fitting parameters

Patient 5_2 Fitting Results

AutoPEEP [cm H_2O] 8

IC 1.26 – 1.92 L

	Inflation			Deflation			
PEEP [cm H_2O]	Mean	SD	Error perc	Mean	SD	Error perc	Number of Units Estimated
10	38.37	15	9.672	19.798	8	3.66	180,000
15	33.025	15	1.884	21.115	8	0.07	160,000
20	30.482	15	0.176	22.417	15	4.39	154,000
25	24.926	15	0.785	20.072	8	6.099	126,000
29	35.912	25	0.012	28.476	15	0.015	192,000

Table 6-7: Patient 6 model fitting parameters

Patient 6 Fitting Results

AutoPEEP [cm H_2O] 10

IC 1.12 – 1.40 L

	Inflation			Deflation			
PEEP [cm H_2O]	Mean	SD	Error perc	Mean	SD	Error perc	Number of Units Estimated
15	29.799	15	2.137	19.647	8	0.652	120,000
20	28.966	15	0.085	18.914	15	3.225	112,000
25	35.174	25	0.065	25.406	15	0.0009	140,000

Table 6-8: Patient 6 (second trial) model fitting parameters

Patient 6_2 Fitting Results

AutoPEEP [cm H_2O] 2.3

IC 1.40 – 2.00 L

	Inflation			Deflation			
PEEP [cm H_2O]	Mean	SD	Error perc	Mean	SD	Error perc	Number of Units Estimated
5	25.057	15	4.547	12.593	8	0.433	180,000
10	19.198	15	0.594	11.964	8	2.527	140,000
15	23.741	15	0.121	17.259	15	0.0008	200,000
20	21.338	15	0.001	13.626	15	2.474	180,000
25	22.082	15	0.451	10.639	15	6.19	180,000

Table 6-9: Patient 6 (third trial) model fitting parameters

Patient 6_3 Fitting Results

AutoPEEP [cm H_2O] 1.6

IC 1.44 – 3.00 L

	Inflation			Deflation			
PEEP [cm H_2O]	Mean	SD	Error perc	Mean	SD	Error perc	Number of Units Estimated
5	28.476	15	1.687	15.133	8	0.317	300,000
10	23.459	15	0.077	17.954	15	2.435	220,000
15	32.32	25	0.040	22.707	15	0.905	280,000
20	14.569	15	0.189	13.866	8	0.037	144,000

Table 6-10: Patient 7 model fitting parameters

Patient 7 Fitting Results

AutoPEEP[cm H_2O] 2

IC 0.72 – 1.00 L

	Inflation			Deflation			
PEEP [cm H_2O]	Mean	SD	Error perc	Mean	SD	Error perc	Number of Units Estimated
5	22.485	15	4.42	11.959	8	9.85	100,000
10	24.562	25	1.064	13.852	15	10.88	100,000
15	18.722	15	0.12	13.359	8	1.25	70,000
16	20.159	15	0.113	14.24	8	0.528	72,000

Table 6-11: Patient 8 model fitting parameters

Patient 8 Fitting Results

AutoPEEP[cm H_2O] 0

IC 1.44 – 6.00 L

	Inflation			Deflation			
PEEP [cm H_2O]	Mean	SD	Error perc	Mean	SD	Error perc	Number of Units Estimated
5	39.231	15	2.501	30.530	15	1.53	600,000
10	29.038	15	0.180	21.196	15	2.506	200,000
15	27.15	15	0.047	20.220	15	0.318	180,000
20	24.498	15	0.030	16.903	15	2.446	156,000
25	19.675	15	1.099	17.337	8	6.047	144,000
30	25.029	15	0.0655	23.374	8	0.044	168,000

Table 6-12: Patient 9 model fitting parameters

Patient 9 Fitting Results

AutoPEEP[cm H_2O] 12

IC 1.4 – 1.8 L

	Inflation			Deflation			
PEEP [cm H_2O]	Mean	SD	Error perc	Mean	SD	Error perc	Number of Units Estimated
15	24.964	15	1.330	17.390	8	0.209	140,000
20	26.870	15	0.056	18.973	15	4.325	168,000
25	23.429	15	0.622	20.380	8	2.505	160,000
29	26.974	15	0.032	23.955	8	0.031	180,000
30	26.427	15	0.039	24.098	8	0.852	180,000

Figure 6-3 illustrates the fitting results obtained for Patient 1 along with the TOP and TCP distributions. Similar results for all the patients recruited are presented in Appendix A in this thesis.

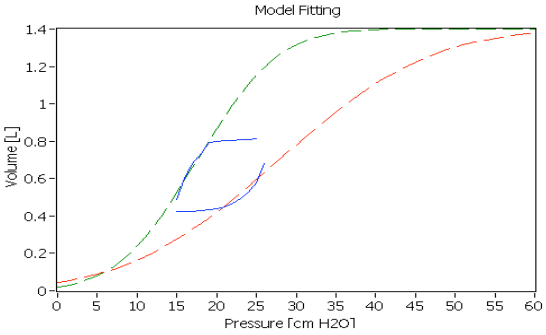

a

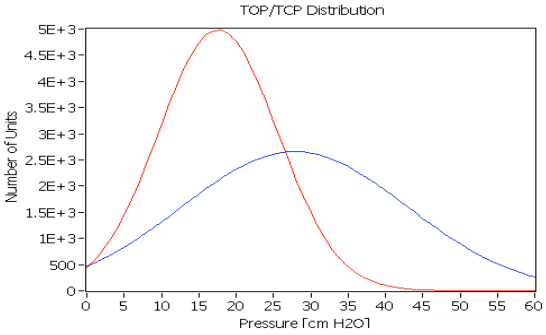

a-1

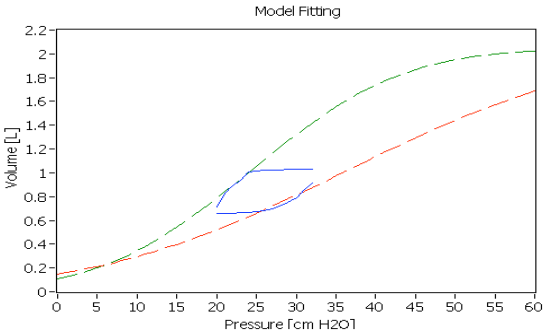

b

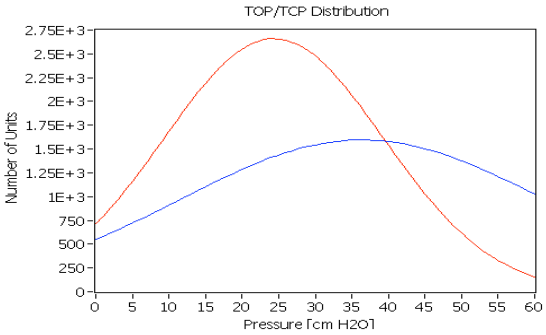

b-1

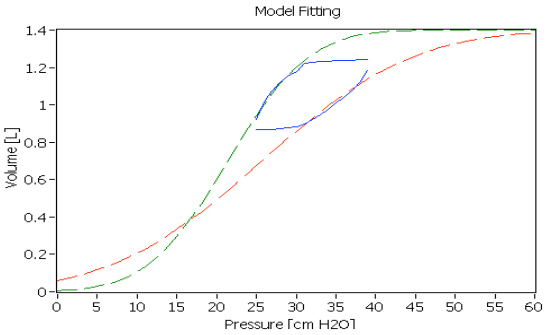

c

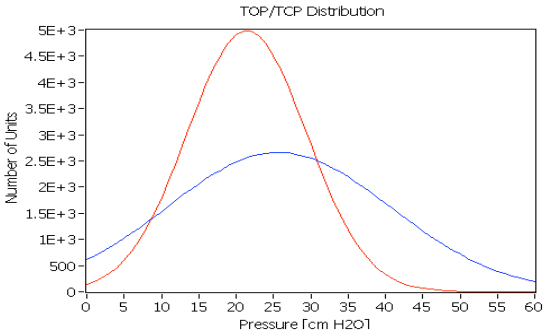

c-1

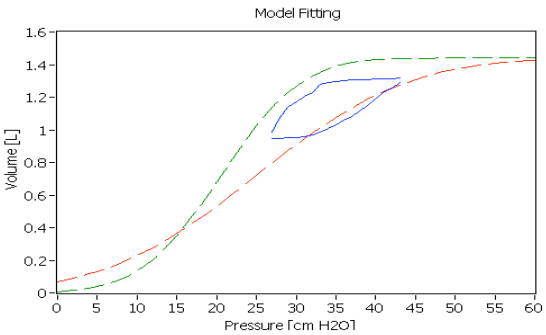

d

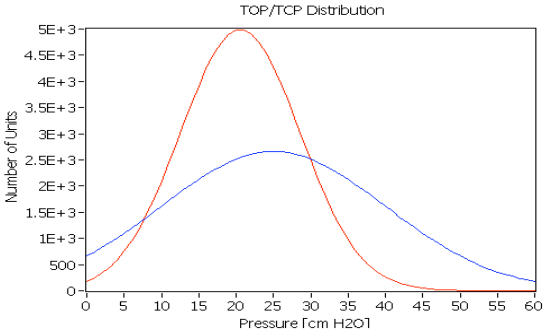

d-1

Figure 6-3: Patient 1 Model Fitting and TOP/TCP Distribution. a-d represent breaths taken at different PEEP levels (breath 4-7) with a-1 – d-1 representing the TOP/TCP distributions for respective breathing cycles. Red curve represents TCP distribution and blue curve represents TOP distributions

6.3 DISCUSSION AND LIMITATIONS

The data sets obtained had information on EEV for PV loops recorded for each PEEP level for all patients. This data allows an accurate assessment of how much of the lung is being ventilated as a fraction of the whole lung.

6.3.1 MODEL FITTING

The fitting percentage errors for the inflation cycle fell between a minimum error of 0.001% and a maximum error of 20.9% with an average percentage error of 1.45% and the fitting errors for the deflation cycle were found to fall between a minimum of 0.00% and a maximum of 44.51 % with an average percentage error of 3.85%. In some patients, the inflation fitting error was found to be relatively high for PV loops recorded at very low PEEP levels. This result can be particularly observed in the percentage error values for Patient 2, as shown in Figure 6-4. However, the inflation errors were found to be comparatively lower and well within acceptable range for PEEP levels normally seen in clinical settings.

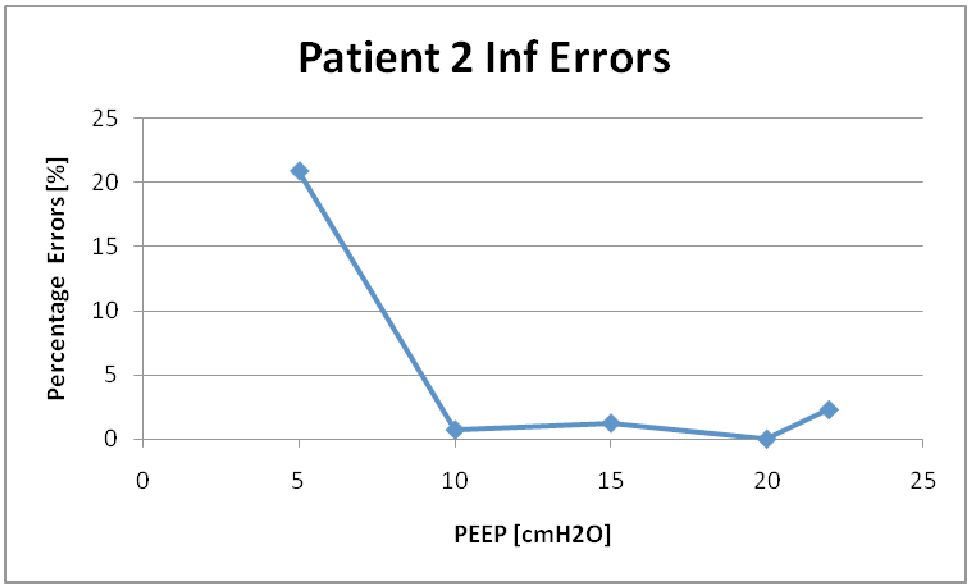

Figure 6-4: Inflation and Deflation Percentage Errors for Patient 2

It should be noted that percentage errors are calculated for an absolute volume. This approach exaggerates the error at lower volumes and understates the error at higher volumes. Low and high volumes generally correspond to lower PEEP and higher PEEP levels, respectively, in tidal ventilation and thus correspond with the observation made with the fitting errors observed.

6.3.2 INSPIRATORY CAPACITY AND NUMBER OF LUNG UNITS

The minimum number of lung units calculated was 70,000 and the maximum was 600,000 corresponding to a total inspiratory capacity of 700 ml and 6 L respectively, since the maximum unit volume for a recruited unit is fixed at 0.01 ml. Inconsistencies in the number of lung units estimated was observed within patients over different PEEP levels. This behaviour is illustrated in Figure 6-5, which shows the number of lung units calculated by the model for Patient 2. It was observed that the model estimated a relatively high number of lung units at low PEEP levels for some patients. Such low PEEP levels are generally not observed in clinical settings. However, such inconsistencies were lower at higher PEEP levels that are commonly used in clinical treatment.

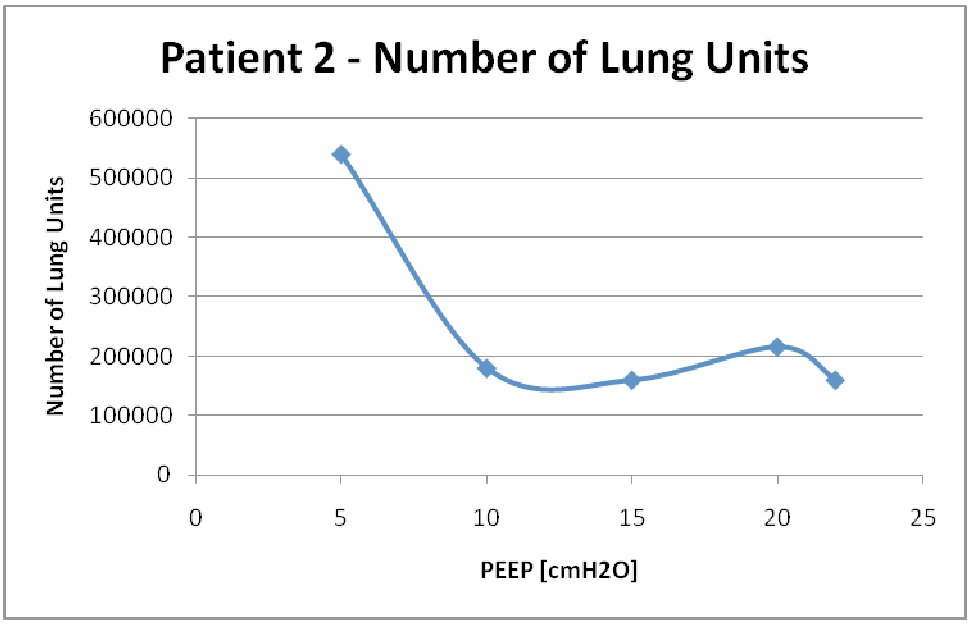

Figure 6-5: Estimated number of lung units with respect to PEEP. The estimated number settles to certain value at higher PEEP levels and is found to be unexpectedly high at low PEEP levels.

The number of lung units calculated were a function of the maximum volume produced during tidal ventilation and the compliance of the curve. As discussed in Chapter 4, the compliance of the lung changes with an increase in PEEP. In particular, the lung compliance was found to decrease at higher PEEP levels. This behaviour can be attributed to higher recruitment of lung units at lower pressures compared to when the lung is ventilated near its inspiratory capacity. When the lung is ventilated at higher PEEP levels near its inspiratory capacity, majority of lung units are already recruited at the beginning of inflation. Hence, more of the volume change occurs because of the stretching of the recruited lung units and airways. Hence, accurate assessment of the lung compliance at clinically relevant PEEP levels is required for an accurate estimation of the number of lung units and inspiratory capacity.

However, the model was still found to offer a good estimate of the IC and thus also offer useful insight into recruitability of the lung by presenting the relative recruitment of the lung compared to the total inspiratory capacity. This outcome can be observed in the fitting results for Patient 1 shown in Figure 6-3, and can be exploited to determine the PEEP levels that are likely to overstretch the recruited lung units, and thus avoiding further damage to lung units.

The model recalculates all the parameters that define the unit compliance curve and threshold pressure distributions based on the lung characteristics observed for each breath. These parameters are ultimately used to calculate the total number of lung units and inspiratory capacity. It should be noted that these parameters may not be consistent throughout the trial for a given patient considering the variation in behaviour of the lung at different PEEP levels.

6.3.3 TOP/TCP DISTRIBUTION PARAMETER

The average TOP distribution mean was found to be higher at 14.57 cmH_2O compared to the average TCP distribution mean which was found to be 10.62 cmH_2O. The average SD of the TOP distribution was also found to be higher at 16.73 cmH_2O compared to TCP distribution which was found to be 11.37 cmH_2O. However, no specific trend in threshold pressure distribution mean and SD values with respect to change in PEEP level was observed for a given patient. This result undermines the physiological relevance of the model in spite of low fitting errors and estimation of the inspiratory capacity of the patient,

since it is difficult to assess the trend in the behaviour of the lung due to lack of such information.

This shortcoming observed in the model fitting can be attributed to recalculation of all the parameters for each breath for a patient as discussed in Section 6.3.2. The parameters calculated that result in minimum errors may not be consistent for a patient for breaths recorded at different PEEP levels due to variability in lung characteristics with change in PEEP and thus result in highly variable threshold pressure distribution and unit compliance parameters. However, the model still offers a strong tool in estimating where the lung is being ventilated with respect to the total inspiratory capacity, as observed in Figure 6-3.

Alternatively, a representative breath as discussed in Chapter 4 can be selected and the unit compliance parameters can be calculated by fitting the model to the selected breath. The number of units estimated by the model and the threshold pressure distribution SD values obtained along with the unit compliance parameters can be considered representative of the patient and kept constant for all the breaths. The threshold pressure distribution mean values can be calculated for the other PV loops obtained at different PEEP levels using the earlier calculated parameters. Table 6-13 shows an example the fitting results obtained for Patient 1 using this specific methodology. Figure 6-6 shows the associated fitting results obtained for Patient 1.

Patient 1 Fitting Results

AutoPEEP [cm H_2O] 10

IC 1.4 – 2.04 L

	Inflation			Deflation			
PEEP [cm H_2O]	Mean	SD	Error perc	Mean	SD	Error perc	Number of Units Estimated
15	27.83	15	0.069	17.58	8	0.43	140,000
20	26.60	15	0.138	19.39	8	0.114	140,000
25	25.70	15	0.012	21.43	8	0.072	140,000
27	24.97	15	0.159	22.29	8	0.001	140,000

Table 6-13: Patient 1 fitting parameters based on lung parameters obtained from fitting the model to a representative breath

It was noted that the model fitted the data well with minimal errors with the new approach. A specific trend in the threshold pressure distribution mean values was also observed. Specifically, the TOP mean was found to decrease and the TCP mean was found to increase with an increase in PEEP. This result is presented in Figure 6-7, which shows the threshold pressure mean values with respect to PEEP. This observation is consistent with the observations made by Yuta (Yuta, 2007). It is thought that once a lung unit is recruited via PEEP, it can be recruited at a lower pressure, effectively decreasing the TOP of the unit. Thus, an increase in PEEP increases the lung volume by two methods: 1) keeping additional lung units recruited at the end of exhalation cycle and 2) by effectively lowering the TOP of lung units. This reduction in TOP of the lung units is represented by the reduction in mean values of the TOP distributions at higher PEEP levels. This mechanism is consistent with several clinical studies (Foti et al., 2000, Henzler et al., 2005).

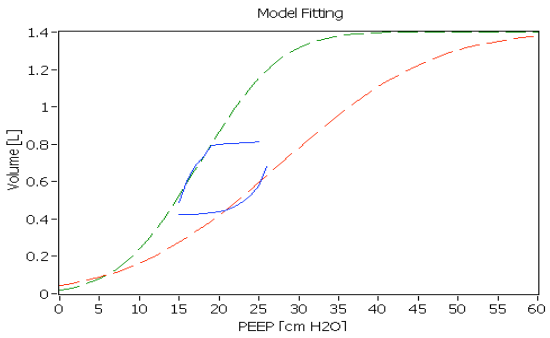

a

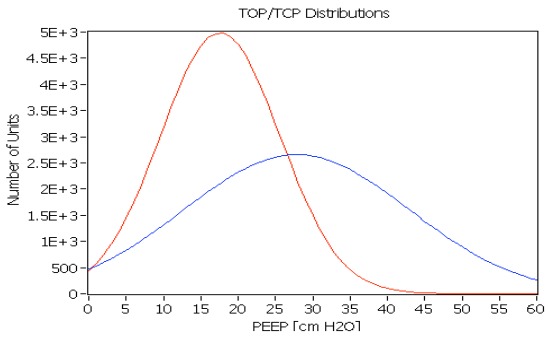

a-1

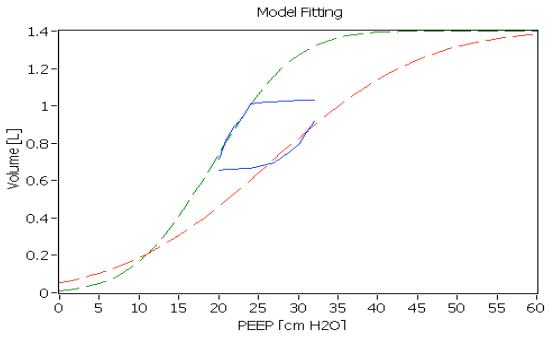

b

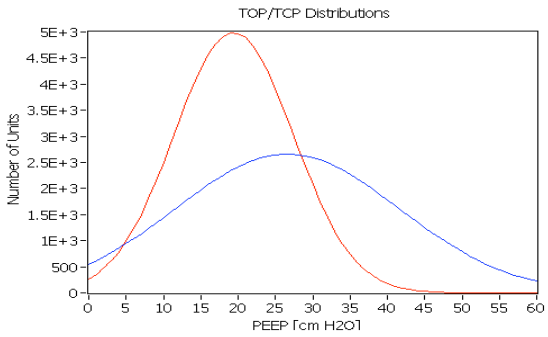

b-1

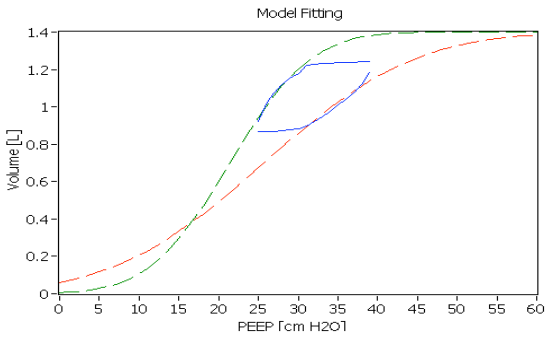

c

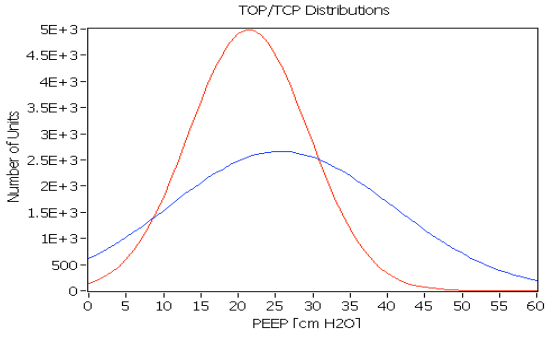

c-1

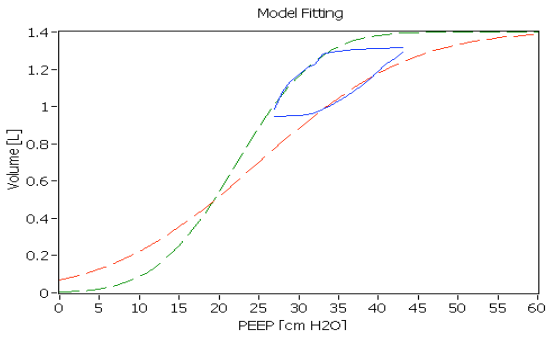

d

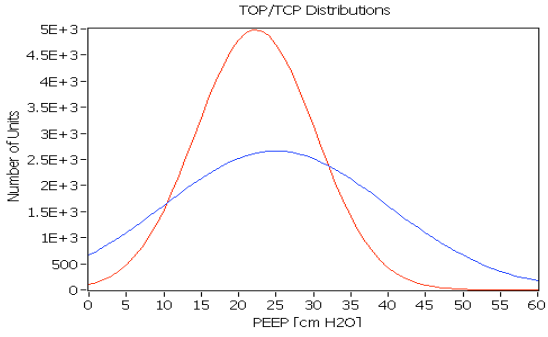

d-1

Figure 6-6: Fitting results for Patient 1. The unit compliance parameters and the threshold pressure SD values were calculated by fitting the model to a representative breath and held constant for the patient for all PEEP levels

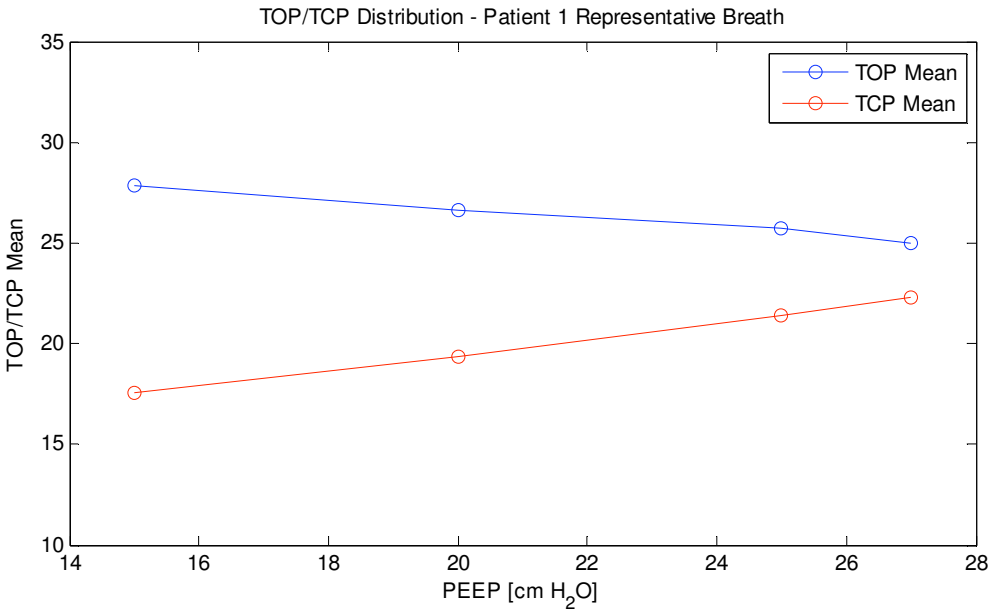

Figure 6-7: TOP/TCP Mean values for Patient 1. The unit compliance parameters and the threshold pressure SD values were calculated by fitting the model to a representative breath and held constant for the patient for all PEEP levels. The mean was calculated for each breath.

The slope of the threshold pressure distributions mean shift with respect to PEEP was also found to be near constant for Patient 1. This trend in mean shift can be exploited to estimate threshold pressure distribution means at different PEEP levels and deduce the lung characteristics at higher PEEP levels without actually setting the ventilator at the particular PEEP level. Equally, the low slope indicates a patient who is not recruitable via PEEP.

6.4 SUMMARY

The model was further validated by fitting it to the clinical data obtained by Sundaresan. Each patient data set obtained included PV loops for different PEEP levels and information on the EEV of the lung for the respective PEEP level. Min to max fitting model discussed in Chapter 5 was used to fit the data.

The model was found to fit the clinical data well with minimum errors. Higher errors were usually found at very low PEEP levels that are not generally employed in normal clinical setting. The average percentage error between the model and the data was found to be

1.45% for the inflation cycle and 3.85% for the deflation cycle which are well within acceptable limits.

The model is also capable of estimating the number of lung units and thus the total inspiratory capacity of the lung. Inconsistencies were observed in the number of lung units calculated for a patient at different PEEP levels. This outcome can be attributed to the variation in the lung characteristics at different PEEP levels, especially the compliance as discussed in Chapter 4. These inconsistencies were particularly high at low PEEP levels and were less at higher PEEP levels normally applied.

The model was also able to identify the threshold pressure distribution parameters, mean and SD, well. The threshold pressure distribution parameters were however also found to vary with changes in PEEP. The variation in these parameters did not follow any particular trend. The model basically calculates the parameters that fit the data well for each PV loop recorded for a patient. This approach invariably leads to inconsistencies in parameters due to variation in the lung characteristics with change in PEEP. However, using a representative breath to calculate the parameters generic to the lung (unit compliance parameters and threshold pressure distribution SD) and fitting the model to all PV loops at different PEEP levels keeping these parameters constant showed potential for accurate fitting and showed a general trend in the TOP and TCP distribution mean values for the patient studied.

In particular, the TOP mean decreased with PEEP and the TCP mean increased with a nearly constant slope in both cases. This consistency in slope can be exploited to estimate lung parameters at higher PEEP levels without any requirement to actually ventilate the patient at that PEEP level. However, only one patient was analysed using this approach and further work needs to be undertaken to validate the approach.

Chapter 7 - Conclusions

7.1 OVERVIEW

Mechanical ventilation (MV) is one of the most common treatments in ICU. It aids patient recovery by completely or partially taking over the breathing process. Determining correct patient specific MV settings is important to avoid any further damage to the lungs and minimise the stay in the hospital. However, current methods of choosing ventilator settings during tidal ventilation are based on medical experience and intuition due to lack of convenient and practical methods of accurately determining the underlying patient specific condition. The result is incorrect or non-optimal MV therapy that can have significant implications on the mortality and length of stay, and thus the total cost of treatment.

Recruitment models are developed to capture the underlying patient condition. Such patient specific models, identified from data, can evaluate clinically useful information such as the lung recruitment status. The models show significant potential to be used as a diagnostic tool to assist clinicians with identifying optimum ventilator settings based on unique patient specific conditions, identified in real - time at the patient's bedside.

7.2 PROJECT OUTCOMES

As discussed earlier, MV forms one of the most common treatments offered in the ICU. It is especially used on patients who experience difficulty in breathing to assist them with the breathing process, especially for patients suffering from ARDS/ALI. ARDS is a severe form of ALI that is characterized by inflammation of the lung and filling of the lungs with fluids. This condition results in the collapse of the lung units that results in an effectively smaller lung. Incorrect MV that do not match the patient - specific condition can cause further damage to the lung, or unnecessarily extend the ventilator treatment of the patient resulting in higher cost.

Currently, there are no established or universally accepted protocols for MV. Past attempts at standardizing MV protocols have mainly focused on controlling the applied PEEP.

Several studies have also suggested the use of low tidal volumes during MV as an effective strategy. However, no specific effective MV protocols have been identified and the final ventilator settings are primarily based on medical experience and intuition.

This lack of a global protocol is partly due to limited data available to the clinicians at the patient's bedside relating to patient – specific lung characteristics and the potential recruitability of the lung. These characteristics also evolve with time and with changes in the disease status, and thus need to be monitored in real-time at the bedside from readily available clinical data. Hence, determining patient – specific ventilation parameters is hindered by lack of convenient methods to determine patient - specific lung condition and the lack of ability to track them in real – time with evolution of disease.

One of the primary goals of the project was to develop an easy and efficient method to measure the flow rate and pressure applied in a breathing cycle during tidal ventilation. The tidal volume is calculated by trapezoidal integration of the flow rate. This measurement was successfully achieved using an instrument called the pneumotachometer. The measured PV data was recorded in a readily usable form (text file) that can be used immediately by clinicians in conjunction with the recruitment model to identify patient specific lung characteristics.

Another important goal of the project was to develop a model to calculate the dFRC of a patient associated with the applied PEEP, by applying a stress – strain theory of lung mechanics. This model was validated using clinical data, which contained the PV loops and associated dFRC values for 9 patients at different PEEP levels. The model developed and validated a generic population parameter, β_1, to accurately estimate dFRC at different PEEP levels.

The results indicated that β_1 values that represented the overall lung characteristics (β_{1rep}) that were calculated using lung characteristics observed in a representative breath chosen for each patient showed a linear trend with respect to PEEP and was found to be more effective in accurate estimation of dFRC. The model also exhibited certain limitations. One of the primary limitations was high estimation errors at low PEEP levels. However, this limitation does not pose significant risk since such low PEEP levels are generally not applied in the ICU. Furthermore, the trends observed between the estimated and measured dFRC values are similar in most cases. The model presented offers an easy method for

estimation of dFRC at the patient's bedside that offers a powerful tool since deflation of lung to ZEEP to measure dFRC may not always be safe and can pose significant risk of added lung damage for many patients.

The research also identifies and validates an overall model-based approach that uses readily available clinical data, such as PV loops, to capture lung dynamics and determine lung conditions unique to the patient. The recruitment model presented here is based on newly hypothesised and accepted lung mechanics that considers recruitment and derecruitment of lung units as the primary mechanisms of volume change during tidal ventilation. The model is fitted to clinical data (PV loops), and the patient – specific and physiologically relevant parameters are identified. The model was validated using clinical data obtained for 9 patients that contained PV data at different PEEP levels and associated EEV information.

The model was able to fit all types of clinical data with average errors less than 4% displaying the significant potential of the model. The outputs of model fitting included unit compliance and threshold pressure distribution parameters (mean and SD) that best indicated the unique underlying lung condition. All parameters except threshold pressure distribution mean values were varied iteratively and the parameters that produced least error were identified. The threshold pressure means were calculated using the model fitting algorithm in Labview. The model also has potential to track these parameters with time and hence identify changes in the patient's condition with evolution of the disease. The model also estimated the total number of lung units for a patient and, thus, the total inspiratory capacity of the patient. Hence, the model also indicates where the lung is being ventilated with respect to the total inspiratory capacity and help in identifying PEEP levels that may cause further damage.

However, the model also displayed certain shortcomings. Inconsistencies in the number of lung units estimated by the model were observed. These inconsistencies were found to be lower at PEEP levels generally applied in the ICU, and were higher at relatively very low PEEP levels. Thus, this shortcoming does not pose significant clinical drawback to the use of the model in clinical settings.

Another shortcoming was related to the unit compliance and threshold pressure distribution parameters observed. The unit compliance and threshold pressure distribution parameters

were found to vary with PEEP. The variation in these parameters did not follow any certain trend. This shortcoming can be overcome by selecting a representative or average breath over a given period, and calculating parameters that are expected to stay constant for a patient over time. These parameters can be kept constant for a patient and the threshold pressure distributions means can be recalculated for each breath. However, further research needs to be carried out to validate this method.

Overall, the fitting model and method presented displayed great usefulness in clinical settings in determining the patient specific characteristics and exploit them to determine optimum PEEP levels for MV.

Chapter 8 - Future Work

The models presented in this thesis have shown very good potential for clinical applications to optimise ventilator treatment and minimise further damage to lung units. However, a comprehensive clinical study is required to fully validate and understand the physiological applications of the model.

8.1 LUNG CHARACTERISTICS

The model assesses the underlying lung characteristics and condition by identifying the parameters that result in minimum errors between the PV data fitted and the model. The parameters identified by the model are considered unique to the patient. The description of the lung characteristics offered by the parameters identified can be further validated through additional data.

8.1.1 NUMBER OF LUNG UNITS

The model estimates the number of recruitable lung units and hence the total inspiratory capacity of the patient based on the lung characteristics observed in individual breaths recorded. Certain inconsistencies were observed in this number when the model was fitted to PV loops individually at different PEEP levels. An alternative to this method has also been proposed where a representative breath at a clinically relevant PEEP is selected and the total number of lung units is estimated by fitting the model to this representative breath. This total number of lung units estimated is kept constant for PV loops recorded at different PEEP levels.

Both these approaches for estimating the number of lung units need to be validated clinically. Additional data that may indicate the total inspiratory capacity such as CT scans should be included in the study to directly compare the estimated inspiratory capacity with the actual inspiratory capacity of the patient.

8.1.2 DFRC

A model to estimate the dFRC of the patient at different PEEP levels is also proposed in this thesis. A constant β_1 was identified and introduced in the model and this new parameter was hypothesised as a population constant for the corresponding PEEP level. A larger dataset is required to validate the hypothesis. Although, the research carried out in this thesis strongly indicates towards validity of this hypothesis and the use of β_1 to estimate dFRC, further trials must be carried out to confirm this outcome and to validate the model for clinical use.

β_1 is defined by the applied tidal volume and lung and chest wall elastance observed during a breathing cycle. The values of β_1 and β_{1rep} defined in this thesis showed variation across different patients, and was significant in some cases. Further research is required in order to determine the relationship between β_1, including β_{1rep}, where a similar approach is used, and lung characteristics such as the lung and chest wall elastance and tidal volume applied.

8.2 SPONTANEOUSLY BREATHING PATIENTS

As mentioned earlier, the patients studied by Sundaresan et al were sedated and paralysed using muscle relaxants, to prevent spontaneous breathing. However, not all patients are sedated or completely reliant on the ventilator for breathing and still breathe spontaneously. The lung mechanics of these patients may be more complicated compared to passively breathing patients. The model presented here does not account for spontaneously breathing patients and thus offers a disadvantage in accommodating all sorts of patients. Thus it is important to introduce a metric that allow application of this model to spontaneously breathing patients.

The primary difficulty when examining spontaneously breathing patients is determination of a metric to quantify the spontaneous breathing effort from the patient. One of the primary reasons behind this is the difficulty in measuring transpulmonary pressure on a regular basis. However, initial investigations can be carried out using the artificial lung connected to two ventilators, with one simulating spontaneous breathing and the other MV applied to a patient. The data can be collected at different lung compliance, different

spontaneous breathing pressures and different modes of MV. A further comprehensive research on spontaneous breathing would be required but this method would allow to develop a metric for quantifying spontaneous breathing which can be validated using clinical data.

8.3 MODEL PARAMETERS

The model fitting outputs include unit compliance curve parameters and threshold pressure distributions parameters. The unit compliance curve is described as a cumulative distribution function in the model and hence is defined by mean and SD. Similarly, the threshold pressure distributions are modelled as Gaussian function and are again described by mean and SD. The model identifies the mean and SD values for both the distributions that result in minimum fitting errors.

It was observed that the unit compliance curve parameters and threshold pressure distribution parameters varied with respect to PEEP for the same patient. Some of the parameters are not expected to change, such as the unit compliance parameters and threshold pressure distributions SD. Further investigation into physiological implications of these variations need to be carried out. The model may also be re-evaluated and redesigned to take this into consideration.

An alternative method as proposed earlier involves selection of a representative breath at a clinically applicable PEEP and fitting of the model to the PV data obtained for the said representative breath. The unit compliance parameters and the threshold pressure SD can be held constant for a particular patient for all PEEP levels and the model can be refitted to the rest of the PV loops keeping these parameters constant.

This method would require recalibration of these parameters every few, hours but would still make the system more autonomous compared to current methods. Recalibration of these parameters with time also allows tracking of changes in the patient's lung characteristics with time. The usefulness of these parameters will be greatly enhanced when used in conjunction with other data, such as CT scans, that could indicate the severity of the disease since they would allow for direct comparison between the two. A

comprehensive database correlating the identified parameters and severity of the disease would greatly help clinicians identify evolution of the disease with time.

8.4 REAL – TIME FITTING

The model, in its current form, can take anywhere between 5-10 mins for comprehensive model fitting to the selected breath. This time is significantly reduced (10-20 seconds) when the unit compliance parameters and threshold pressure distributions SD are determined by fitting the model to a representative breath and fixed as constants instead of determining them iteratively. This time is still very high to be considered for real time fitting of the model to the PV data. Thus, the model needs to be optimised and modified to fit the requirements. The built – in curve fitting algorithm in Labview used to determine the means of the threshold pressure distributions can be rewritten and optimised for the purpose.

Use of a laptop computer with a faster processer speed is also expected to reduce the fitting time. The model can be further optimised by further reducing the number of parameters that are determined. It should be however noted that real time model fitting may be difficult to achieve. However, the observed time taken to fit the model to PV loops is reasonable for clinical applications. The labview program saves the necessary PV data in a readily usable form (txt files). Initially this data may be collected for a patient and stored. The model can then be fitted to the obtained data independently later on to determine optimum ventilator settings. The time taken to determine these settings is insignificant compared to the length of the patient's stay in the ICU and MV treatment offered

Appendix A – Recruitment Model Results

Patient 1

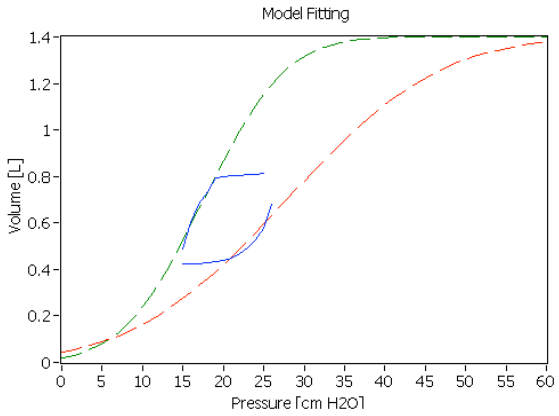

a

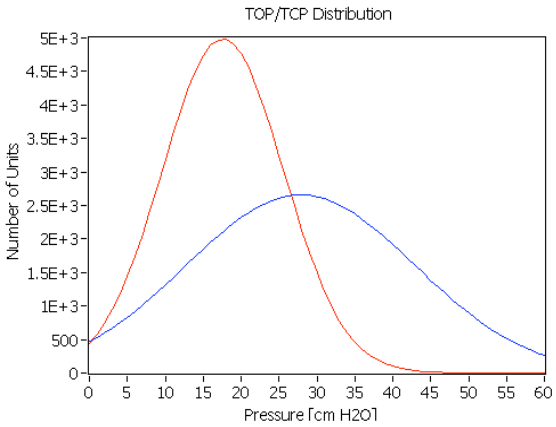

a-1

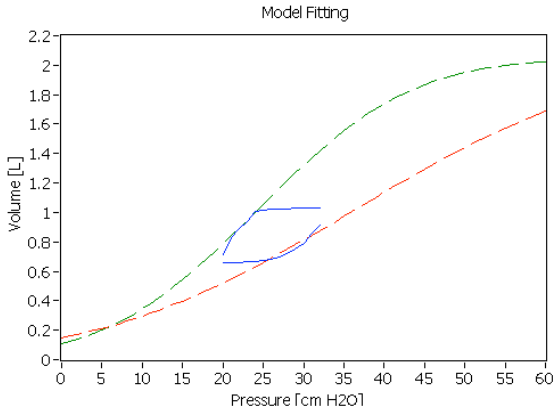

b

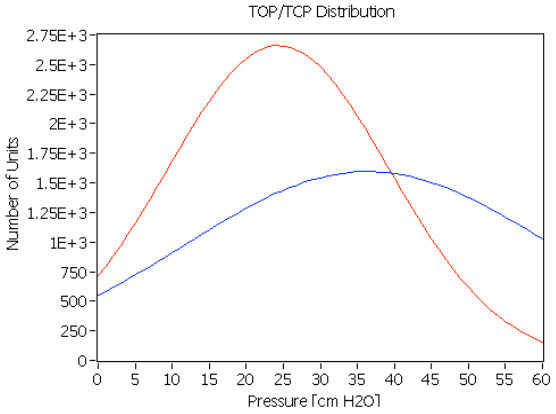

b-1

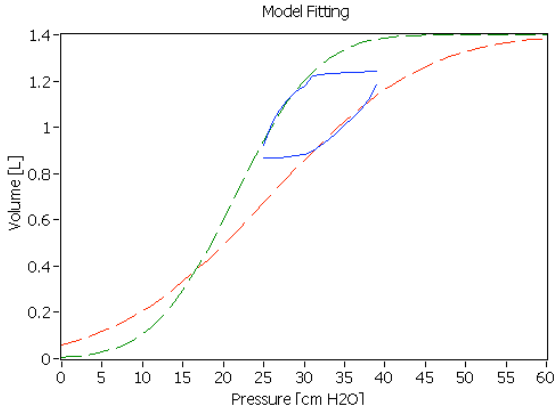

c

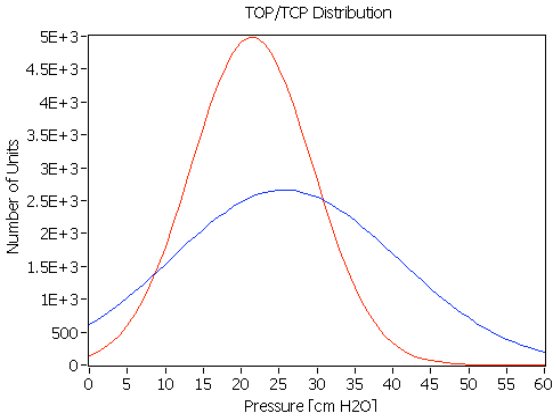

c-1

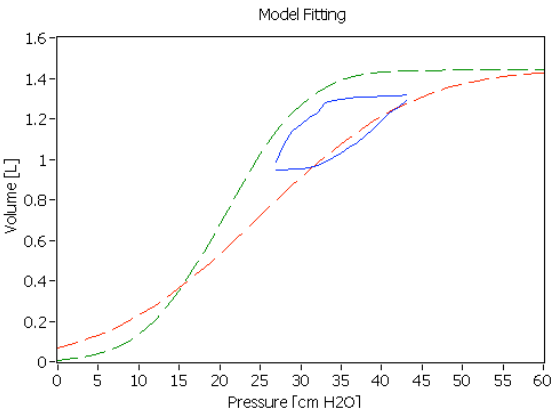

d

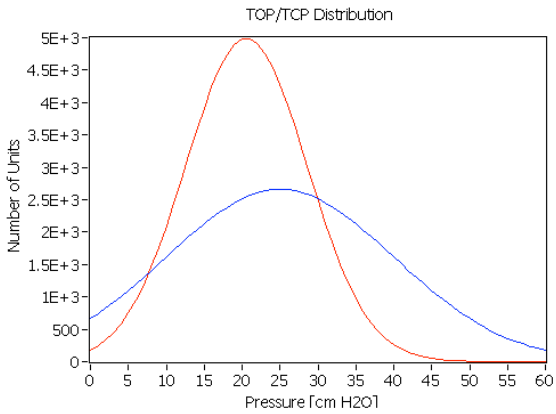

d-1

Figure A-1: Patient 1 Model Fitting and TOP/TCP Distribution. a-d represent breaths taken at different PEEP levels with a-1 – d-1 representing the TOP/TCP distributions for respective breathing cycles. Red curve represents TCP distribution and blue curve represents TOP distributions

Patient 2

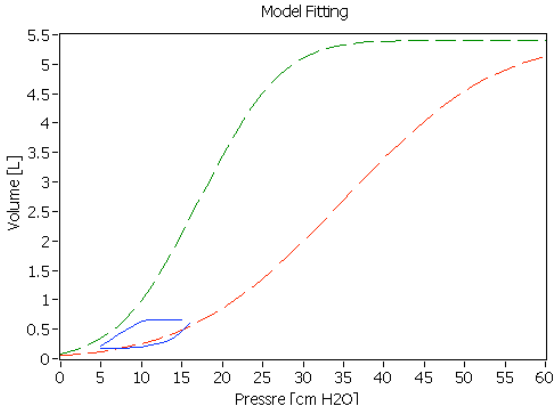

a

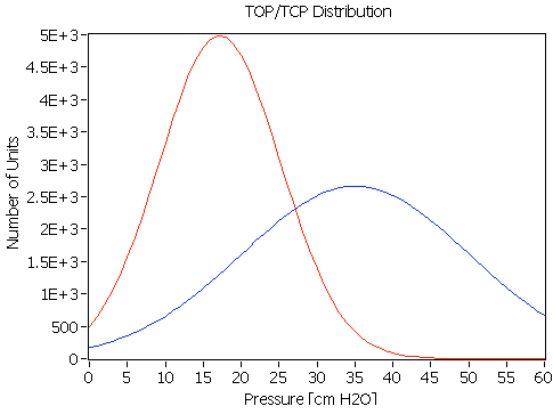

a-1

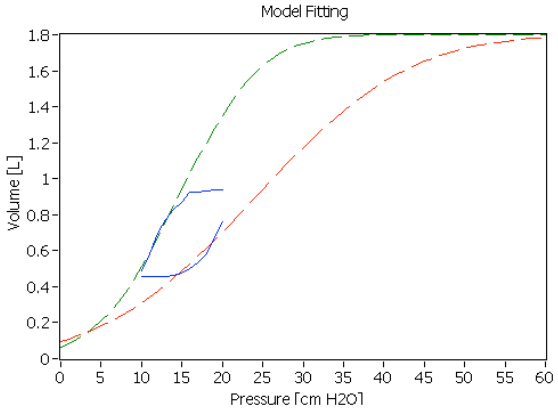

b

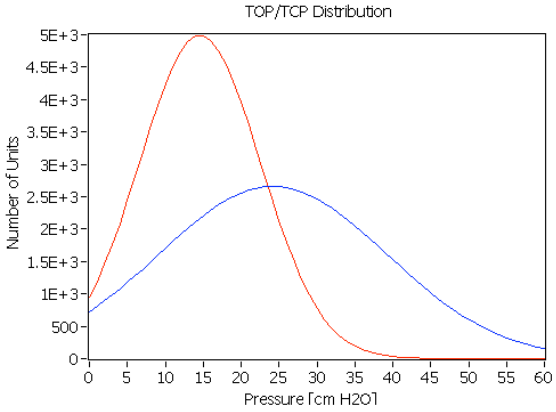

b-1

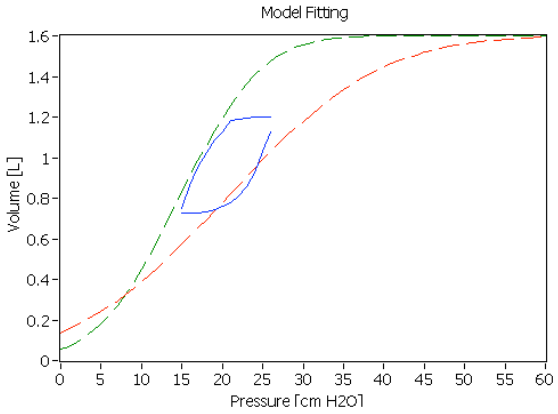

c

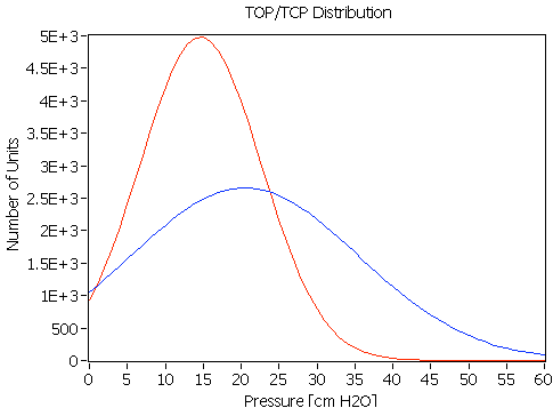

c-1

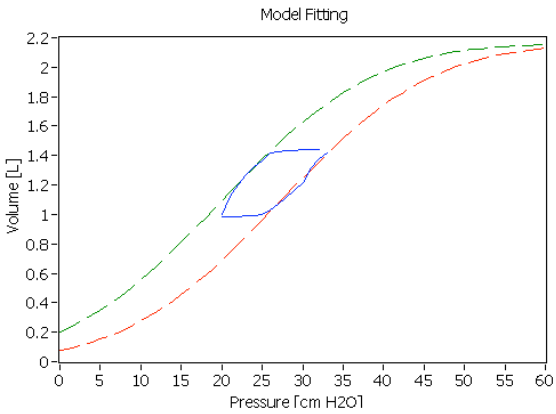

d

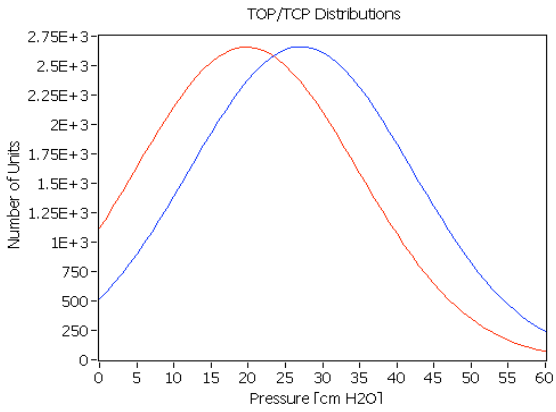

d-1

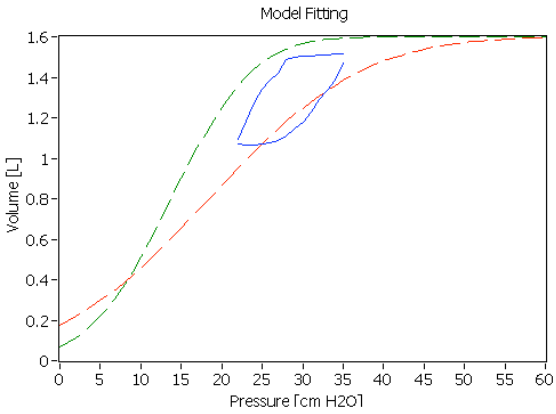

e

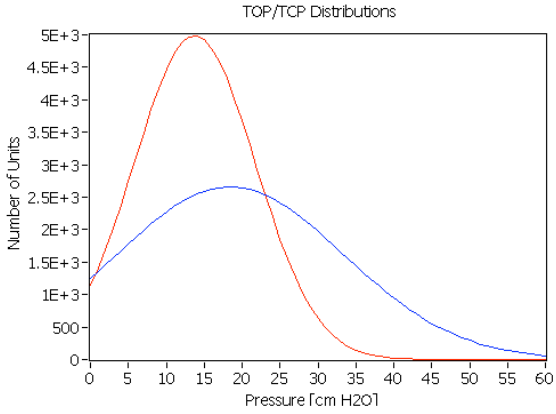

e-1

Figure A-2: Patient 2 Model Fitting and TOP/TCP Distribution. a-e represent breaths taken at different PEEP levels with a-1 – e-1 representing the TOP/TCP distributions for respective breathing cycles. Red curve represents TCP distribution and blue curve represents TOP distributions

Patient 3

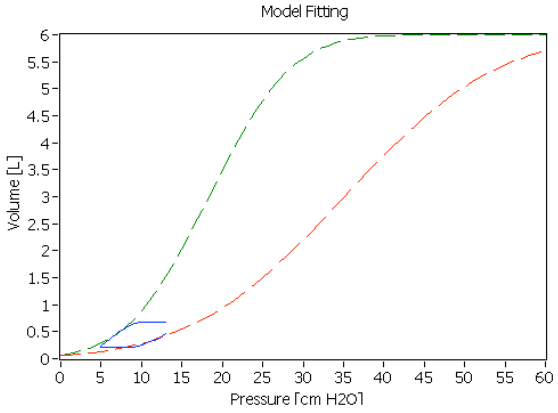

a

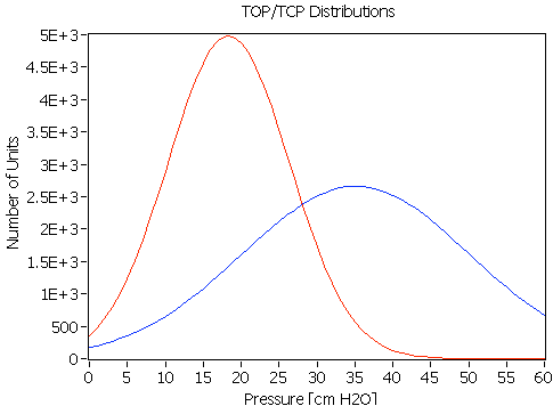

a-1

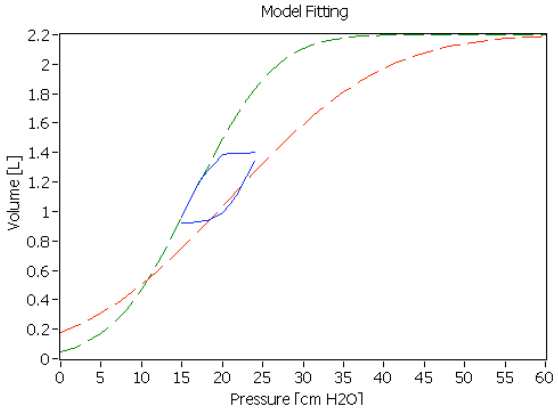

b

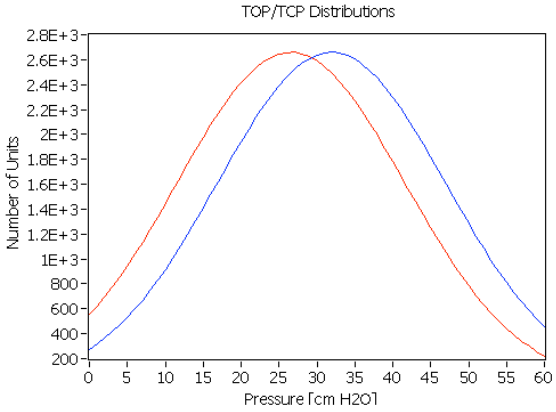

b-1

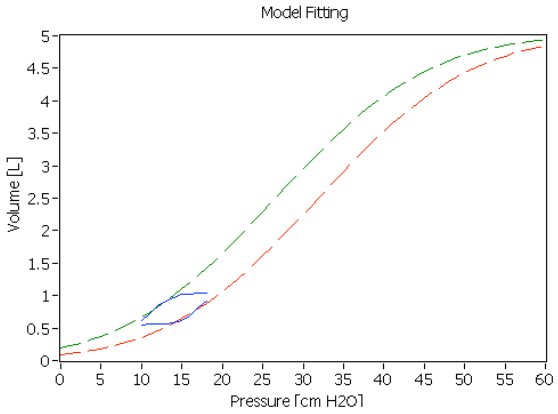

c

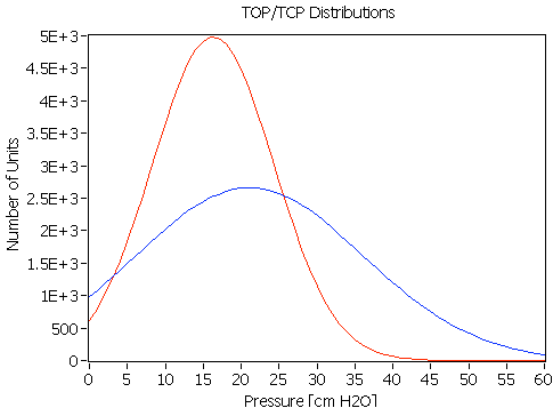

c-1

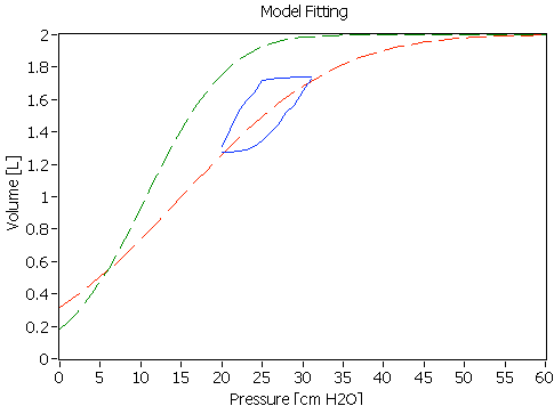

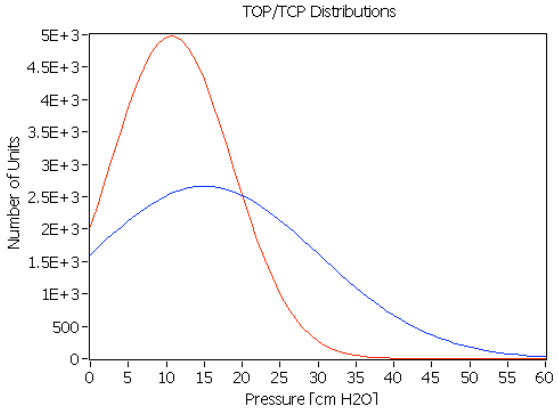

d **d-1**

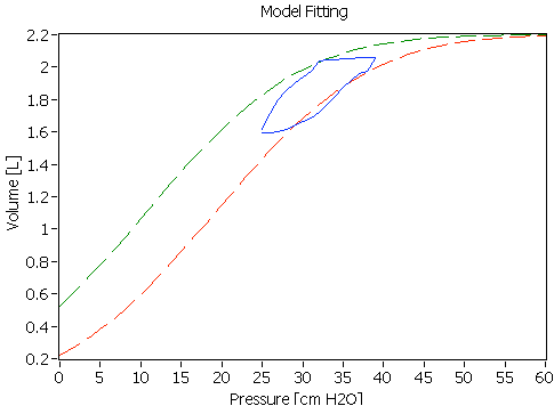

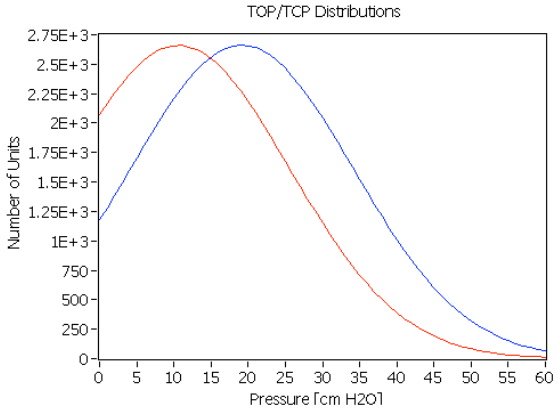

e **e-1**

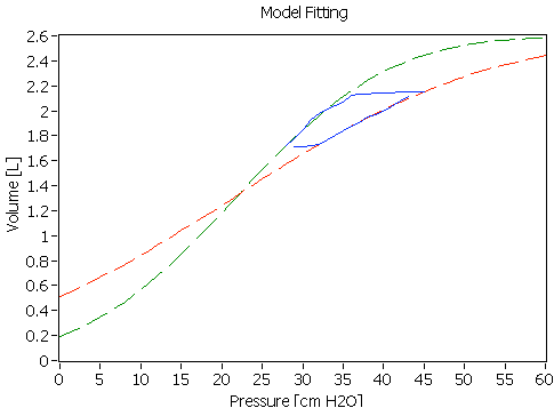

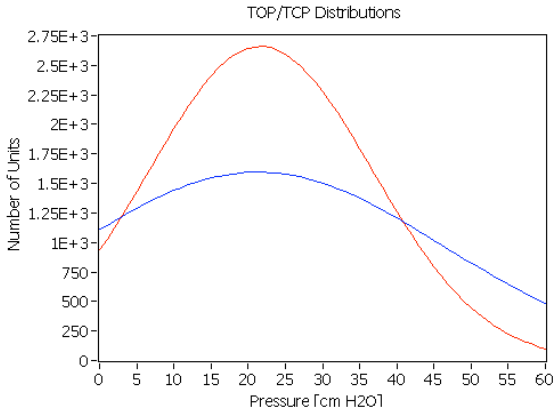

f **f-1**

Figure A-3: Patient 3 Model Fitting and TOP/TCP Distribution. a-f represent breaths taken at different PEEP levels with a-1 – f-1 representing the TOP/TCP distributions for respective breathing cycles. Red curve represents TCP distribution and blue curve represents TOP distributions

Patient 4

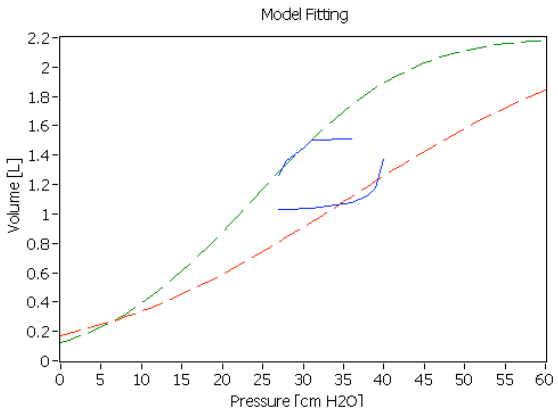

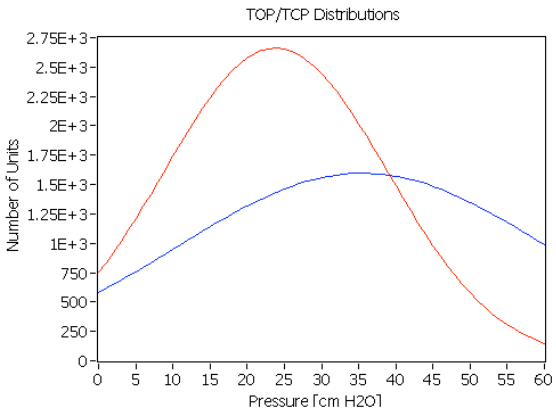

a **a-1**

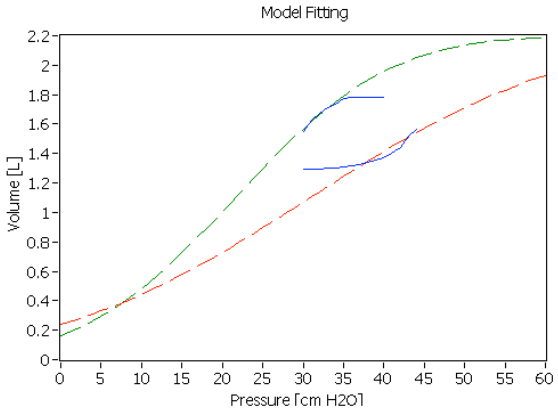

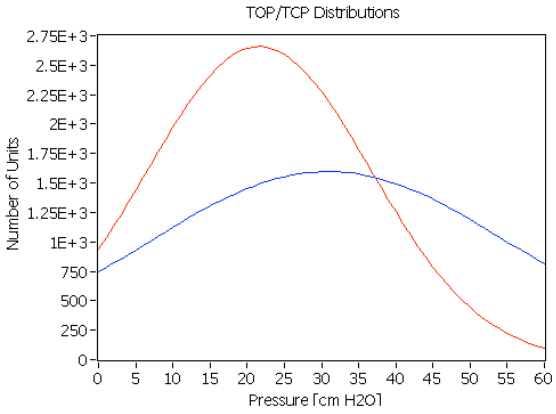

b **b-1**

Figure A-4: Patient 4 Model Fitting and TOP/TCP Distribution. a-b represent breaths taken at different PEEP levels with a-1 – b-1 representing the TOP/TCP distributions for respective breathing cycles. Red curve represents TCP distribution and blue curve represents TOP distributions

Patient 5

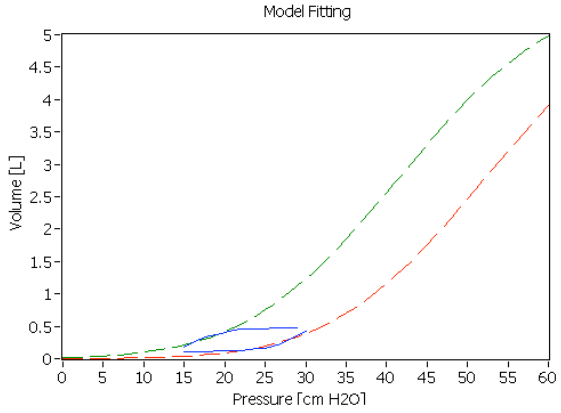

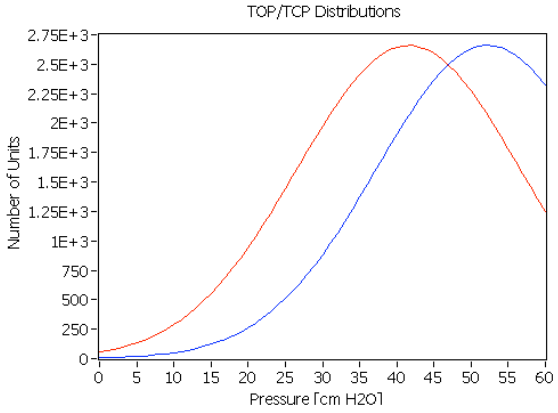

a **a-1**

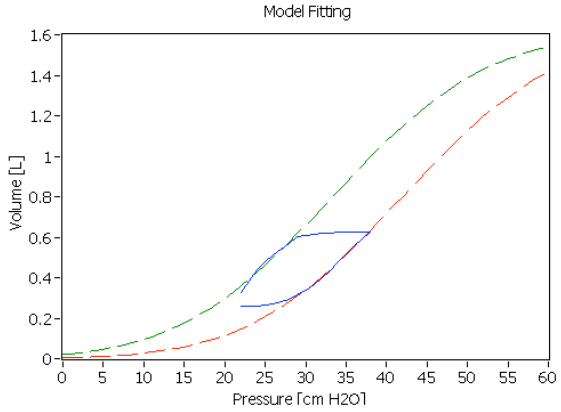

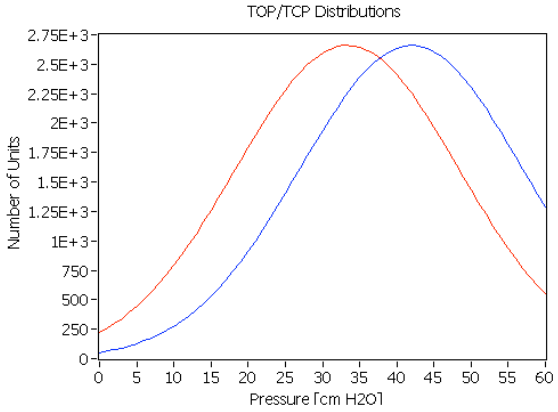

b **b-1**

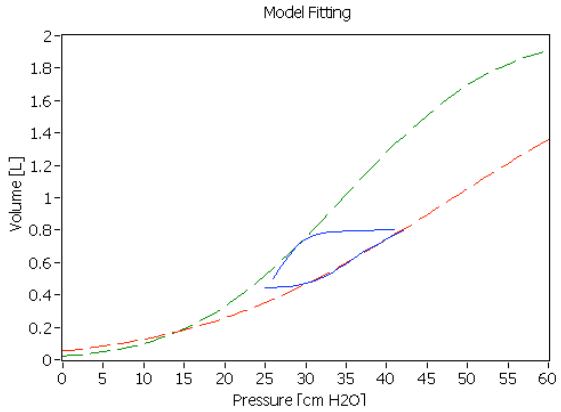

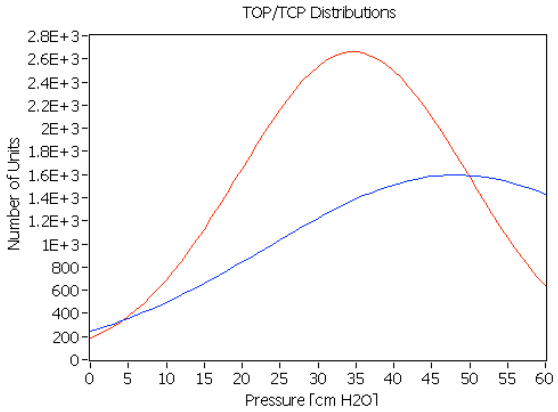

c **c-1**

Figure A-5: Patient 5 Model Fitting and TOP/TCP Distribution. a-c represent breaths taken at different PEEP levels with a-1 – c-1 representing the TOP/TCP distributions for respective breathing cycles. Red curve represents TCP distribution and blue curve represents TOP distributions

Patient 5 Trial 2

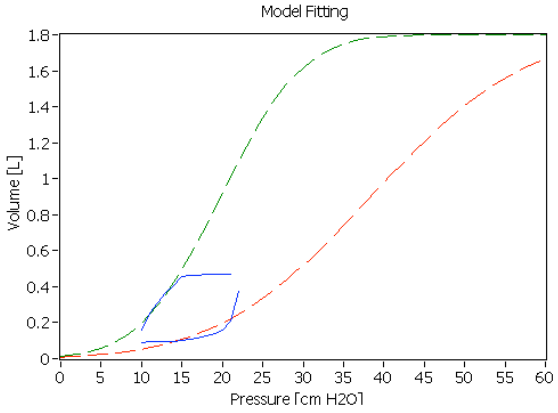

a

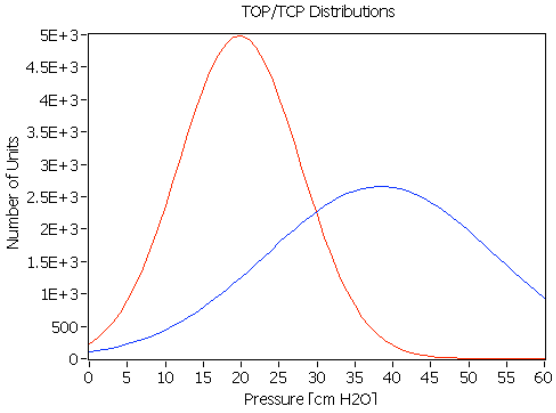

a-1

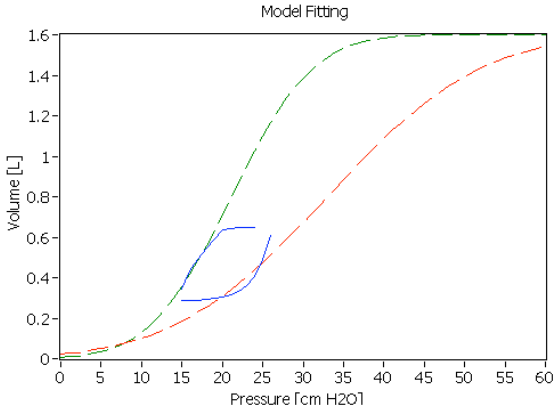

b

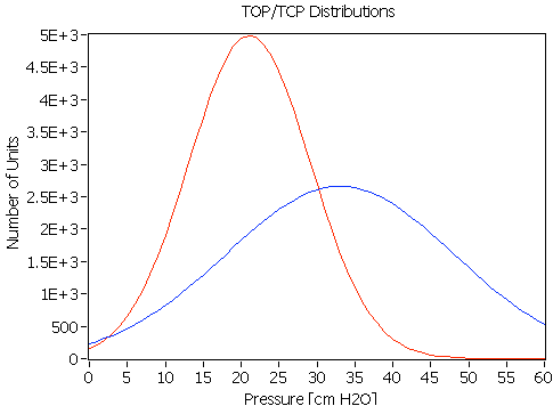

b-1

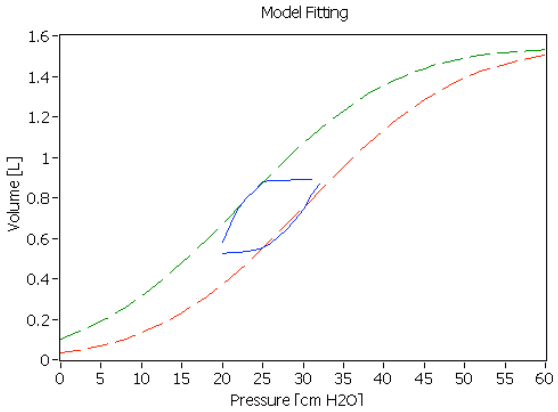

c

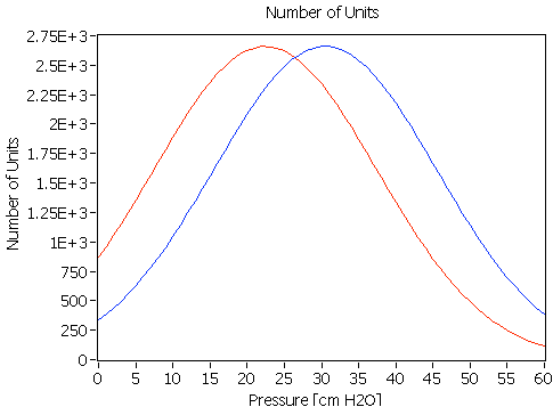

c-1

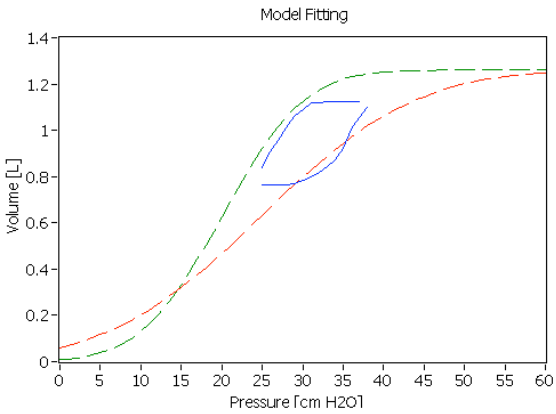

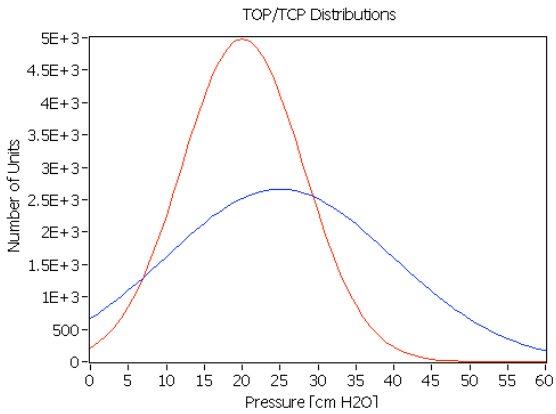

d **d-1**

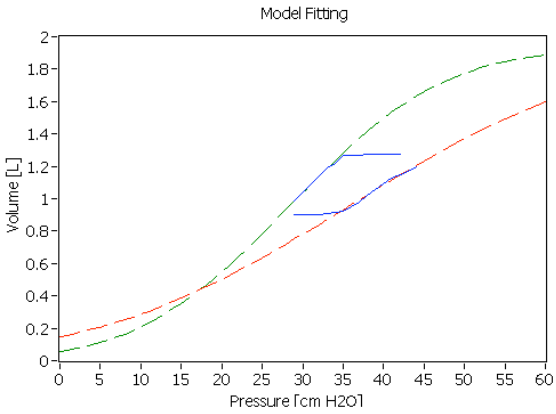

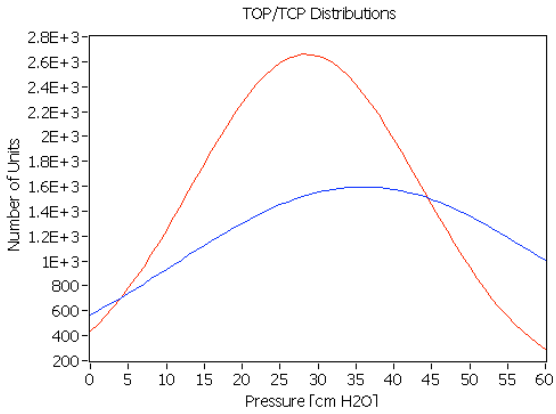

e **e-1**

Figure A-6: Patient 5 Trial 2 Model Fitting and TOP/TCP Distribution. a-e represent breaths taken at different PEEP levels with a-1 – e-1 representing the TOP/TCP distributions for respective breathing cycles. Red curve represents TCP distribution and blue curve represents TOP distributions

Patient 6

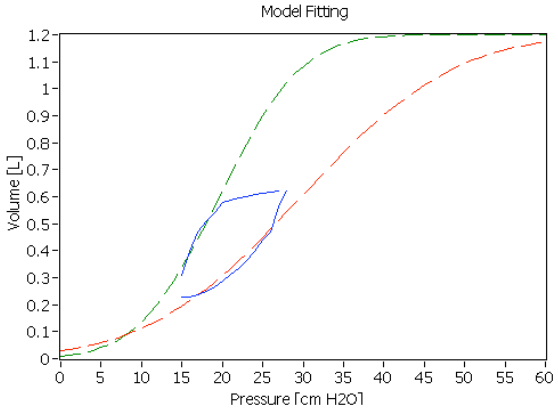

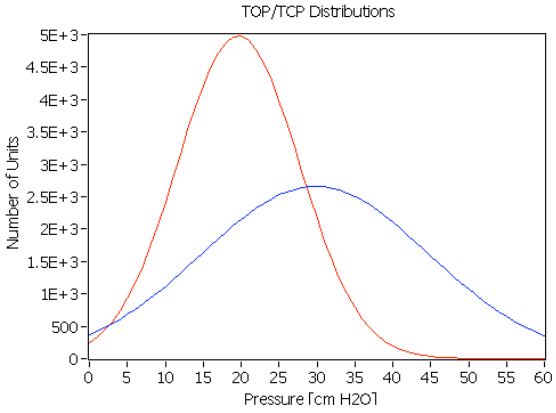

a **a-1**

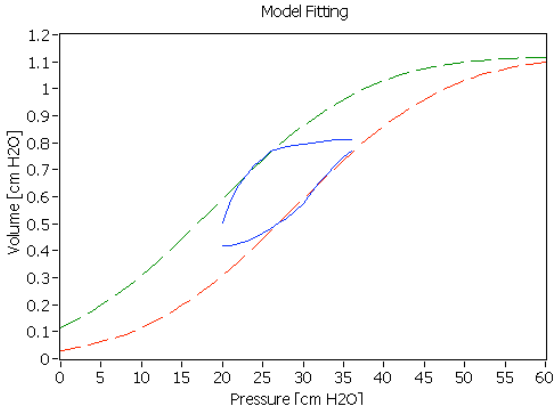

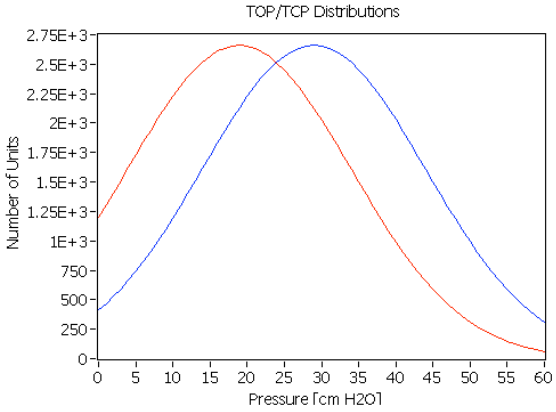

b **b-1**

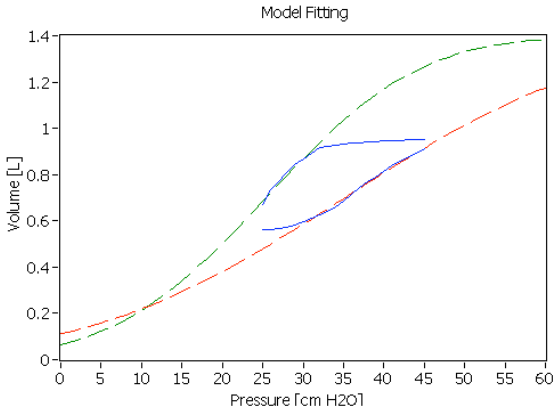

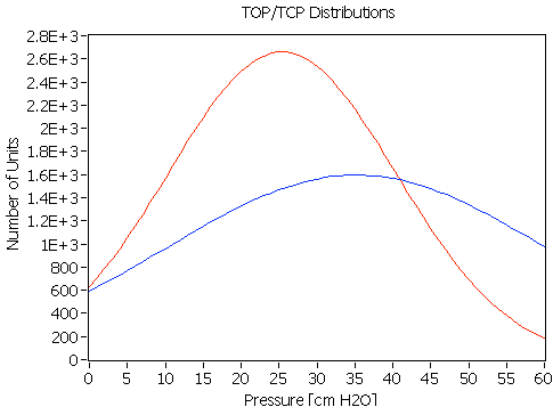

c **c-1**

Figure A-7: Patient 6 Model Fitting and TOP/TCP Distribution. a-c represent breaths taken at different PEEP levels with a-1 – c-1 representing the TOP/TCP distributions for respective breathing cycles. Red curve represents TCP distribution and blue curve represents TOP distributions

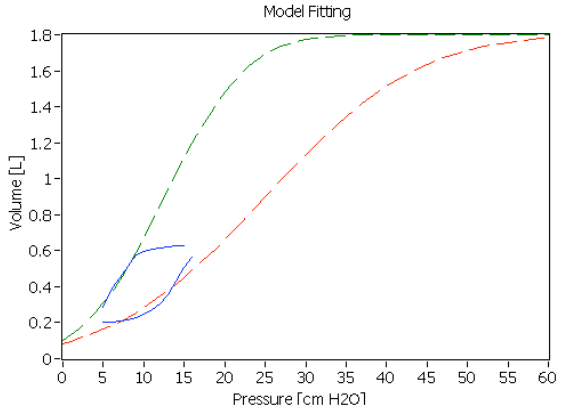
Model Fitting
Volume [L]
Pressure [cm H2O]

a

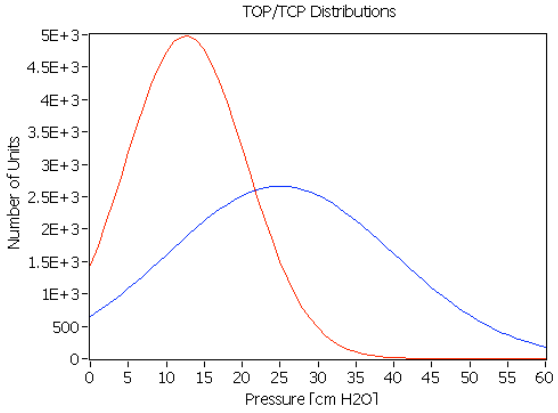
TOP/TCP Distributions
Number of Units
Pressure [cm H2O]

a-1

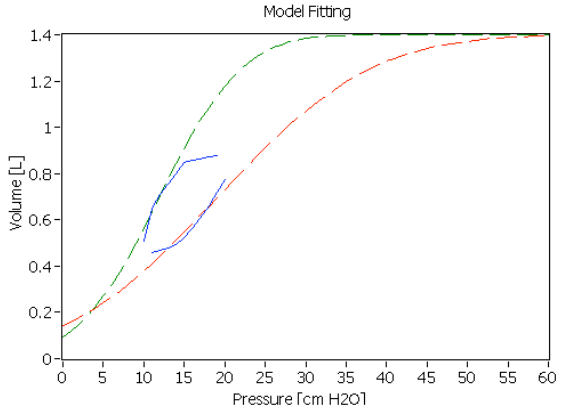
Model Fitting
Volume [L]
Pressure [cm H2O]

b

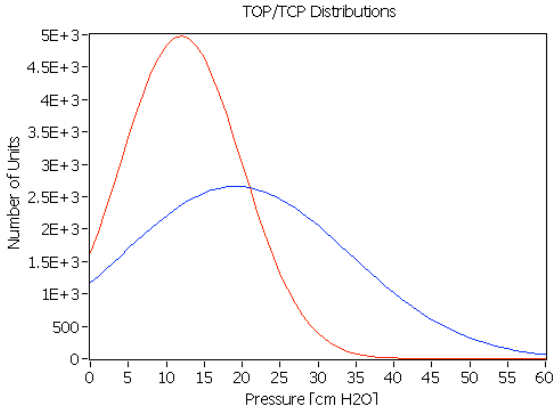
TOP/TCP Distributions
Number of Units
Pressure [cm H2O]

b-1

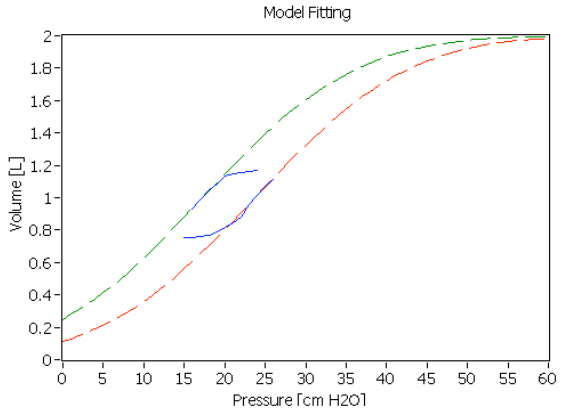
Model Fitting
Volume [L]
Pressure [cm H2O]

c

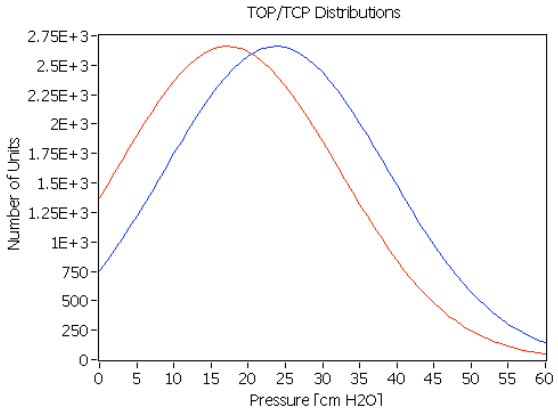
TOP/TCP Distributions
Number of Units
Pressure [cm H2O]

c-1

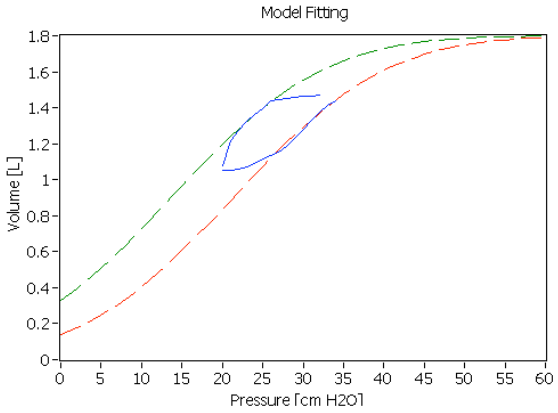

d

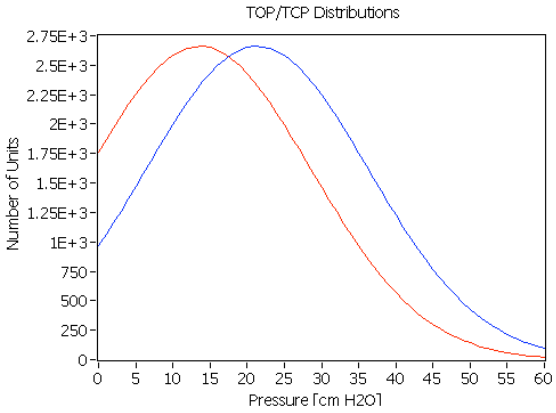

d-1

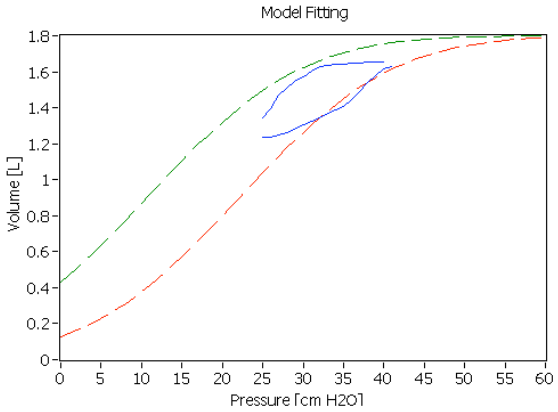

e

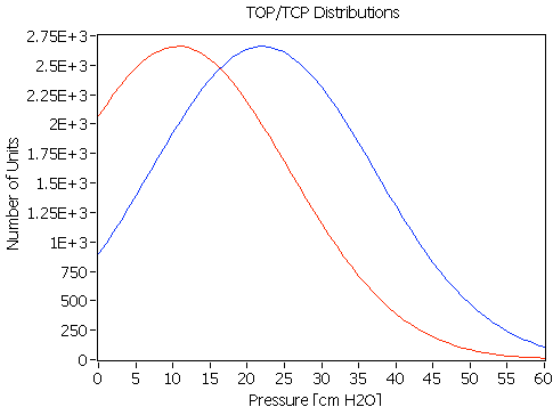

e-1

Figure A-8: Patient 6 Trial 2 Model Fitting and TOP/TCP Distribution. a-e represent breaths taken at different PEEP levels with a-1 – e-1 representing the TOP/TCP distributions for respective breathing cycles. Red curve represents TCP distribution and blue curve represents TOP distributions

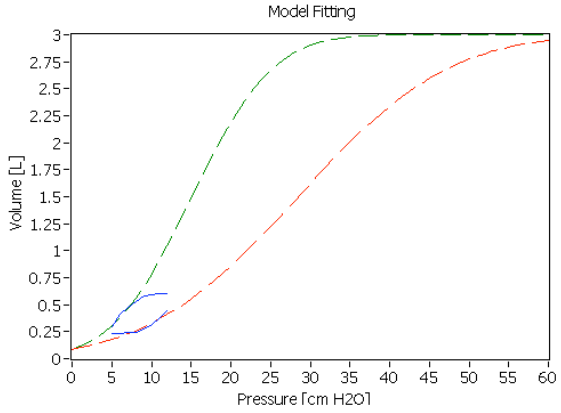
Model Fitting
Volume [L]
Pressure [cm H2O]

a

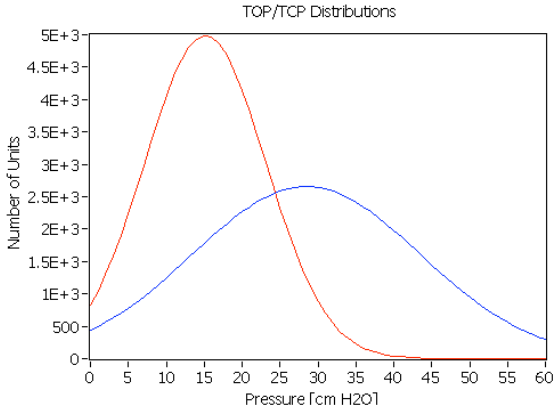
TOP/TCP Distributions
Number of Units
Pressure [cm H2O]

a-1

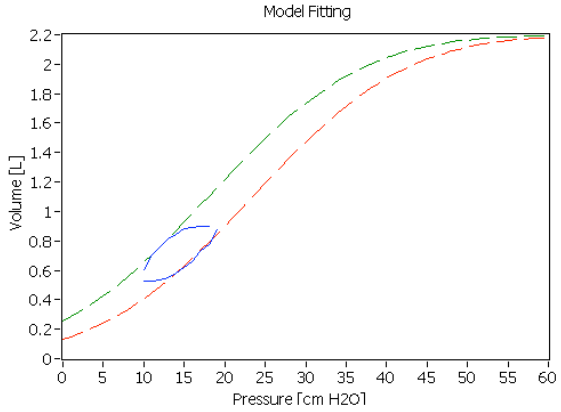
Model Fitting
Volume [L]
Pressure [cm H2O]

b

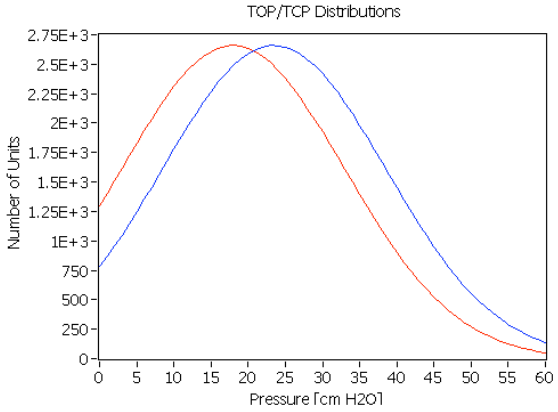
TOP/TCP Distributions
Number of Units
Pressure [cm H2O]

b-1

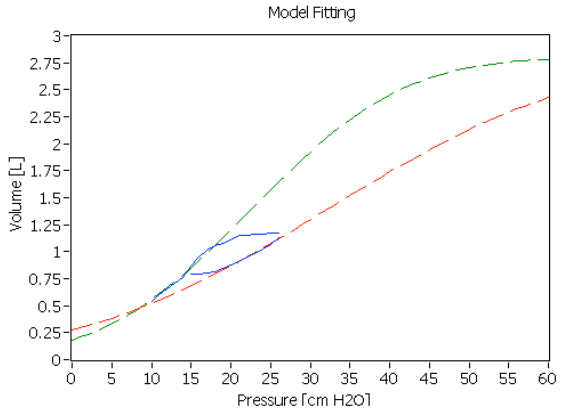
Model Fitting
Volume [L]
Pressure [cm H2O]

c

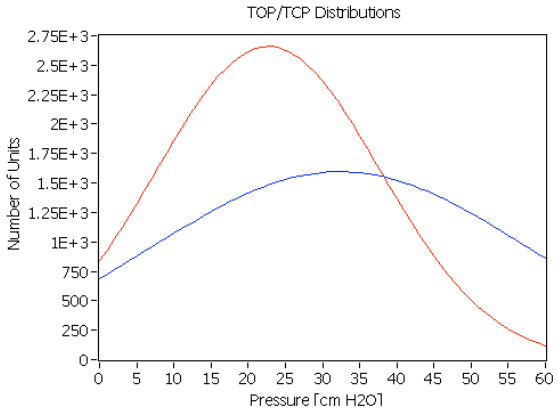
TOP/TCP Distributions
Number of Units
Pressure [cm H2O]

c-1

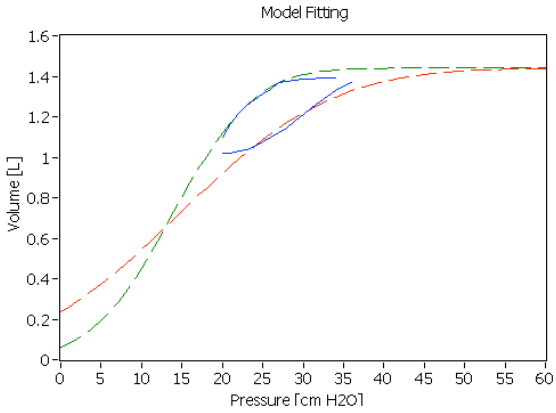

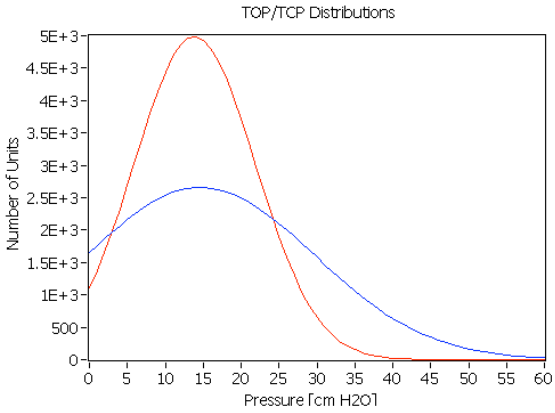

d **d-1**

Figure A-9: Patient 6 Trial 3 Model Fitting and TOP/TCP Distribution. a-d represent breaths taken at different PEEP levels with a-1 – d-1 representing the TOP/TCP distributions for respective breathing cycles. Red curve represents TCP distribution and blue curve represents TOP distributions

Patient 7

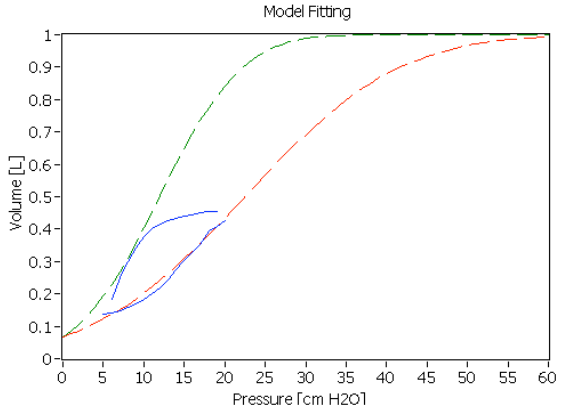

a

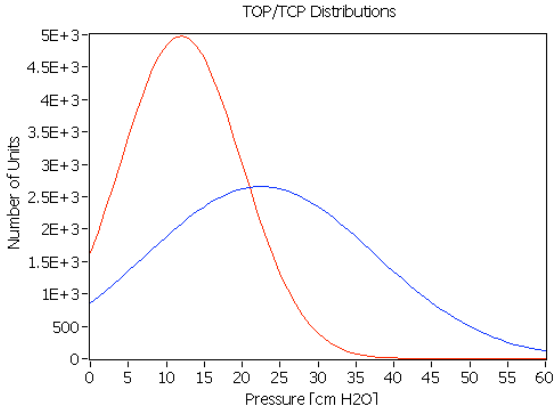

a-1

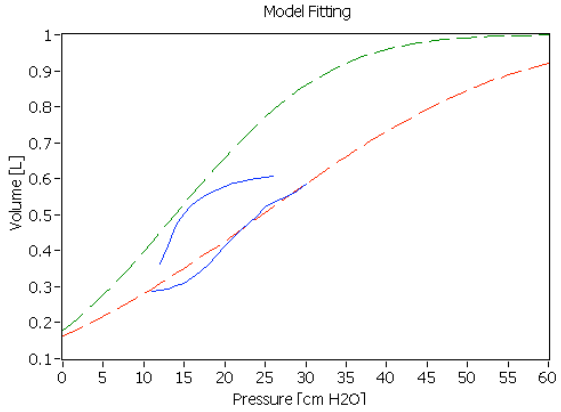

b

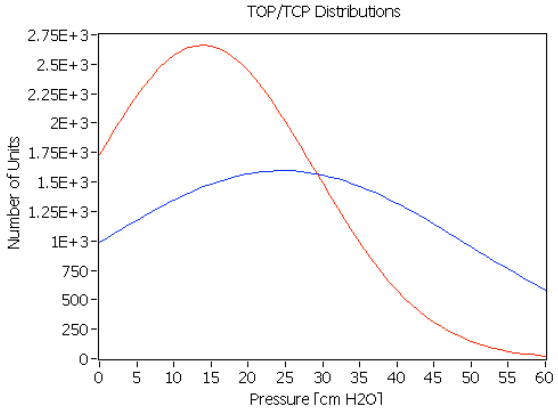

b-1

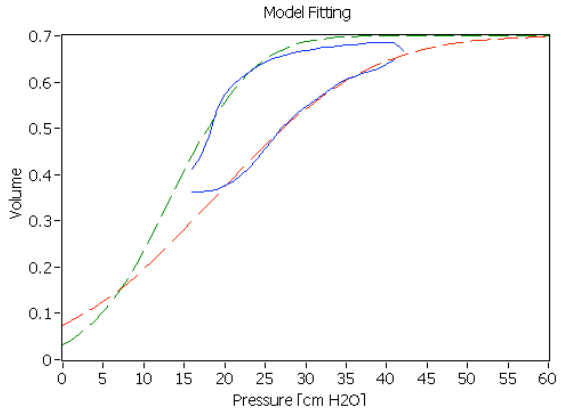

c

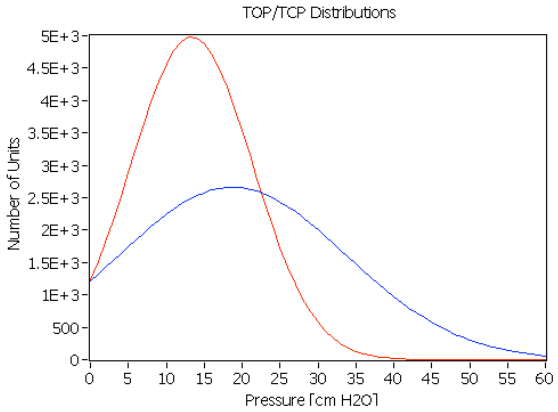

c-1

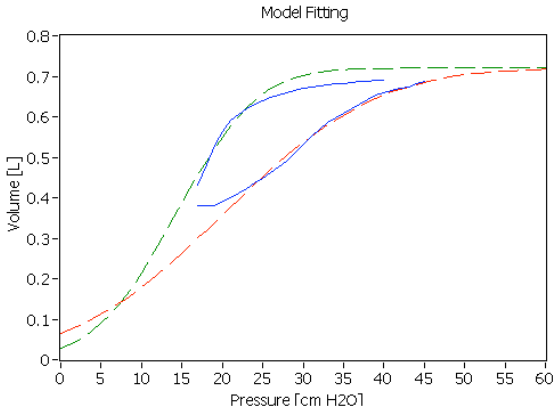

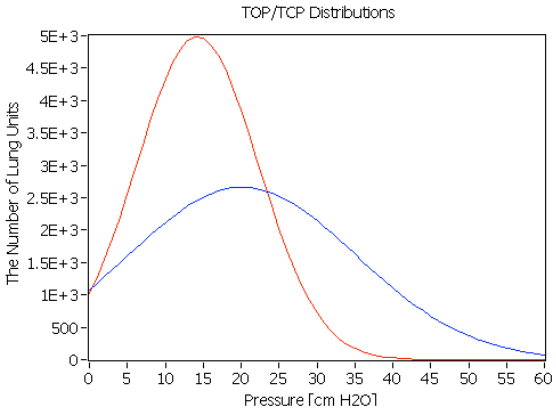

d **d-1**

Figure A-10: Patient 7 Model Fitting and TOP/TCP Distribution. a-d represent breaths taken at different PEEP levels with a-1 – d-1 representing the TOP/TCP distributions for respective breathing cycles. Red curve represents TCP distribution and blue curve represents TOP distributions

Patient 8

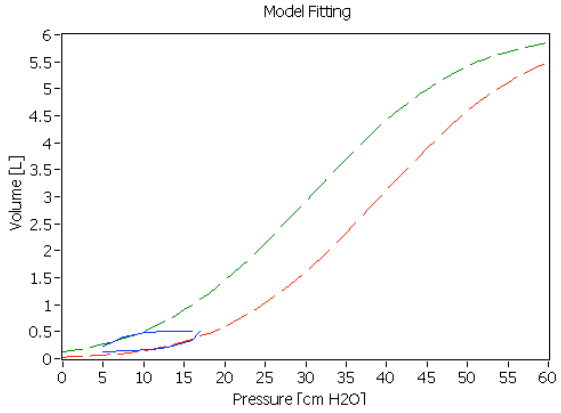

a

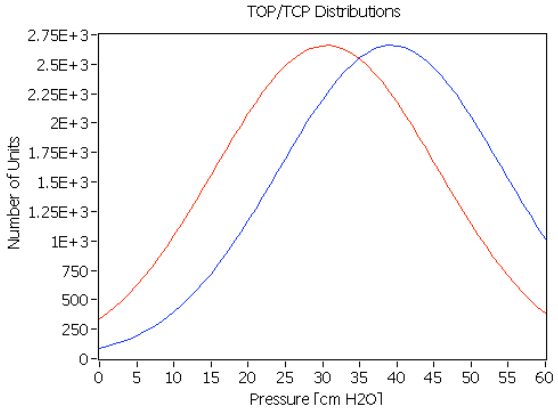

a-1

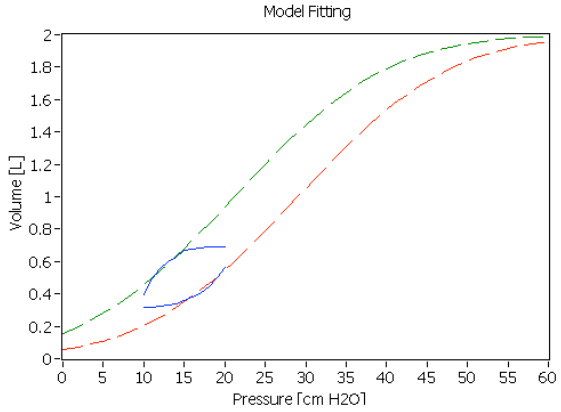

b

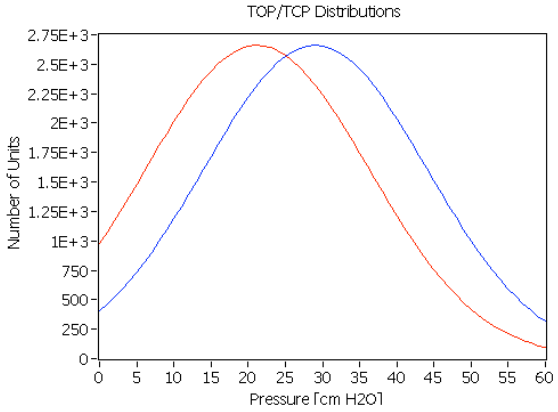

b-1

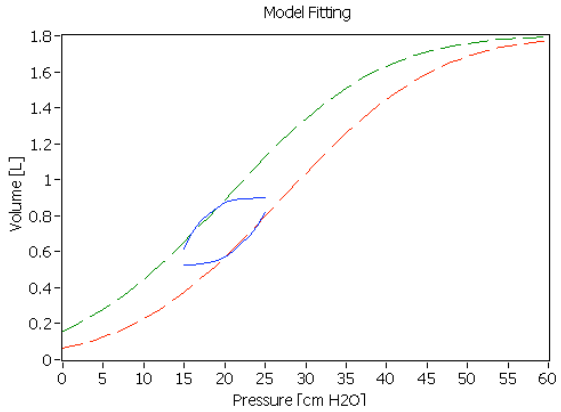

c

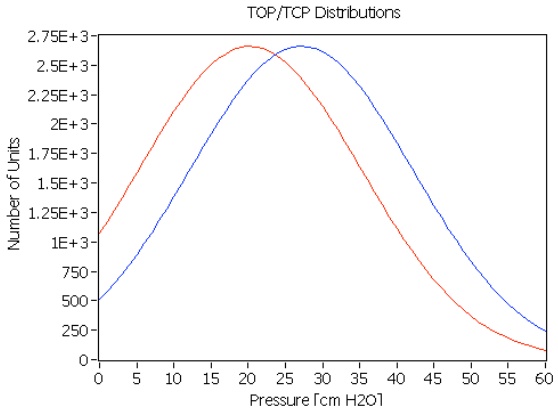

c-1

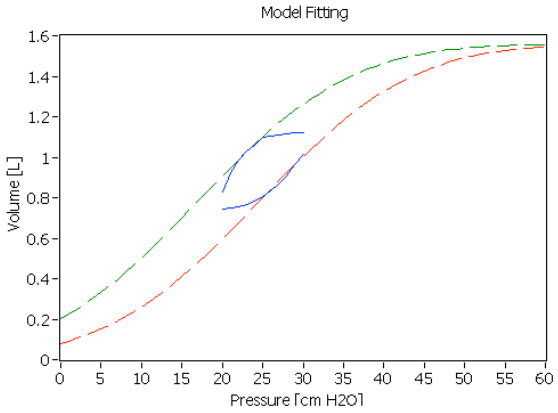

d

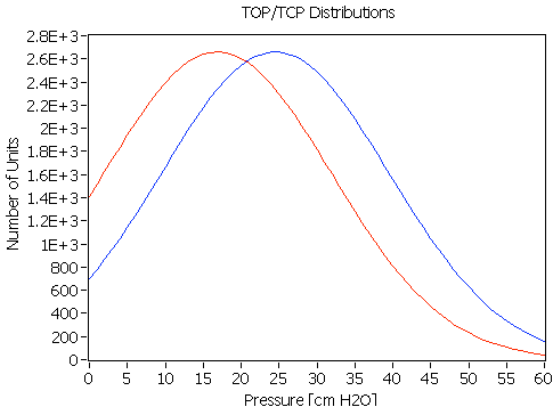

d-1

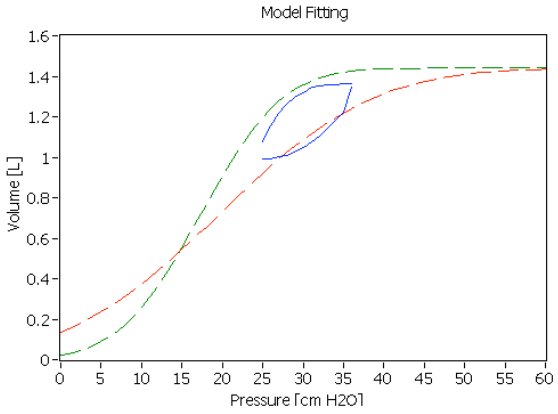

e

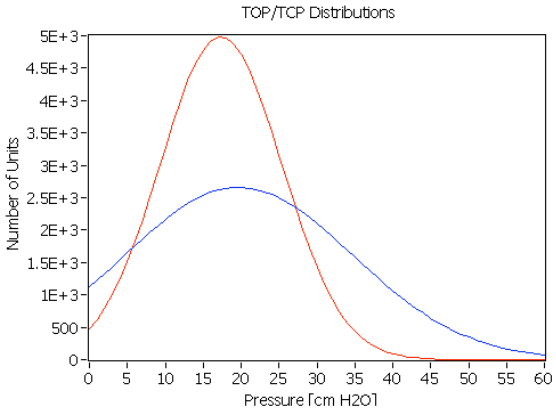

e-1

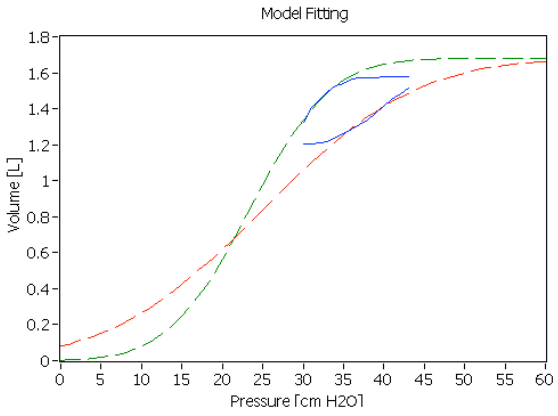

f

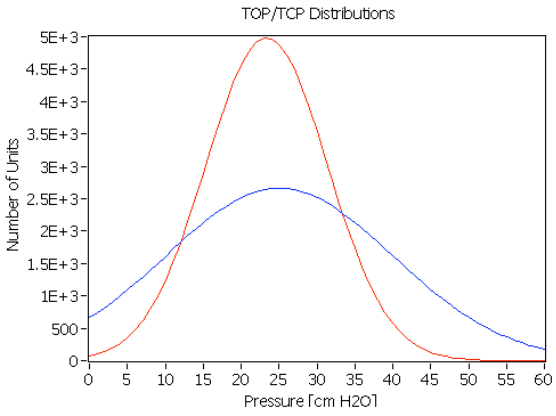

f-1

Figure A-11: Patient 8 Model Fitting and TOP/TCP Distribution. a-f represent breaths taken at different PEEP levels with a-1 – f-1 representing the TOP/TCP distributions for respective breathing cycles. Red curve represents TCP distribution and blue curve represents TOP distributions

Patient 9

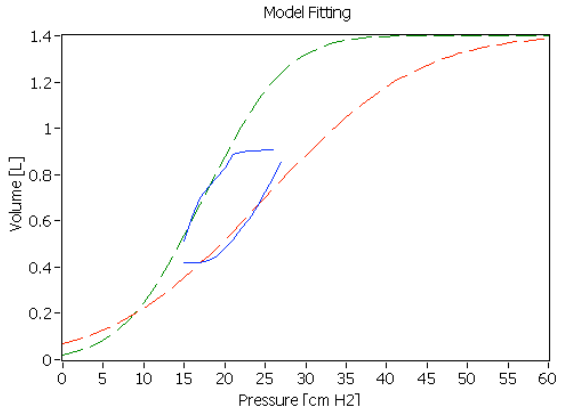

a

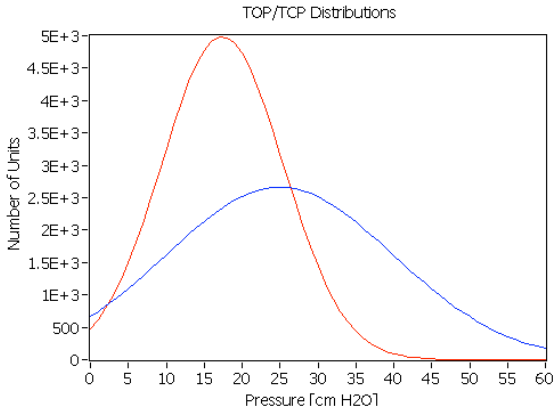

a-1

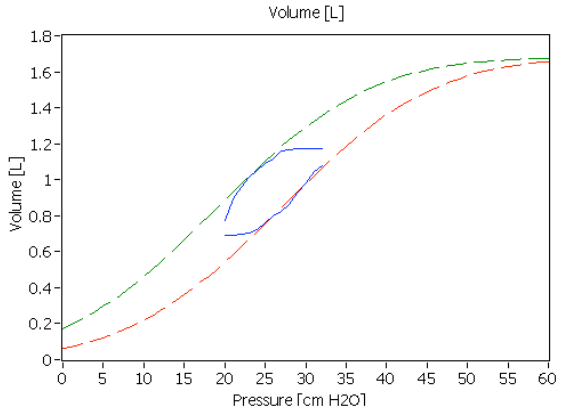

b

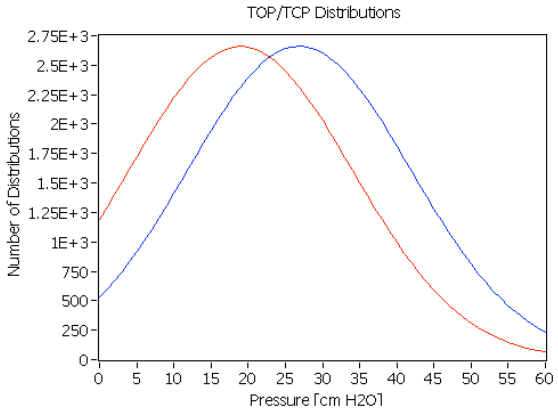

b-1

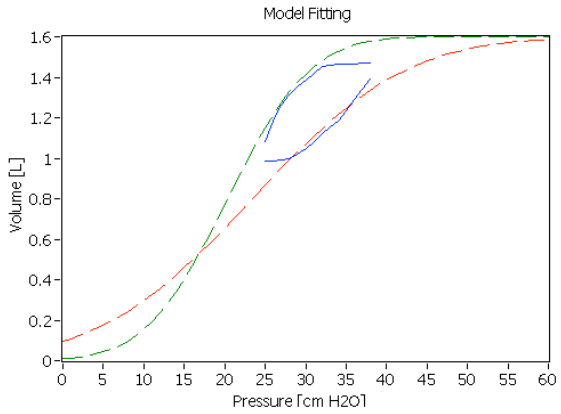

c

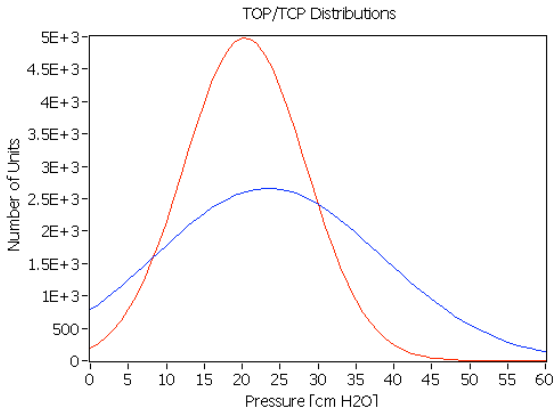

c-1

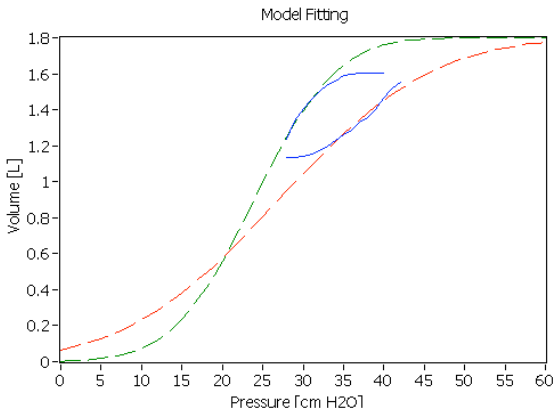

d

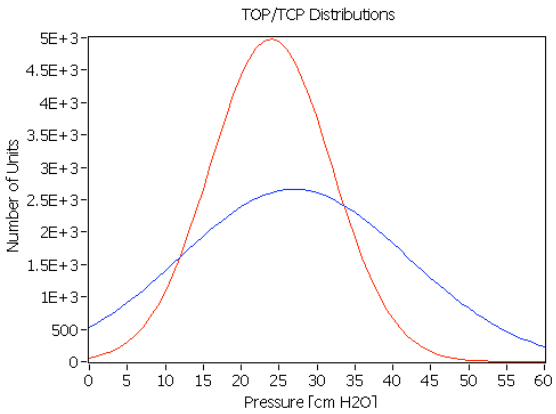

d-1

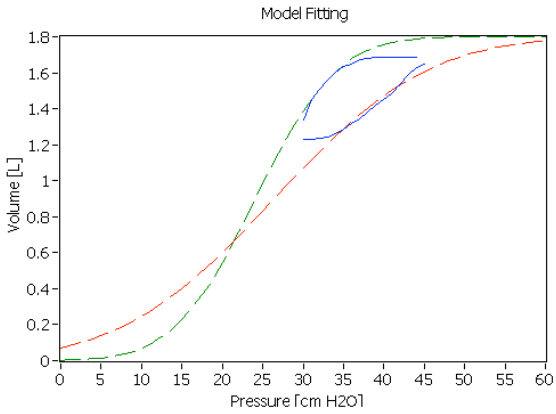

e

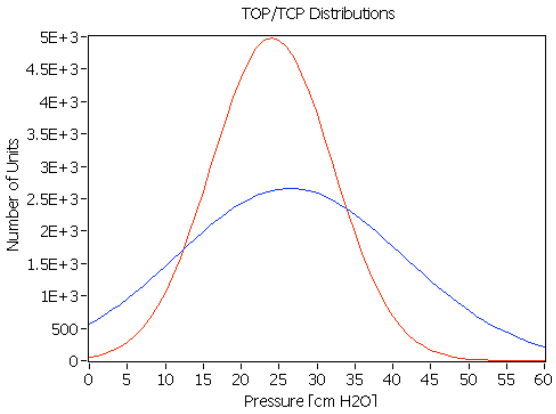

e-1

Figure A-12: Patient 9 Model Fitting and TOP/TCP Distribution. a-e represent breaths taken at different PEEP levels with a-1 – e-1 representing the TOP/TCP distributions for respective breathing cycles. Red curve represents TCP distribution and blue curve represents TOP distributions

References

ALBAICETA, G. M., TABOADA, F., PARRA, D., , LUYANDO, L. H., CALVO, J., MENENDEZ, R. & OTERO, J. 2004. Tomographic Study of the Inflection Points of the Pressure-Volume Curve in Acute Lung Injury. *Am J Respir Crit Care Med,* 170**,** 1066-1072.

AMATO, M. B. P., BARBAS, C. S. V., MEDEIROS, D. M., MAGALDI, R. B., SCHETTINO, G. P., LORENZI-FILHO, G., KAIRALLA, R. A., DEHEINZELIN, D., MUNOZ, C., OLIVEIRA, R., TAKAGAKI, T. Y. & CARVALHO, C. R. R. 1998. Effect of a Protective-Ventilation Strategy on Mortality in the Acute Respiratory Distress Syndrome. *New England Journal of Medicine,* 338**,** 347-354.

ARTIGAS, A., BERNARD, GORDON R., CARLET, J., DREYFUSS, D., GATTINONI, L., HUDSON, L., LAMY, M., MARINI, JOHN J., MATTHAY, MICHAEL A., PINSKY, MICHAEL R., SPRAGG, R., SUTER, PETER M. & THE CONSENSUS COMMITTEE 1998. The American-European Consensus Conference on ARDS, Part 2 . Ventilatory, Pharmacologic, Supportive Therapy, Study Design Strategies, and Issues Related to Recovery and Remodeling. *Am. J. Respir. Crit. Care Med.,* 157**,** 1332-1347.

ASHBAUGH, D., BOYD BIGELOW, D., PETTY, T. & LEVINE, B. 1967. Acute Respiratory Distress in Adults. *The Lancet,* 290**,** 319-323.

ATABAI, K. & MATTHAY, M. A. 2002. The pulmonary physician in critical care â€¢ 5: Acute lung injury and the acute respiratory distress syndrome: definitions and epidemiology. *Thorax,* 57**,** 452-458.

BERSTEN, A. D. 1998. Measurement of overinflation by multiple linear regression analysis in patients with acute lung injury. *Eur. Respir.J,* 12**,** 526-532.

BERSTEN, A. D., EDIBAM, C., HUNT, T. & MORAN, J. 2002. Incidence and Mortality of Acute Lung Injury and the Acute Respiratory Distress Syndrome in Three Australian States. *Am. J. Respir. Crit. Care Med.,* 165**,** 443-448.

BROCHARD, L., ROUDOT-THORAVAL, F., ROUPIE, E., DELCLAUX, C., CHASTRE, J., FERNANDEZ-MONDEJAR, E., CLEMENTI, E. V. A., MANCEBO, J., FACTOR, P., MATAMIS, D., RANIERI, M., BLANCH, L., RODI, G., MENTEC, H., DREYFUSS, D., FERRER, M., BRUN-BUISSON, C., TOBIN, M. & LEMAIRE, F. 1998. Tidal Volume Reduction for Prevention of Ventilator-induced Lung Injury in Acute Respiratory Distress Syndrome. *Am. J. Respir. Crit. Care Med.,* 158**,** 1831-1838.

BROWER, R. G., LANKEN, P. N., MACINTYRE, N., MATTHAY, M. A., MORRIS, A., ANCUKIEWICZ, M., SCHOENFELD, D. & THOMPSON, B. T. 2004. Higher

versus Lower Positive End-Expiratory Pressures in Patients with the Acute Respiratory Distress Syndrome. *New England Journal of Medicine,* 351**,** 327-336.

CARNEY, D. E., BREDENBERG, C. E., SCHILLER, H. J., PICONE, A. L., MCCANN, U. G., GATTO, L. A., BAILEY, G., FILLINGER, M. & NIEMAN, G. F. 1999. The mechanism of lung volume change during mechanicalventilation *Am J Respir Crit Care Med,* 160**,** 1697-1702.

CHENG, W., DELONG, D. S., FRANZ, G. N., PETSONK, E. L. & FRAZER, D. G. 1995. Contribution of opening and closing of lung units to lung hysteresis. *Respiration Physiology,* 102**,** 205-215.

CHIUMELLO, D., CARLESSO, E., CADRINGHER, P., CAIRONI, P., VALENZA, F., POLLI, F., TALLARINI, F., COZZI, P., CRESSONI, M., COLOMBO, A., MARINI, J. J. & GATTINONI, L. 2008. Lung Stress and Strain during Mechanical Ventilation for Acute Respiratory Distress Syndrome. *Am J Respir Crit Care Med,* 178**,** 346-355.

CROTTI, S., MASCHERONI, D., CAIRONI, P., PELOSI, P., RONZONI, G., MONDINO, M., MARINI, J. J. & GATTINONI, L. 2001. Recruitment and Derecruitment during Acute Respiratory Failure . A Clinical Study. *Am J Respir Crit Care Med,* 164**,** 131-140.

DASTA, J. F., MCLAUGHLIN, T. P., MODY, S. H. & PIECH, C. T. 2005. Daily cost of an intensive care unit day: the contribution to mechanical ventilation. *Crit Care Med,* 33**,** 1141-3.

DEANS, K. J., MINNECI, P. C., CUI, X., BANKS, S. M., NATANSON, C. & EICHACKER, P. Q. 2005. Mechanical ventilation in ards: One size does not fit all. *Crit Care Med,,* 33**,** 1141–3.

DREYFUS, D., BASSET, G., SOLER, P. & SAUMON, G. 1985. Intermittent positive-pressure hyperventilation with high inflation pressures produces pulmonary microvascular injury in rats. *Am Rev Respir Dis,* 132**,** 880-884.

EICHACKER, P. Q., GERSTENBERGER, E. P., BANKS, S. M., CUI, X. & NATANSON, C. 2002. Meta-Analysis of Acute Lung Injury and Acute Respiratory Distress Syndrome Trials Testing Low Tidal Volumes. *Am. J. Respir. Crit. Care Med.,* 166**,** 1510-1514.

ESTEBAN, A., ANZUETO, A., FRUTOS, F., ALIA, I., BROCHARD, L., STEWART, T. E., BENITO, S., EPSTEIN, S. K., APEZTEGUIA, C., NIGHTINGALE, P., ARROLIGA, A. C. & TOBIN, M. J. 2002. Characteristics and Outcomes in Adult Patients Receiving Mechanical Ventilation: a 28 day international study. *JAMA: The Journal of the American Medical Association,* 287**,** 345-355.

FERNÁNDEZ, R., MANCEBO, J., BLANCH, L., BENITO, S., CALAF, N. & NET, A. 1990. Intrinsic PEEP on static pressure-volume curves. *Intensive Care Medicine,* 16**,** 233-236.

FOTI, G., CEREDA, M., SPARACINO, M. E., DE MARCHI, L., VILLA, F. & AND PRESENTI, A. 2000. Effects of periodic lung recruitment maneuvers on gas

exchange and respiratory mechanics in mechanically ventilated acute respiratory distress syndrome (ARDS) patients. *Intensive Care Med,* 26**,** 501-7.

GAJIC, O., DARA, S. I., . , MENDEZ, J. L., ADESANYA, A. O., FESTIC, E., CAPLES, S. M., RANA, R., ST. SAUVER, J. L., LYMP, J. F., AFESSA, B. & HUBMAYR, R. D. 2004. Ventilator-associated lung injury in patients without acute lumg injury at the onset of mechanical ventilation. *Crit Care Med,* 32**,** 1817-1824.

GATTINONI, L., CAIRONI, P., PELOSI, P. & GOODMAN, L. R. 2001. What has Computed Tomograpy taught us about the Acute Respiratory Distress Syndrome. *Am J Respir Crit Care Med,* 164**,** 1701-1711.

GATTINONI, L., CHIUMELLO, D., CARLESSO, E. & VALENZA, F. 2004. Bench-to-bedside review: Chest wall elastance in acute lung injury/acute respiratory distress syndrome patients. *Critical Care,* 8**,** 350:355.

GATTINONI, L., LUCIANO P & ANTONIO 2005. The concept of "baby lung". *Intensive Care Medicine,* 31**,** 776-784.

GE HEALTHCARE. 2006. *The INview Suite: SpiroDynamics and FRC INview.* .

GIRGIS, K., HAMED, H., KHATER, Y. & KACMAREK, R. M. 2006. A decremental peep trial identifies the peep level that maintains oxygenation after lung recruitment. *Respir Care,* 51**,** 1132–9.

HAMILTON MEDICAL. New HAMILTON single use Flow Sensor - brochure.

HAMILTON MEDICAL. 2006. Galileo gold ventilator brochure and technical specifications.

HEINZE, H., SCHAAF, B., GREFER, J., KLOTZ, K. & EICHLER, W. 2007. The Accuracy of the Oxygen Washout Technique for Functional Residual Capacity Assessment During Spontaneous Breathing. *Anesth. Analg.,* 104**,** 598-604.

HENZLER, D., PELOSIM P., DEMBINSKI, R., ULLMAN, A., MAHNKEN , A. H., ROSSAINT, R. & AND KUHLEN, R. 2005. Respiratory compliance but not gas exchange correlates with changes in lung aeration after a recruitment maneuver: an experimental study in pigs with saline lavage lung injury,. *Am J Respir Crit Care Med,* 158**,** 194-202.

HICKLING, K. G. 1998. The pressure-volume curve is greatly modified by recruitment, a mathematical model of ARDS lungs. *Am J Respir Crit Care Med,* 158**,** 194-202.

HICKLING, K. G. 2001. Best compliance during a decremental, but not incremental, positive end-expiratory pressure trial is related to open-lung positive end-expiratory pressure: a mathematical model of acute respiratory distress syndrome. *Am J Respir Crit Care Med,* 163**,** 69-78.

HICKLING, K. G. 2002. Reinterpreting the pressure-volume curve in patients with acute respiratory distress syndrome. *Curr Opin Crit Care,,* 8**,** 32–8.

IOTTI, G. A. & BRASCHI, A. 1999. Measurements of Respiratory Mechanics During Mechanical Ventilation. *Hamilton Medcal AG, Rhazuns, Switzerland.*

JONSON, B. & SVANTESSON, C. 1999. Elastic pressure-volume curves: what information do they convey. *Thorax,* 54**,** 82-7.

JONSON, B. & UTTMAN, L. 2005. Elastic pressure-volume curves in acute lung injury and acute respiratory distress syndrome. *Intensive Care Med,* 31**,** 205-12.

JONSON, B. & UTTMAN, L. 2007. Efficient gas exchange with low tidal volume ventilation in acute respiratory distress syndrome. *Journal of Organ Dysfunction,* 3**,** 82-89.

KACMAREK, R. M. 2005. Lung protection: the cost in some is increased work of breathing. is it too high? *Respir Care,* 50**,** 1614–6.

KALLET, R. H. & R.M. JASMER. 2005. Clinical implementation of the ARDS network protocol is associated with reduced hospital mortality compared with historical controls. *Critical Care Medicine,* 33**,** 925-9.

KARASON, S., KARLSEN, K. L., LUNDIN, S. & STENQVIST, O. 1999. A simplified method for separate measurements of lung and chest wall mechanis in ventilator-treated patients. *Acta Anaesthesiol Scand,* 43.

KARASON, S., SONDERGAARD, S., LUNDIN, S., WIKLUND, J. & AND SENQVIST, O. 2000. Evaluation of pressure/voume loops based on intratracheal pressure measurements during dynamic conditions. *Acta Anaesthesiol Scand,* 44**,** 571-7.

KARASON, S., SONDERGAARD, S., LUNDIN, S., WIKLUND, J. & SENQVIST, O. 2001. Direct tracheal airway pressure measurements are essential for safe and accurate dynamic monitoring of respiratory mechanics. A laboratory study. *Acta Anaesthesiol Scand,* 45**,** 173-9.

LUHR, O. R., ANTONSEN, K., KARLSSON, M., AARDAL, S., THORSTEINSSON, A., FROSTELL, C. G. & BONDE, J. A. N. 1999. Incidence and Mortality after Acute Respiratory Failure and Acute Respiratory Distress Syndrome in Sweden, Denmark, and Iceland. the arf study group. *Am. J. Respir. Crit. Care Med.,* 159**,** 1849-1861.

MALBOUISSON, L. M., MULLER, J. C., CONTANTIN, J. M., LU, Q., PUYBASSET, L., ROUBY, J. J. & GROUP, A. T. C. S. S. A. 2001. Computed Tomography Assessment of Positive End-expiratory Pressure-induced Alveolar Recruitment in Patients with Acute Respiratory Distress Syndrome. *American Journal of Respiratory and Critical Care Medicine,* 163**,** 1444-1450.

MANZANO, F., YUSTE, E., COLMENERO, M., ARANDA, A., GARCÍA-HORCAJADAS, A., RIVERA, R. & FERNÁNDEZ-MONDÉJAR, E. 2005. Incidence of acute respiratory distress syndrome and its relation to age. *Journal of Critical Care,* 20**,** 274-280.

MAQUET MEDICAL SYSTEMS. 2006. Servo-i ventilator brochure.

MCLEAN, S. E., JENSEN, L. A., SCHROEDER, D. G., GIBNEY, N. R. T. & SKJODT, N. M. 2006. Improving Adherence to a Mechanical Ventilation Weaning Protocol for Critically Ill Adults: Outcomes After an Implementation Program. *American Journal of Critical Care,* 15**,** 299-309.

MUGHAL, M. M., CULVER, D. A., MINAI, O. A. & ARROLIGA, A. C. 2005. Auto-positive end expiratory pressure: mechanisms and treatment. *Cleveland Clinical Journal of Medicine,* 72**,** 801-809.

OCHS, M., NYENGAARD, J. R., JUNG, A., KNUDSEN, L., VOIGT, M., WAHLERS, T., RICHTER, J. & GUNDERSEN, H. J. G. 2004. The Number of Alveoli in the Human Lung. *Am. J. Respir. Crit. Care Med.,* 169**,** 120-124.

OLEGARD, C., SONDERGAARD, S., HOULTZ, E., LUNDIN, S. & STENQVIST, O. 2005. Estimation of Functional Residual Capacity at the Bedside Using Standard Monitoring Equipment: A Modified Nitrogen Washout/Washin Technique Requiring a Small Change of the Inspired Oxygen Fraction. *Anesth. Analg.,* 101**,** 206-12.

PELOSI, P., GOLDNER, M., MCKIBBEN, A., ADAMS, A., ECCHER, G., CAIRONI, P., LOSAPPIO, S., GATTINONI, L. & MARINI, J. J. 2001. Recruitment and Derecruitment During Acute Respiratory Failure . An Experimental Study. *Am J Respir Crit Care Med,* 164**,** 122-130.

RELLO, J., OLLENDORF, D. A., PSTER, F., VERA-LLONCH, M., BELLM, L., REDMAN, R. & KOLLEF, M. H. 2002. Epidemiology and outcomes of ventilator-associated pneumonia in a large us US database. *Chest,* 122**,** 2115-21.

REYNOLDS, H. N., MCCUNN, M., BORG, U., HABASHI, N., COTTINGHAM, C., BAR-LAVI, Y., 1998. Acute respiratory distress syndrome: estimated incidence and mortality rate in a 5 million-person population base. *Critical Care,* 2**,** 29 - 34.

RICARD, J. D., DREYFUSS, D. & SAUMON, G. 2003. Ventilator-induced lung injury. *Eur. Respir.J,* 22**,** 2s-9.

ROUBY, J. J., LU, Q. I. N. & GOLDSTEIN, I. 2002. Selecting the Right Level of Positive End-Expiratory Pressure in Patients with Acute Respiratory Distress Syndrome. *Am. J. Respir. Crit. Care Med.,* 165**,** 1182-1186.

ROUBY, J. J., PUYBASSET, L., CLUZEL, P., RICHECOEUR, J., LU, Q. & GRENIER, P. 2000. Regional distribution of gas and tissue in acute respiratory distress syndrome. II. Physiological correlations and definition of an ARDS Severity Score. *Intensive Care Medicine,* 26**,** 1046-1056.

RUBENFELD, G. D., CALDWELL, E., PEABODY, E., WEAVER, J., MARTIN, D. P., NEFF, M., STERN, E. J. & HUDSON, L. D. 2005. Incidence and Outcomes of Acute Lung Injury. *New England Journal of Medicine,* 353**,** 1685-1693.

SALAZAR, E. & KNOWLES J.H. 1964. An analysis of the pressure-volume characteristics if the lungs. *J Appl Physiol,* 19**,** 97-104.

SCHILLER, H. J., STEINBERG, J., HALTER, J., MCCANN, U., DASILVA, M., GATTO, L. A., CARNEY, D. & NIEMAN, G. 2003. Alveolar inflation during generation of a quasi-static pressure/volume curve in the acutely injured lung. *Crit Care Med,* 31**,** 1126-1133.

SEBEL, P., STODDART, D. M., WALDHORN, R. E., WALDMANN, C. S. & WHIFIELD, P. 1985. Respiration: the breath of life. *The Human Body*.

SEELEY, R. R., STEPHENS, T. D. & TATE, P. 2003. *Anatomy & Physiology,* New York, McGraw-Hill.

STEWART, T. E., MEADE, M. O., COOK, D. J., GRANTON, J. T., HODDER, R. V., LAPINSKY, S. E., MAZER, C. D., MCLEAN, R. F., ROGOVEIN, T. S., SCHOUTEN, B. D., TODD, T. R. J., SLUTSKY, A. S. & GROUP, T. P.-A. V. L. V. S. 1998 Evaluation of a Ventilation Strategy to Prevent Barotrauma in Patients at High Risk for Acute Respiratory Distress Syndrome. . *N Engl J Med,* 338**,** 355-361.

SUCHYTA, M. R., CLEMMER, T. P., ELLIOTT, C. G., ORME, J. F., MORRIS, A. H., JACOBSON, J. & MENLOVE, R. 1997. Increased Mortality of Older Patients With Acute Respiratory Distress Syndrome. *Chest,* 111**,** 1334-1339.

SUNDARESAN, A., CHASE, G., HANN, C. & SHAW, G. 2011. Dynamic functional residual capacity can be estimated using a stress–strain approach. *Computer Methods and Programs in Medicine,* 101**,** 135-143.

SUNDERESAN, A. 2010. *Applications of Model-Based Lung Mechanics in the Intensive Care Unit.* Doctor of Philosophy, The University of Canterbury.

TAKEUCHI, M., GODDON, S., DOLHNIKOFF, M., SHIMAOKA, M., HESS, D., AMATO, M. B. P. & KACMAREK, R. M. 2002. Set Positive End-expiratory Pressure during Protective Ventilation Affects Lung Injury. *Anesthesiology,* 97**,** 682-692.

THE ACUTE RESPIRATORY DISTRESS SYNDROME NETWORK. 2000. Ventilation with lower tidal volumes as compared with traditional tidal volumes for acute lung injury and the acute respiratory distress syndrome. *N Engl J Med.*

VANDER, A., SHERMAN, J. & LUCIANO, D. 2001. The Mechanism of Body Function. *Human Physiology*.

VENEGAS, J. G., HARRIS, R. S. & SIMON, B. A. 1998. A comprehensive equation for the pulmonary pressure-volume curve. *J Appl Physiol,* 84**,** 389-395.

VILLAR, J., KACMAREK, R. M., PEREZ-MENDEZ, L. & AGUIRRE-JAIME, A. 2006. A high positive end-expiratory pressure, low tidal volume ventilatory strategy improves outcome in persistent acute respiratory distress syndrome: A randomized, controlled trial. *Crit Care Med,* 34**,** 1311-1318.

WALSH, T. S., DODDS, S. & MCARDLE, F. 2004. Evaluation of simple criteria to predict successful weaning from mechanical ventilation in intensive care patients. *British Journal of Anaesthesia,* 92**,** 793-799.

WARE, L. B. & MATTHAY, M. A. 2000. The acute respiratory distress syndrome. *N Engl J Med,* 342**,** 1334-49.

YUTA, T. 2007. *Minimal Model of Lung Mechanics for Optimising Ventilator Terapy in Critical Care.* Doctor of Philosophy The University of Canterbury.

ZILBERBERG, M. D. & EPSTEIN, S. K. 1998. Acute Lung Injury in the Medical ICU . Comorbid Conditions, Age, Etiology, and Hospital Outcome. *Am. J. Respir. Crit. Care Med.,* 157**,** 1159-1164.